NTNU
Norwegian University of
Science and Technology

Flexible Bulbous Bow Design

A Hydrodynamic Study

Andreas Watle

Marine Technology
Submission date: June 2017
Supervisor: Håvard Holm, IMT

Norwegian University of Science and Technology
Department of Marine Technology

NTNU Trondheim
Norwegian University of Science and Technology
Department of Marine Technology

MASTER THESIS IN MARINE TECHNOLOGY

SPRING 20017

FOR

STUD. TECHN. ANDREAS WATLE

In the thesis the candidate shall present his personal contribution to the resolution of problem within the scope of the thesis work.

This project is intended to investigate the value of having a flexible bulb, which is being able to dynamically change the geometry of the bulb during operations. The purpose of the bulb is to reduce the ships wave resistance, by generating a wave that cancel out the wave generated from the hull. It has proven to be an important part of the resistance minimizing means. Bulbous bows have traditionally been designed and optimized for a specific, or narrow range of, service speed and loading condition. However, ships face a broad spectrum of operating conditions, as they have to take on a broad variety of trades, and one aspect of this is variation in speed. Speed variations may occur on a trip-to-trip basis, or on longer time scales. An example of the latter is container ships that recently have seen large reductions in operating speeds - also known as slow steaming.

As ship owners have reacted to this trend and how ship speeds correlate to the state of the global economy, recent developments have been towards designing the bulb for a broader range of operating conditions. This design strategy is known as robust design, and is essentially suboptimal for each speed scenario. However, based on the variety of operating conditions ships are facing, the strategy is superior to optimizing the bulb for a fixed service speed. Lately there have also been several examples of bulb retrofits, where bulbs designed for a fixed speed are replaced by robust bulb designs.

Bearing this in mind, the hypothesis is that there exists a untapped potential with respect to resistance minimization, by introducing a flexible bulb design. A flexible bulb design implies the option of changing the length of the bulb according to the desired speed for one specific trade –or ultimately during operations. Numerical resistance simulations coupled with a parameterized bulb body are an important part of the decision basis for the potential of the flexible bulb configuration.

This MSc thesis shall build on the work done in the project thesis work during autumn 2016. Several numerical simulation suites exist. This thesis shall use the panel code SIPFLOW within the CAESES framework.

The candidate shall analyze the effect on resistance due to a change in the bulb geometry. The bulb should be parameterized and a geometry which works well for a range of conditions should be identified. A procedure on how to identify the optimal bulb geometry should be used and explained.

The program SHIPFLOW should be used for analyzing the ship resistance. The candidate shall familiarize himself with the program, study its background/theory and limitations.

Further, if time permits, the program CAESES should be used to paremetrize the bulb. This would make it possible to search for the optimal bulb geometry in a systematic manner.

Theories and conclusions should be based on mathematical derivations and/or logic reasoning identifying the various steps in the deduction.

The candidate should utilize existing possibilities for obtaining relevant literature.

The thesis should be organized in a rational manner to give a clear exposition of results, assessments, and conclusions. The text should be brief and to the point, with a clear language. Telegraphic language should be avoided.

The thesis shall contain the following elements: A text defining the scope, preface, list of contents, summary, main body of thesis, conclusions with recommendations for further work, list of symbols and acronyms, reference and (optional) appendices. All figures, tables and equations shall be numerated.

The supervisor may require that the candidate, in an early stage of the work, present a written plan for the completion of the work. The plan should include a budget for the use of computer and laboratory resources that will be charged to the department. Overruns shall be reported to the supervisor.

The original contribution of the candidate and material taken from other sources shall be clearly defined. Work from other sources shall be properly referenced using an acknowledged referencing system.

The thesis shall be submitted in two copies:

- Signed by the candidate
- The text defining the scope included
- In bound volume(s)
- Drawings and/or computer prints that cannot be bound should be organized in a separate folder.
- The bound volume shall be accompanied by a CD or DVD containing the written thesis in Word or PDF format. In case computer programs have been made as part of the thesis work, the source code shall be included. In case of experimental work, the experimental results shall be included in a suitable electronic format.

Supervisor   : Associate Professor Håvard Holm
Start   : 15.01.2017
Deadline   : 11.06.2017

Trondheim, date ⁹/₍ - ⁷

Supervisor

Preface

This thesis is written as the final part of my Master's degree specializing in Marine Hydrodynamics at the Marine Technology Department at the Norwegian University of Science and Technology (NTNU) in Trondheim. This thesis has been written at NTNU during the spring semester of 2017. The workload corresponds to 30 ECTS.

The master thesis build upon the work of the project thesis written in the autumn of 2016, under the name "Flexible Bulbous Bows-A Hydrodynamic Study. The primary focus of the project thesis was to investigate and evaluate suitable software to be used during the master thesis.

Although the thesis is carried out as an individual project, the project is conducted in partly collaboration with stud. techn. Jon Hovem Leonhardsen, who specializes in Marine Systems Design. His work provided input data the operating profile used in the scenario based optimization procedure of this thesis. Furthermore, a total of seven Bachelor students at the Department of Mechanical Engineering at NTNU campus Kalvskinnet worked on concept development and the structural mechanics of the flexible bulbous bow concept.

<div align="center">

Trondheim, June 11, 2017

Andreas Watle

Andreas Watle

</div>

Acknowledgment

I would like to thank the following persons for their support and guidance during this project:

My supervisor, Associate Professor Håvard Holm, for great support and guidance during the compilation and writing of the master thesis through weekly meetings.

PhD candidate Carl Fredrik Rehn for giving me the opportunity to work on this project.

Olav Rognebakke for valuable input on the state-of-the-art wave resistance calculations and bulb retrofitting procedures.

Stud. techn. Jon hovem Leonhardsen for valuable input data.

The support staff at CAESES for great support and feedback.

A.W.

Executive Summary

With varying fuel costs and the pressure from International Maritime Organizations(IMO) Energy Efficient Design Index(EEDI) regulations regarding CO_2 emissions, new economical and environmentally-friendly technologies are becoming an integral part of ship design. Vessels today face a broad spectrum of operating conditions, as they must take on a broad variety of trades, and one aspect of this is variation in sailing speed. The variation in operating conditions due to both long and short term effects in the global economy opens an untapped potential for further fuel savings, by introducing a flexible bulb that could adopt to the change in operating conditions in real time. This thesis aims to investigate the value of bulbous bows that can reconfigure the length during transit from a hydrodynamic point of view.

To fit merchant vessels with bulbous bows to reduce the total resistance of the hull is customary practice. Although the bulbs differ in terms of shape and size for the different vessel segments, the primary objective is to reduce the ships wave resistance, by generating a wave that interferes with the wave generated by the hull, resulting in a minimization the wave resistance. As ship owners have reacted to how ship speeds correlates to the state of the global economy, recent developments have been towards designing the bulb for a broader range of operating conditions. This design strategy is known as robust design, and is essentially suboptimal for each speed scenario. However, based on the variety of operating conditions ships are facing, the strategy is superior to optimizing the bulb for a fixed service speed. The introduction of the flexibility to the bulb design is an active method of creating value, contrasting the standard passive robust design approach.

Large scale effects such as the wave making of the vessel is mostly unaffected by viscous effects, and this supports the use of a potential flow code to evaluate the wave resistance of the hull. By evaluating the difference in wave resistance for the different length configurations of the flexible bulb, the potential of such a device can be stated. The potential flow code SHIPFLOW is used to rank the different bulb design modifications with respect to hydrodynamic performance.

The design procedure of the flexible bulbous bow is divided in two stages. The first stage is to analyze Automatic Identification System(AIS) data for a reference vessel to establish an applicable operating profile for the design model. The operating profile for the reference vessel ANL BAREGA was obtained from a study carried out in parallel, which has the objective of analyzing AIS data for the global fleet to identify the fuel savings from being able to reconfigure the bulb during transit. The second stage of the design cycle consists of an optimization procedure of

the flexible bulb geometry, with respect to reduction in the weighted effective power over the operating profile.

The optimization of the flexible bulb configuration is a process which is divided into four separate parts. Firstly, the length, breadth and height parameters of the bulb geometry is parametrized with the use of parametric B-spline curves and surfaces. Parameterization with B-spline curves and surfaces hold the desired ability to morph the bulb geometry in an effective and efficient manner while retaining the typical bulb shape, with the movement of a set of control points on the bulb surface. The parameterization is derived and implemented within the workbench of the CAESES framework. The second part constitutes a search of the design space to identify the influence of the design parameters on the wave resistance for the various speeds in the operating profile. Furthermore, this part will establish a set of flexible bulb geometry candidates to be studied later in the optimization procedure. The third part of the optimization procedure is to establish a robust optimized bulb configuration with the use of a particle swarm optimization algorithm implemented in MATLAB. This bulb design will be used as reference for the flexible bulb, since it is industry standard. The last part consists of evaluating the flexible bulb candidates with a change in the length parameter. The performance of the flexible bulb configurations and the robust bulb configuration are compared establish the potential of flexibility in the bulb design.

To validate the design method and estimates the value of having a reconfigurable bulb, a case study on the KRISO container ship(KCS) coupled with the operating profile of the comparable container ship ANL BAREGA is presented. The results from the case study indicated a clear trend which states that the potential of flexibility in the bulb design is largely governed by the breadth parameter in the lower to mid speed regime, while in the higher speed regime the length parameter is the governing factor. As a result, the best flexible bulb configuration yielded a reduction in the weighted effective power of 0.22%. The reduction is too small to account for the assumed affiliated additional costs, leaving limited incentives for such a configuration to be implemented in ship design.

Sammendrag

Med varierende drivstoffkostnader og press fra reglene til den Internasjonale Maritime Organisasjon(IMO) sitt Energi Effektive Design Indeks (EEDI) angående CO_2-utslipp, har nye økonomiske og miljøvennlige teknologier blitt en integrert del av skipsdesign. Skip i dag står overfor et bredt spekter av operasjonsprofiler, da de må ta på seg et bredt spekter av frakter, og ett aspekt av dette er variasjon i seilingshastigheter. Variasjonen i operasjonsprofilet på grunn av både lange og kortsiktige effekter i verdensøkonomien åpner et uutnyttet potensial for ytterligere drivstoffbesparelser ved å innføre en fleksibel bulb som kan adaptere til forandringene i operasjonsprofilene i sann tid. Denne oppgaven tar sikte på å undersøke verdien av bulber som kan rekonfigurere lengden under seiling fra et hydrodynamisk synspunkt.

Å utstyre containerskip med bulber for å redusere skrogets totale motstand, er vanlig praksis. Selv om bulbene er forskjellige med hensyn til form og størrelse for de forskjellige skipssegmentene, er det primære målet å redusere skipets bølgemotstand ved å generere en bølge som interfererer med bølgen som genereres av skroget, noe som resulterer i en reduksjon av bølgemotstanden. Rederier verden over har reagert på hvordan skipets hastighet korrelerer med tilstanden i verdensøkonomien, og en reaksjon av dette har vært å designe bulben for et bredere spekter av driftsforhold. Denne designstrategien er kjent som robust design, og er i hovedsak suboptimal for hvert hastighetsscenario, men basert på de ulike operasjonsprofilene som skipene står overfor, er strategien bedre enn å optimalisere bulben for en fast servicehastighet. Innføringen av fleksibilitet bulb designet er en aktiv metode for å skape verdier, i motsetning til en standard passiv robust designtilnærming.

Storskala effekter som bølgedannelsen til skipet er for det meste upåvirket av viskøse effekter, og dette støtter bruken av en panelkode for å beregne bølgemotstanden. Ved å evaluere forskjellen i bølgemotstanden for de forskjellige lengdekonfigurasjonene av den fleksible bulben, kan potensialet for en slik anordning angis. panelkoden SHIPFLOW brukes til å rangere de forskjellige bulb konfigurasjonene med hensyn på bølgemotstanden.

Designprosedyren til den fleksible bulben er delt i to trinn. Det første trinnet er å analysere data fra automatisk identifiseringssystem (AIS) for et referansefartøy for å etablere en aktuell driftsprofil for designmodellen. Driftsprofilen for referansefartøyet ANL BAREGA ble hentet fra en parallellstudie som har til formål å analysere AIS-data for den globale flåten for å identifisere drivstoffbesparelsene ved å kunne rekonfigurere bulben under seiling. Den andre fasen av designprosedyren består av en optimaliseringsprosedyre for den fleksible bulbgeometrien, med

hensyn på reduksjon i den vektede effektive ytelsen over operasjonsprofilet.

Optimaliseringen av den fleksible bulbkonfigurasjonen er en prosess som er delt inn i fire separate deler. Først parameteriseres lengden, bredden og høydeparameteren til bulbgeometrien ved bruk av parametriske B-spline kurver og overflater. Parameterisering med B-spline kurver og overflater innehar de ønskede muligheten til å endre bulbgeometrien på en effektiv måte mens den typiske bulbgeometrien er beholdt, ved å flytte på et sett av kontrollpunkter på bulboverflaten. Parameteriseringen er utført og implementert i programmet CAESES. Den andre delen utgjør et søk i designrommet for å identifisere påvirkning av designparametrene på bølgemotstanden for de forskjellige hastighetene i operasjonsprofilet. Videre vil denne delen også etablere et sett med fleksible bulbgeometrikandidater som skal studeres senere i optimaliseringsprosedyren. Den tredje delen av optimaliseringsprosedyren er å etablere en robust optimalisert bulbkonfigurasjon, som vil bli brukt som referanse, da denne bulbkonfigurasjonen er industristandard. Den siste delen består av å evaluere de fleksible bulbkandidatene med en endring i lengdeparameteren. De fleksible bulbkonfigurasjonene og den robuste bulbkonfigurasjonen blir sammenlignet for å etablere nytteeffekten av den fleksible bulben

For å validere designmetoden samt å etablere potensialet av fleksibilitet i bulbdesignet, presenteres et case-studie på KRISO-containerskipet (KCS) kombinert med driftsprofilen til det lignende containerskipet ANL BAREGA. Resultatene fra casestudien indikerte en klar trend som fastslår at potensialet for fleksibilitet i bulbdesignet i stor grad styres av breddeparameteren i det nedre til midterste hastighetsregimet, mens i DET høyere hastighetsregimet er lengdeparameteren den styrende faktoren. Som et resultat av dette ga den beste fleksible bulbkonfigurasjonen en reduksjon i den vektede effektive ytelsen på $0,22\%$. Reduksjonen i ytelse for den fleksible bulbkonfigurasjonen er for liten i forhold til de antatte tilknyttede tilleggskostnadene ved implementering av fleksibilitet i bulbdesign for skip.

Contents

List of Figures

List of Tables

Chapter 1

Introduction

1.1 Background

The International Maritime Organizations(IMO) Energy Efficient Design Index(EEDI), is prompting the use of more energy efficient and less polluting hull and machinery configurations. New ship design needs to meet the minimum criteria for energy efficiency level per capacity mile for the given ship type and size segment. In the future the minimum criteria is thought to be tightened, in order to drive the innovation and technological development IMO (2016).

Globally, approximately 90% of the world's trade is transported by ship, and accordingly the shipping industry has a major role to play on ensuring that the world's fleet are able to comply with the new EEDI regulations. With the varying fuel costs and the pressure from IMOs strict EEDI regulations regarding CO_2 emissions, new economical and environmentally-friendly technologies are becoming an integral part of ship design. There is pressure on the ship owners to push innovative technologies that will minimize both production costs and running costs, and these new technologies must be considered both at the retrofit stage as well as the new-build stage. As a consequence, there is a lot of on-going research into energy saving devices(ESDs) for ships. ESDs are defined as flow directing, hydrodynamic devices intended to reduce the energy losses around the propeller Kim et al. (2015). The various ESDs available on the marked today differs substantially in their working principles and they concern different parts of the ship. However, the main objective of the ESDs is to increase the propulsive efficiency, reduce the resistance or a combination of both simultaneously. This thesis will concern around the improvement of the hydrodynamic performance of the bulbous bow.

1

1.1.1 Variations in the Operating Conditions

Vessels today face a broad spectrum of operating conditions, as they have to take on a broad variety of trades, and one aspect of this is variation in speed. Speed variations may occur on a trip-to-trip basis, or on longer time scales. An example of the latter is container ships that over the last years have seen large reductions in operating speeds - known as slow steaming Grey (2014). Slow steaming is simply the term for ships steaming at lower engine speeds, and because fuel consumption is roughly proportional to sailing speed to the power of three, reduction in speed results in a significant reduction in fuel expenses, at the cost of time of the given trade. Slow steaming was initially introduced as a reaction to the rapidly rising fuel prices in 2007, and later established by the lowering of trade volumes and freight rates as a result of the financial crisis in 2008. Naturally, slow steaming affected the vessel segment which operates in the higher Froude regimes hardest, and the change in speed for container ships has drawn a lot of attention. In the case study done by Olav (2016), represented in figure 1.1a and 1.1b it is evident that the operating profile of a 8500 TEU container vessel have changed drastically from a narrow operating profile with a mean sailing speed of $23[kn]$ in 2008 to a broad operating profile ranging from $11[kn]$ to $21[kn]$ in 2013 as a result of the slow steaming profile. As seen in the latter figure 1.1b, the operating profile of the vessel is concentrated far away from the initial design point, leading to suboptimal ship design for the current oprating profile.

(a)   (b)
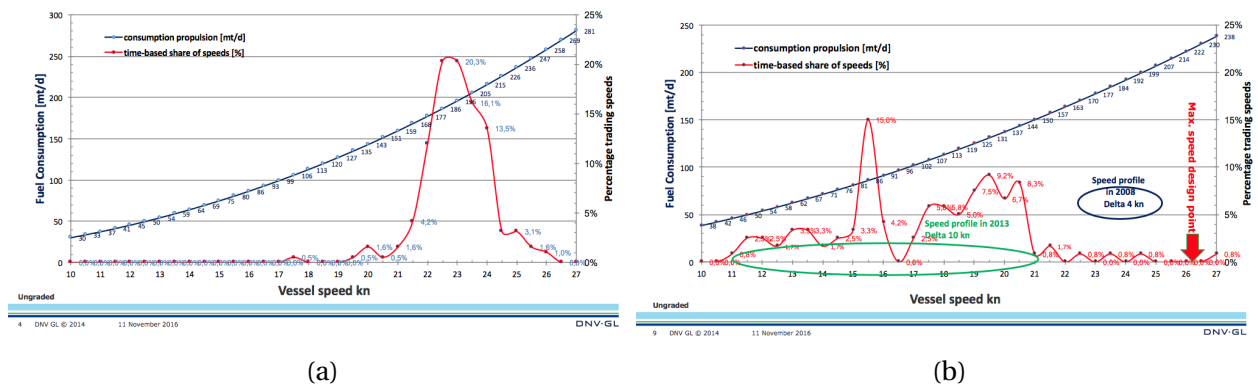
Figure 1.1: Breakdown of the operational profile of a container ship with respect to speed and fuel consumption during the time period 2008 to 2013.

As a consequence of slow steaming, container ships designed and built before 2008 have been designed for service speeds which are no longer relevant. As a result of the non-optimal designs, ship owners have started to replace bulbous bows and propellers with bulbs and propellers designed for the new speed and loading regimes, known as retrofit projects. Maersk conducted the first retrofit project in 2012, and had claimed potential fuel savings of 20 % Maersk (2013). Due

to the potential fuel saving of such a project, and thus the short payback period, retrofit projects are done extensively on container vessels. DNV GL have been involved with approximately 150 retrofit projects for container ships, and reports a payback period of approximately 12 months; assuming an investment cost of $600,000\ USD$, a bunker price of $600\ USD$ per tonnes and a six percent reduction in bunker consumption DNVGL (2016). Additionally, even without big events like the finical crisis, the process of designing performance with respect to one operating condition is outdated. Research done by Røe (2010) indicates that merchant vessels only operate at the design condition for a small amount of time. The variation in operating conditions due to both long and short term effects opens up an untapped potential for further fuel savings, by introducing a flexible bulb that could adopt to the operating conditions in real time.

1.1.2   State of the Art Bulbous Bow Design

Shipbuilders and shipyards produce vessels that meets draft, speed and fuel consumption specifications in calm water for specific design conditions. This implies that the vessels are designed to have superior hydrodynamic performance under the specified operating condition. Vessels are either designed and optimized for one specific operating condition, with superior hydrodynamic performance properties at this one condition, or they are optimized for a limited range of operating conditions, with slightly reduced hydrodynamic performance properties for the specified operating conditions compared to the point based design, but experience an overall improvement when the operating profile is considered. The design and optimization of the bulbous bow follows the same design procedure, either a design for a single operating condition, or a robust design for a small range of operating conditions. Due to the complexity of the bulbous bow and how it affects the different resistance components, it is difficult to design the geometry of the bulb for more than one draft and speed condition. Today the common practice in bulb design, is to adopt the bulb shape of ships with similar features in terms of geometry and operating profile, and use this a starting point in the design process. Sophisticated calculation methods such as computational fluid dynamics(CFD) and computer aided parametric modelling provide the possibilities of testing several bulb designs at a low cost, and is often used to optimize the bulb performance. Although CFD methods have gained foothold in the shipbuilding industry, the use of CFD codes requires a skilled user in order to evaluate and validate the results.

1.1.3 The Value of Flexibility

The concept of flexibility in engineering design can be described as a method of handling uncertainties. The flexibility, also described as changeability, constitutes the ability of a system to alter its form and therefore its function at an acceptable expenditure Rehn (2015). The introduction of flexibility in the bulbous bow design enables the bulb to take advantage of the change in the operating profile and therefore minimize the potential downside risks of a change in the operating profile. However, with the addition of flexibility in the design, there will always be an affiliated extra cost. As a means to evaluate the respectable affiliated extra cost of introducing flexibility to the bulb design, the potential savings of such a device in therms of resistance reduction, and subsequently the fuel consumption, needs to be established.

1.1.4 The General Idea of a Flexible Bulb
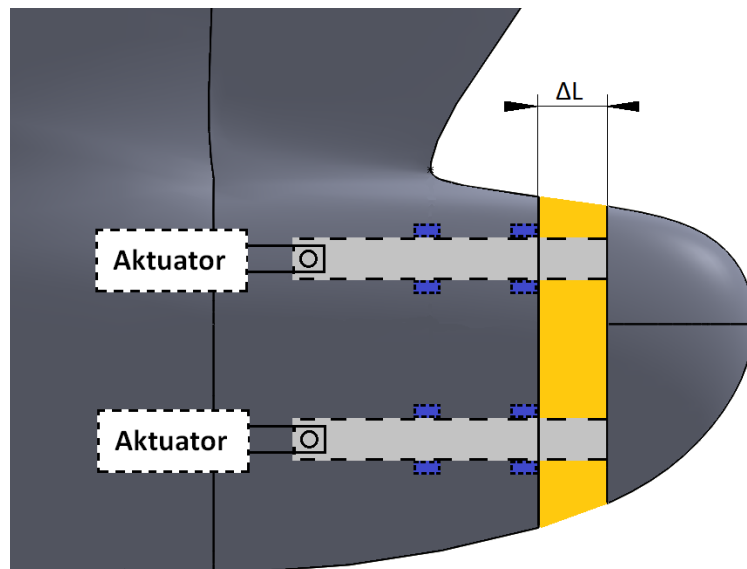
Figure 1.2: Illustrative figure describing the concept of the flexible bulb design Bang et al. (2017).

Figure 1.2 illustrates a general idea of how the flexible bulb will work in practice, and aims to provide an understanding of the concept. It is thought that the bulb will have the ability to change a set of the main parameters(e.g. the length as seen in figure 1.2) during operation. This theses aims to investigate the potential savings of fuel consumption by introducing a flexible bulb to ship design. From an engineering standpoint, knowledge of the potential savings, in terms of reduced operating costs, by introducing flexibility in the bulb design is valuable input

for the next stage of the design of the flexible bulb, namely the structural. The balance between the additional extra costs of the structural design of the flexible bulb compared to a robust bulb design, and the possible reduction of operating costs by introducing the flexible bulb design compared to the robust bulb design will establish the payback period. Given that the structural design of the flexible bulb is feasible, the factors mentioned above will constitute if the flexible bulb design is in fact profitable.

1.2 Objectives

The main objectives of this thesis can be summarized by the following:

1. Establish the working principles of the bulbous bow and how it affects the different hydrodynamic characteristics of the ship through a literature study.

2. Study the background, theory and limitations of potential flow code SHIPFLOW. This includes validating the resistance calculations with a comparable potential flow code.

3. Find a suitable method for parameterizing the bulb geometry to be aggregated towards flow simulations with SHIPFLOW.

4. Analyze the effect on resistance due to a change in the bulb geometry.

5. Propose a suitable and efficient method for a design procedure of the flexible bulb configuration.

6. Conduct a case study on a suitable vessel to establish the value of having a flexible bulb.

1.3 Limitations

The study of the flexible bulbous bow configuration in this thesis is only assessing the hydrodynamic aspect of having such a flexible bulb available. The structural design of the flexible bulb is outside the scope of this thesis, as it evolves around a complete different engineering discipline, and will therefore not be a subject of study in this thesis.

The resistance characteristics of the vessel is mostly dependent on speed. The variation of the operating profile for container vessels also see a large variance in draft and trim angle, which also have an impact on the resistance characteristics. However, the only reliable dynamic data

included in AIS messages is speed and position, therefore the analysis of the flexible bulb is only concerned around the variation in speed.

The complexity of the design of the flexible bulb configuration introduces a large design space concerning several separate optimization procedures with a large amount of design and input parameters, presenting a computationally demanding task. To keep the optimization process within the time constraints of the thesis input variables such as the draft condition, and design parameters such as the height of the bulb were excluded from parts of the optimization procedure. Naturally, this imposes limitations of the design model.

1.4 Structure of the Report

The rest of the report is structured as follows.

Chapter 2 gives an introduction to ship resistance and the purpose bulbous bow has in this context. It provides a taxonomy of bulbous bows, based on different operational conditions and requirements. This chapter is largely based on the project thesis and is written in cooperation with stud. techn. Jon Hovem Leonhardsen.

Chapter 3 Evaluates the state-of-the-art-methods for resistance calculations for ships, and when they are suited. Additionally, the background, theory and limitations of potential flow code SHIPFLOW is presented.

Chapter 4 aims to validate the potential flow code SHIPFLOW for further work in the thesis. Comparisons with the potential flow code ShipX WaveRes as well as experimental data is evaluated.

Chapter 5 is devoted to provide an understanding of parametric design for engineering problems. This includes a literature study of the current state-of-the-art modeling features and optimization processes. Moreover, a description of how the parameterization of the bulb geometry is modelled in the CAESES framework is explained.

Chapter 6 presents a design procedure for the flexible bulb geometry. The different optimization procedures within the design procedure are discussed and explained. In addition, the chapter presents the input data for the case study.

Chapter 7 presents the results form the case study, and chapter 8 is concerned around the discussion of the results and findings of the from the case study as well as the methodology used to

find them.

Chapter 9 presents the conclusion of the thesis, and give recommendations for further work.

Chapter 2

System Description - Resistance and Bulbous Bows

In order to understand the bulbous bow and when it is beneficial, it is important to understand the breakdown of the ship resistance. This chapter will address the ship resistance components, the bulb's purpose in this context, and describe how different operating conditions call for different bulb designs. The following sections are written in cooperation with stud. techn. Jon Hovem Leonhardsen.

2.1 Resistance

The resistance forces acting on a ship moving through water can be divided into two main components; pressure force and shear force. The pressure force is acting in a direction normal to the surface of the body, and is mainly caused by the wave making of the hull. The shear force, often referred to as viscous resistance, is acting tangentially to the surface, that is, in the direction of the local relative fluid motion. This force is caused by the friction between the fluid and the body. In ship resistance theory, a common simplification is to divide the total resistance into wave making resistance and viscous resistance, under the assumption that these components are independent of each other (Steen, 2011).

2.1.1   Resistance Components

The following section will elaborate the resistance components, as presented by Steen (2011). The wave resistance is a significant component to the total resistance of the ship. The wave generation of the hull moving through the water is a result of the pressure difference induced by the free surface effects. It is common to assume that the pressure resistance and the wave resistance of the ship are equal, although viscous effects such as flow separation will create pressure resistance, called viscous pressure resistance. For ships, the viscous pressure resistance is usually small compared to the wave resistance, and is therefore studied separately. The wave resistance can be described with a hull moving through water. As the hull moves through water, the volume displacement alters the velocity along the hull. At the forward part of the hull, the water is forced outwards, and at the aft, it flows back towards the centre line of the ship. Bernoulli's equation describes the wave making

$$\frac{\rho}{2}v^2 + \rho g z + p = constant \tag{2.1}$$

Here, ρ is the water density, v is the flow velocity along the hull, g is the gravitational acceleration, z is the surface elevation and p is the atmospheric pressure. The velocity of the flow around the ship hull will be retarded and accelerated in the bow and after body respectively. This will lead to a change in the free surface elevation, as the pressure at the surface has to be equal to the atmospheric pressure. The velocity around the ship will increase towards the middle of the ship, and the same physical phenomena results in a change in wave elevation along the hull.

A typical distribution of the resistance components as a function of Froudes number F_N is shown in figure 2.1[1]. Froudes number is a dimensionless ratio of the flow velocity, i.e. the ship speed, to the ship length, given by $F_N = \frac{v}{\sqrt{gL}}$. The figure is only illustrative, and aims to provide an understanding of how the main resistance components vary as a function of speed.

---

[1]Simplified sketch based on resistance breakdown presented by Steen (2011)
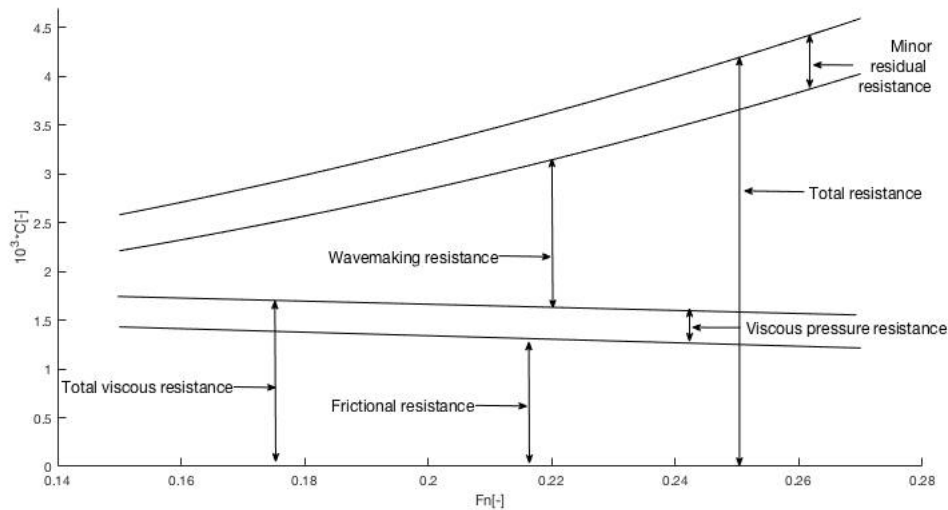
Figure 2.1: Resistance breakdown as function of Fn[-].

2.1.2 Reduction of Total Resistance

To improve the hydrodynamic performance of the vessel, a typical approach is often to min-imise the total resistance of the ship. There are several energy saving devices that can improve a vessel's hydrodynamic features in order to reduce the total resistance, and ultimately minimis-ing the vessel's energy consumption. The different energy saving devises vary broadly in terms of their working principals and claimed energy savings. That being said, the typical way to im-prove the hydrodynamic characteristics is to investigate the influence of the key hydrodynamic aspects such as the fore and aft shoulders, the stern shape, the bulbous bow, flow alternating devices such as propellers and form parameters etc.(Grech La Rosa et al., 2015).

Since the different hydrodynamic aspects affect the performance of the vessel and the resistance component in different ways, obtaining an optimal design is a difficult task. Nonetheless, some of these aspects is possible to asses within a certain set of constraints to obtain an improved overall hydrodynamic performance. To improve the hull's resistance characteristics, a bulbous bow can be fitted to the forward part of the hull. The primary aim of the bulb is to generate a wave forward of the vessel, with the purpose of minimizing the waves propagating down the length of the hull. This would occur by the principle of destructive interference when the waves interact. The superposition of the two wave contributions which may result in destructive inter-ference of the bow wave, and the wave generated by the bulb is described by figure 2.2 [2].

---

[2]https://en.wikipedia.org/wiki/Bulbous_bow#/media/File:Bulbous_Bow_NT.PNG
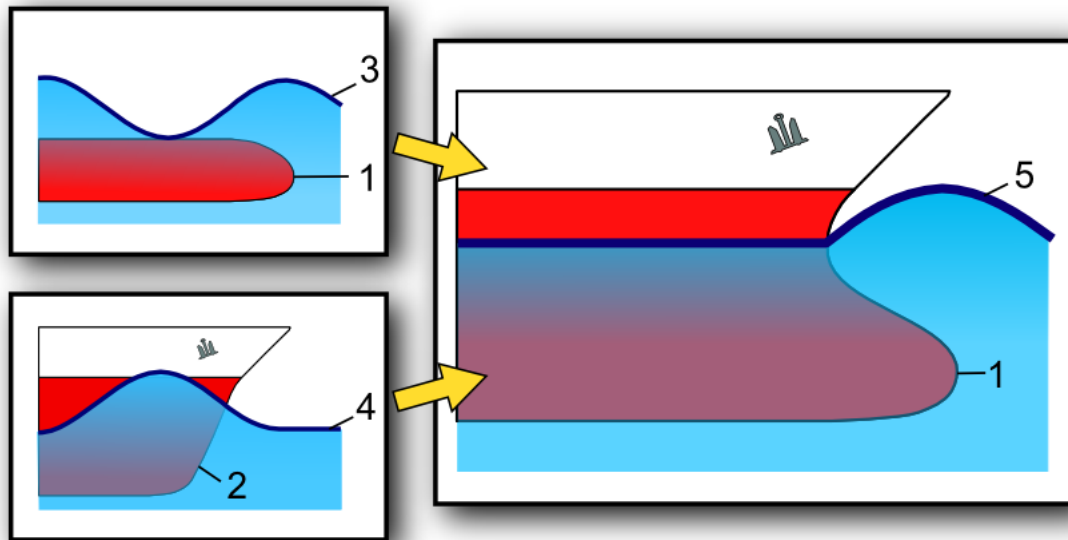
Figure 2.2: An illustrative figure of how the superposition of the waves generated by the bulb and bow may cause a reduction of the propagating wave down the length of the hull.

As seen in figure 2.2, the small bulb(1) placed in front of the main bow the hull generates its own wave system(3). The ship hull(2) generates a separate wave system(4). If these two wave generating components are carefully arranged, the through of the bulb's wave system will align with the crest of the main bow wave. As a result, the bow wave(5) is partially canceled, leading to recovery of the initially lost energy. The interaction affects the wave making resistant component, which becomes more dominating as the ship's velocity increases as shown in figure 2.1.

In addition to influencing the hull's wave system, bulbous bows also affect the frictional resistance. The additional wetted surface of the body introduced by the bulb, will always increase the frictional resistance, which is the biggest contributor to the viscous resistance. The introduction of the bulb will in some cases improve the fairing around the forebody, and thus change the hull's viscous pressure field, which can reduce the viscous resistance. For full, slow ships the reduction of viscous resistance due to the smoothing of the fore body can take presence over the wave canceling effects of the bulb. Kracht (1978)

Calm Water Conditions and Added Resistance.

In real operating conditions, the presence of waves will have an effect of the resistance of the ship, also known as added resistance. The methods of calculating the added resistance in waves of a ship are often complex, and the validity of the methods results is often insufficient for var-

ious ship types. The common practice of predicting the added resistance is to evaluate the increase in power due to the waves for similar ships sailing the same route. As a result, a sea margin, often 15–30% of the ship calm water resistance, is added at the design stage Arribas (2007).

Bulbous bows are in general designed assuming calm water conditions, which in reality is rarely not the case. However, the effect of waves on the hydrodynamic performance of the bulb varies for vessels in terms of their shape and operational profile as described by Blume and Kracht (1985): **"As a rule, for fast ships with low block coefficient and pronounced wavemaking, the thrust increases very strongly at very low wave steepnesses while for slow ships with high block coefficient and pronounced wavebreaking, this increase in thrust is less."**

Bearing this in mind, this thesis will follow the assumption that the the effect of waves on the hydrodynamic properties of the hull is largely based on the vessel type, and the sea sate of the sailing route, and not by small changes in the bulb geometry. The connection of the presence of the bulbous bow and the added resistance of the ship is outside the scope of this thesis, and will not be investigated further.

2.2 Geometry of Bulbous Bows

Like for a ship, describing the form and geometry of the bulb with simple parameters is not an easy task, as the curvatures are complex and intersect each other. The shape of the cross section of the bulb at the forward perpendicular (FP) can roughly be divided into three different categories. They are named after their geometric shape, divided into the Δ-type, the O-type, and the ∇-type. Table 2.1 offers a description of the different types, and figure 2.3 presents a visualization of the cross section for the different the bulb types.

Table 2.1: Description of bulb-types.

Type	Description
Δ-Type	The delta-type features a drop shaped sectional area, with center of gravity positioned in the lower half part of the bulb. The volume is concentrated near the base of the the bulb.
O-Type	A bulb with an oval cross-section, with center of gravity and volume concentration positioned in the centre of the bulb.
∇-Type	The nabla-type is similar, but opposite to the delta-type, with a drop shaped sectional area, with center of gravity positioned in the upper half part of the bulb close to the free surface. The volume is concentrated near the free surface of the the bulb.
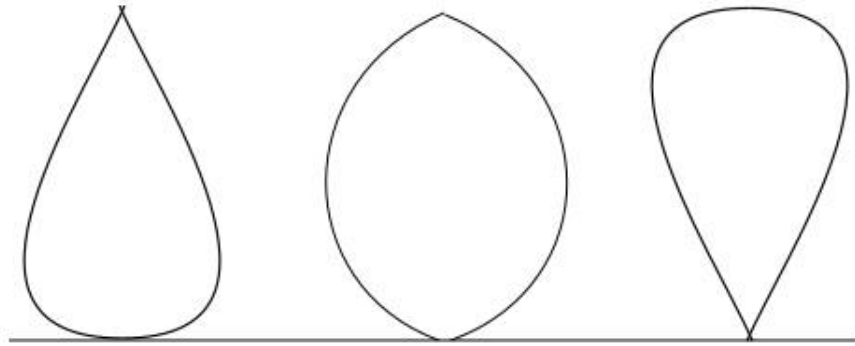
Figure 2.3: Bulb types.

2.2.1 Parameters and Dimensions of the Bulbous Bow
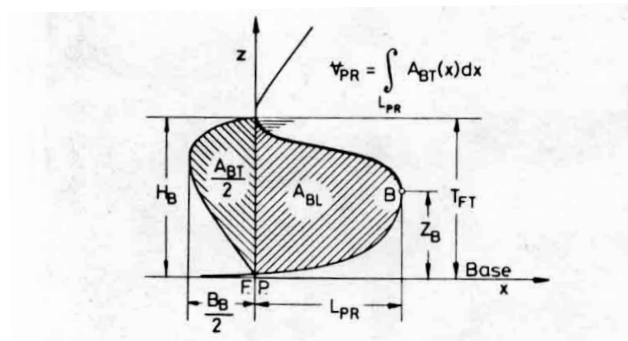
Figure 2.4: Linear and nonlinear bulb parameters.

In order to describe the shape of the specific bulb form, quantitative bulb parameters is nec-

essary. As described by (Kracht, 1978) the bulbous bow can be described with three linear, and three nonlinear dimensionless quantitative parameter normalized by the main dimensions of the ship. The parameters of the bulb is illustrated in figure 2.4.The three linear bulb parameters are:

The breadth parameter is described by the maximum breadth(B_B) of the bulb cross-section at FP, divided by the beam of the ship(B_{MS})

$$C_{BB} = \frac{B_B}{B_{MS}} \tag{2.2}$$

The length parameter is described by the protruding length(L_{PR}) of the bulb, divided by the the length between the perpendiculars of the ship(L_{PP}).

$$C_{LPR} = \frac{L_{PR}}{L_{PP}} \tag{2.3}$$

The depth parameter is described by the height(Z_B) of over the base line at the foremost point of the bulb, divided by the draft (T_{FP}) of the ship at FP.

$$C_{ZB} = \frac{Z_B}{T_{FP}} \tag{2.4}$$

The non-linear bulb parameters are:

The cross-section parameter, which described the cross-sectional area A_{BT} of the bulbous bow at the FP, devided by the midship-section area A_{MS} of the ship

$$C_{ABT} = \frac{A_{BT}}{A_{MS}} \tag{2.5}$$

The lateral parameter, which describes the area of ram bow A_{BL} in the longitudinal plane, divided by A_{MS}.

$$C_{ABL} = \frac{A_{BL}}{A_{MS}} \tag{2.6}$$

The volumetric parameter, which describes the volume ∇_{PR} of the protruding part of the bulb, divided by the volume displacement ∇_{WL} of the ship

$$C_{\nabla PR} = \frac{\nabla_{PR}}{\nabla_{WL}} \tag{2.7}$$

The parameters listed in equation 2.2 to 2.7 gives a description of the bulb shape and geometry that is sufficient to provide a general representation of the bulb.

2.2.2 Influence of the Bulb Parameters on the Hydrodynamic Effect of the Bulb

According to linearized wave theory, the addition of a bulb to the hull is considered to be a interference problem of the free wave system of the ship and the bulb. The phase of the bulb wave is manly determined by the position of the bulb body, while the amplitude of the bulb wave is related to the volume of the bulb. As a consequence of this, the phase difference and amplitude of the interfering free wave systems may cause a cancellation Kracht (1978).

Effect of the Volume

The volumetric coefficient $C_{\nabla PR}$ of the bulb is linked to the amplitude of the wave pattern. With an increase in the bulb volume, the amplitude of the wave pattern created by the bulb will increase. As the volume of the bulb is affected by the breadth C_{BB} and the cross section C_{ABT} parameter, these parameters will affect the interfering wave system in a similar way.

Effect of the Length

The length parameter C_{LPR} of the bulb is a key factor of the phase relation of the interfering bulb-ship free wave system. Of all the parameters describing the bulb, the length parameter has the greatest influence on the interference effect of the bulb and ship wave system. The lateral parameter C_{ABL} is strongly related to the length parameter, and will accordingly affect the bulb-ship free wave system in a similar manner.

Effect of the Depth

The depth parameter C_{ZB} influences the interference effect, and it can be described by linear wave theory. If the centre of the bulb is positioned in the water surface, the effect of the bulb would be negative, with added resistance. A lowering of the position from the water surface down to the deepest point of the vessel would show an increase in the interference effect until a maximum, and by lowering it further the effect would go to zero.

2.2.3 Seakeeping and Maneuverability

In general, with regards to seakeeping and maneuverability, there are little to non side effects to fitting the ship with a bulbous bow, compared to the contrary. Classic maneuverability tests such as the overshoot angle and zigzag tests show no significant difference when comparing ships with and without a bulb(Kracht, 1978). Most bulb designs for new vessels is designed with a ∇-characteristic, with emphasis on seakeeping problems such as slamming and pitch-motion. In fact, the bulb reduces the pitch motion of the ship due to its higher damping. In conclusion , further investigation on the influence of the bulb parameters on the hydrodynamical aspects of the ship will be concentrated on the reduction of resistance.

2.3 Taxonomy of Bulbous Bows

The operational requirements and profile are important factors in the design stage of a vessel. The following sections will adapt some of the notation of Grech La Rosa et al. (2015) and describe the standard geometry of bulbous bows for different combinations of displacement and Froude number regimes.
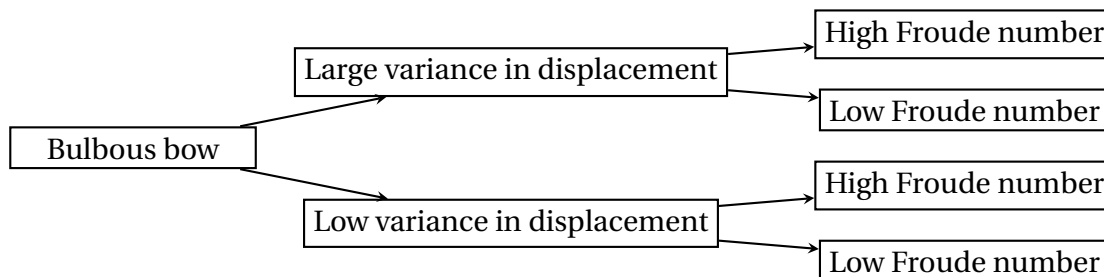
Figure 2.5: Breakdown of operational profiles.

Large Variance in Displacement and High Froude Number

For vessels operating in high speed regimes, wave making will be the dominating resistance component. The length of the bulb is correlated to the speed regime, and ships with high operational speeds are generally fitted with long protruding bulbs. This is because the length of a bulb is roughly proportional to its internal volume, meaning that small increments in length will increase the potential of the wave generated, in addition to manipulating the phase of the wave.

As a consequence of this, the resulting wave will lead to increased resistance should the vessel sail at lower speeds thus generating waves that will interact in a suboptimal way.

Figure 2.6: Bulb design, container vessel.

Large variance in displacement makes it hard to control the bulb's depth beneath the waterline. In order to account for this, the bulbs fitted on vessels with such operating profiles are generally of large height. However, different displacements will lead to different waves generated by the bulbous bow, and it is clear that bulbous bows fitted on vessels operating in high speed regimes with large variance in displacement are optimised for selected conditions, and not for the whole operational range. Examples of vessels facing such operational requirements are container and RoRo (Roll On Roll Off) vessels, and figure 2.6 shows a typical bulb for a container vessel.

Large variance in displacement and low Froude number

For vessels operating with large variance in draught and in the lower speed regime, typically tankers and bulk carriers, the viscous resistance component is dominant. They are generally fitted with short and deep bulbs, as the main purpose is to improve the viscous characteristics, and not the wave making. The viscous characteristics are improved by extending the waterline, which will be constant for a large range of draughts

Figure 2.7: Bulb design, tanker.

because of the large height of the bulb. This means that the bulbs are optimised for a wider range of operating profiles. Figure 2.7 shows a typical bulb for a tanker.

Low variance in displacement and high Froude number

For vessels operating with relatively fixed draught and high speed, the purpose of the bulb is solely to generate an independent wave to interact with the wave generated by the hull. As for the large variance in displacement and high Froude number case, the bulbs are optimised for a limited range of operating speeds. Cruise vessels and ferries are examples of vessels operating within this category.

Low variance in displacement and low Froude number

Vessels operating with low variance in displacement and in low Froude regimes are in general not fitted with bulbous bows.

2.4 Defining the System

As section 2.3 showed, bulb design depends heavily on the operating conditions or requirements the ship in question is exposed to. Optimal bulb geometry varies across different operating conditions, hence, the design of bulbs is closely attached to analyses of operating profiles. Especially for this project, for which the idea was based on the hypothesis that operating conditions vary significantly, it is important to couple bulb design with analyses of the operating environment. Thus, the system subject for investigation in this project includes both the physical bulb itself, and the operating environment in which the bulb is intended to function.

Flexible bulb design

From the classification of the various bulb designs and their typical operational profile, it is clear that container ships have a large potential for reduction of resistance due to their large variance in both Froude number and displacement in the operational profile. The length of the bulb strongly influence the phase of the wave generated by the bulb, and the phase of the wave generated by the ship is strongly influenced by the speed of the ship. With a flexible bulb that could change the length(L_{PR}), the operational time with a bulb that produces a wave without a bow wave from the ship to interact with, and thus an increase in the resistance, can be significantly reduced. An increase in length has minimal impact on the main particulars of the vessel, including the displacement, while it can significantly change the wave making resistance, suggesting that the the length can be studied separately. In addition, it is clear that the bulbs influence on the resistance is manly concerned around the reduction of wave resistance, and subsequently, this will be the main focus in the resistance calculations in this report.

Chapter 3

Prediction of Wave Resistance

As discussed in chapter 2, the main goal of the bulb is to reduce the wave resistance of the ship, and subsequently it is important to establish a suitable method to calculate the wave resistance of ships to be used later in this thesis. This chapter will discuss the different state of the art methods for resistance calculations for ships, and when they are beneficial. Secondly this chapter concludes on the particular method and software to used for resistance calculations later in the case study of the flexible bulb, found in chapter 6. The software and its underlying theory and assumptions will be discussed in detail. In general, there are three main methods for predicting the resistance of a ship:

1. Experimental methods

2. Empirical methods

3. Numerical methods

3.1   Experimental and Empirical Methods

The benchmark for accurate resistance prediction of the ship hull is obtained by testing the ships in model scale in towing tanks. The drawback of predicting the resistance in model scale in the towing tanks is tripartite; the scaling of the results from model scale to full scale introduces uncertainties, the cost and time it takes to produce a ship model, as well as the availability of the towing tank facilities. Due to the expense of producing the ship and bulb shape variants in model scale, this method is not considered suitable for an early stage design process, and will

not be discussed further. From series of model scale predictions for various ship types and ship dimensions, empirical formulas such as Holtroop-Mennen, Guldhammer and Harvald and Hollenbachs methods have been derived Steen (2011). These methods gives fairly good resistance predictions for an early stage design for the ship types they are intended for. However, the empirical formulas are not well suited when predicting difference in resistance for small changes in the geometry is the goal, as these factors are not taken into account.

3.2   Numerical Methods

The numerical methods that predicts the resistance of ships can be divided depending on the assumptions of the fluid. The governing equations which describes the motions of any viscous fluid or gas are the so called Navier Stokes(NS) equations. The equations arise from applying Newton's second law to fluid motion, and the assumption that the stress of the fluid is the sum of a pressure term and a diffusing viscous term. The derivation of the NS-equations can be found in a number of textbooks concerning aerodynamics and hydrodynamics, hence only the results will be mentioned in this thesis.

3.2.1   Navier Stokes Equations

Depending on the assumptions made, the NS equations are generally described by three equations all related to the conservation of a property within a control volume. The equations consists of: the conservation of mass, conservation of momentum and the balance of energy. The balance of energy is largely related to the change in temperature, and since the flow around a vessel is assumed to be of low speed, and the fluid flow is incompressible, the change in temperature will be insignificant, and the energy balance equation is therefore excluded.

Conservation Laws

The statement of the conservation of mass is achieved through the mass continuity equation describes as:

$$\frac{D\rho}{Dt} + \rho \operatorname{div} V = 0 \tag{3.1}$$

where

$$\frac{D}{Dt} = \frac{\partial}{\partial t} + u\frac{\partial}{\partial x} + v\frac{\partial}{\partial y} + w\frac{\partial}{\partial z} \tag{3.2}$$

and

$$divV = \frac{\partial u}{\partial x} + \frac{\partial v}{\partial y} + \frac{\partial w}{\partial z} \tag{3.3}$$

With the same reasoning as for the energy balance equation mentioned above, the density, ρ, is assumed to be constant, and the continuity equation reduces to:

$$divV = 0 \tag{3.4}$$

As described by Newton's laws of motion, the amount of momentum remains constant within some problem domain. The conservation of momentum is described by the NS-equation:

$$\rho\frac{Du_i}{Dt} = \rho g_i - \frac{\partial p}{\partial x_i} + \frac{\partial}{\partial x_j}\left[\mu\left(\frac{\partial u_i}{\partial x_j} + \frac{\partial u_j}{\partial x_i}\right) + \delta_{i,j}\lambda divV\right] \tag{3.5}$$

Although the viscosity of water is temperature dependent, it is assumed to be constant. With the same reasoning as for the energy conservation; the temperature difference for the fluid flow is assumed to be insignificant, thus the assumption of constant viscosity is supported. The NS equation for constant viscosity, incompressible flow reduces to:

$$\rho\frac{Du_i}{Dt} = \rho g_i - \frac{\partial p}{\partial x_i} + \mu\frac{\partial}{\partial x_j}\left(\frac{\partial u_i}{\partial x_j} + \frac{\partial u_j}{\partial x_i}\right) \tag{3.6}$$

Approximation techniques for the Navier Stokes equation

The NS equations are a set of coupled differential equations that could, in theory, be solved analytically with the use of calculus. However, the analytical solution to the equations are too difficult to obtain. In order to make use of the equations, a set of simplifications and approximations to the equations are implemented in order to solve them numerically. Numerical approximation methods like finite difference, finite volume, finite element and spectral methods are commonly coupled with the NS equations known as computational fluid dynamics (CFD) NASA (2017).

There are however, two main problems when applying CFD in hydrodynamics and the field of marine. The first problem evolves around the large Reynolds number subjected to large scale

ships which makes the flow turbulent. The smallest eddies induced by the turbulent flow are very small compared to the computational domain, which compose difficulties for the discretization. The discretization in space and time for these numerical schemes calls for an extreme amount of cells, which is not available by today's computational standards. The second problem is related to the free surface. The location of the free surface is initially unknown, which makes it impossible to satisfy the correct boundary conditions from the start. The solution to this problem is to solve a time dependent problem, where the free surface is allowed to grow from zero to a steady state solution. This solution technique is however computationally demanding Larsson and Broberg (1990).

As means to reduce the computational cost introduced by the turbulent flow, methods to model the turbulent flow is applied. The large scale effects of the mean flow is not largely affected by the smallest eddies induced by the turbulent flow. The Reynold-averaged Navier-Stokes equations(RANS) methods make use of this physical phenomena, integrating the NS equations in time and space before they are solved numerically. With this method, the eddies appear to contain quantities known as the Reynold stresses which makes for a reduction in computational cost and complexity compared to direct numerical simulation methods. For the calculations of ship motions and resistance predictions most commercial CFD codes today evolve around the RANS methods. The use of two-equation turbulence models such as the $\kappa - \omega$ models, coupled with a sophisticated grid technique and discritization of higher order are known to give results of good quality Larsson et al. (2010).

3.2.2   Euler Equations

The Euler equations are a subset of the Navier-Stokes equations, not accounting for the viscosity of the fluid, and subsequently it does not capture the viscous effects. In theory, the Euler equations could be well suited to evaluate the wave making of the ship hull, since the viscous terms reduces the complexity of the equation. However, the numerical schemes are often as time consuming as the RANS methods, and with the loss of the viscous term in the NS equation, the numerical schemes often experience dissipation and becomes unstable and is therefore not commonly used.

An alternative to the approximation of the Navier-Stokes and Euler equations, if the wave resistance is to be investigated, is the use of potential theory. Potential theory methods compared to RANS methods can be advantageous if the computational cost and time is a subject of matter.

While RANS methods typically can take up to 12 hours on a powerful computer, a potential theory solver can take between a couple of minutes to a couple of hours depending on the amount of panels on the hull and the free surface Steen (2011). This makes potential theory methods advantageous in the early stage design when the change in wave resistance and small changes in geometry are the subject of investigation.

3.2.3 Potential Theory

The dominating principle to predict the wave resistance of ship is with the use of potential flow theory. Today it is normal to divide it into two categories dependent on how the hull geometry is represented with sinks and sources.

1. Thin ship theory

2. 3-D panel methods

In thin ship theory the geometry is represented with a distribution of sinks and sources at the centerplane of the hull. This means that the distribution of the buoyancy is modeled both longitudinally and vertically. Thin ship theory has proven to be a useful calculation method for when a quick estimation of the wave resistance is needed for slender multihull configurations.

In 3-D panel methods, the sinks and sources are distributed over the wetted surface of the ship hull. The hull is then discretized into panels. Panel methods are divided into first order and higher order methods, dependent on how the source strength is allowed to vary over the panel. If the strength of the sources is constant, the method is considered to be of the first order, and if the source strength is allowed to vary the method is considered to be of higher order.

Panel methods are also classified into linear and non-linear methods, dependent on how the panelling of the free surface is defined. The linear method panels the hull up to the free surface of the hull at zero speed. For the linear methods, the paneling of the free surface is avoided by the use of Green's function. For the non-linear method, the panels needs to be defined up to the real waterline at the speed studied, as well as panelling of the free surface. The introduction of panelling of the free surface introduces more panels than for the linear method, and thus it is computationally more demanding. Since the real waterline at forward speed is unknown, an iteration procedure is required, and this is computationally challenging. Non-linear methods are known to be more accurate than linear methods. Steen (2011)

3.3   Potential Theory Solver

By applying potential theory, it is possible to predict the wave resistance of the hull without considering the viscous effects. When predicting the wave making and the wave resistance of the hull, it is possible to the evaluate the potential of the various bulb shapes on the hull. Although the bulb also will have an effect on the viscous resistance of the hull, the bulb that contributes to the lowest wave resistance will have the potential to be the most suitable bulb for the hull. In the early design stage it is of great advantage to have a numerical code that can predict the wave resistance to a satisfactory degree without the need of large computational power and time. This is especially advantageous when when evaluating different concepts with small shifts in geometry.

3.3.1   SHIPFLOW

In this thesis, the CFD software SHIPFLOW developed by FLOWTECH International AB will be used to calculate the wave resistance of the ship. The software is a product of research conducted over the last decades in close cooperation between FLOWTECH International AB, SSPA and the Naval Architecture Department at Chalmers University of Technology. SHIPFLOW promises to be an efficient and powerful tool for optimization of the forebody of ships. The strength of the program lies in the ability to rank different design modifications in combination with short computing time, and is therefore well suited for a parametric modeling optimization procedure Shipflow (2017). In the following section, the potential code used in SHIPFLOW, the underlying assumptions of the code as well as the method for solving the problem will be discussed. The underlying theory of the code, and the notation used in this chapter is manly based on the work of Janson (1996) and Mierlo (2006)

3.3.2   Non Linear Free Surface Potential Flow Code : SHIPFLOW

The potential flow code used in SHIPFLOW follows the governing assumptions of potential theory, stating that the the flow is assumed to be inviscid, irrotational, incompressible and at steady state. Only a very thin layer close to the hull surface and the wake region is dominated by viscous effects, and for the application of predicting the flow around a ship, the assumption of inviscid and irrotational flow is valid for the major part of the flow field Janson (1996). Large scale effects such as the wave making and wave pattern generated by the vessel is mostly unaffected by the

viscous effects and this supports the use of the potential flow code to evaluate the change in wave resistance and wave pattern.

Mathematical Description of the Problem

The mathematical problem consists of a ship surface, S, disturbing the uniform distributed flow-field with a constant velocity U. The axis system is defined such that the origin of the co-ordinate system moves with the ship, and is located at the undisturbed free surface at the stern. The x-axis extends through the center of the ship and the main flow direction, the y-axis extends to port, while the z-axis extends vertically upwards. The free surface is defined as $z = 0$ at the mean undisturbed waterline when the forward speed of the ship is zero.

Following the assumptions of potential theory, the NS equations 3.6 reduces to:

$$\frac{1}{2}\nabla\mathbf{V}^2 = \rho g - \nabla p \tag{3.7}$$

Under the assumption of potential flow, the irrationality of the flow field is preserved, and the velocity vector may be defined as a gradient of the velocity potential, ϕ.

$$\mathbf{V} = \nabla\phi \tag{3.8}$$

Substituted into the Bernoulli and continuity equations then yields:

$$p + \rho gz + \frac{1}{2}(\nabla\phi\nabla\phi) = const. \tag{3.9}$$

$$\nabla^2\phi = 0 \tag{3.10}$$

The continuity equation 3.4 is now governed by the Laplace equation 3.10 in the fluid region. The Laplace equation is homogeneous and linear, which allows for superposition of the total velocity potential. The decoupling of the pressure and velocity terms in equation 3.9 and 3.10 facilitates the computation of the pressure by solving the Laplace equation first then pressure later. The mathematical problem for the ship can be established by solving the Laplace equation with the specified boundary conditions:

1) The no-slip boundary condition from the NS equation at the hull surface simplifies to tangential boundary condition. The fluid particle should not penetrate the surface of the hull, and the normal velocity component on the hull surface must be zero.

$$\phi_n = 0 \tag{3.11}$$

where $_n$ is the unit normal vector.

2) For ship flow calculations, where the free surface effects are important, two additional boundary conditions must be added to the analysis. At the free surface, the velocity potential must satisfy the dynamic and the kinematic free surface conditions. Since the location of the free surface at the undisturbed waterline is defined by $\zeta(x, y)$, the effects of spray and breaking waves are not accounted for. The effects of spray and breaking waves are considered to have minor impact on the global wave pattern. The dynamic boundary condition states that the pressure at the free surface must be equal to the atmospheric pressure, meaning that the flow velocities and wave elevations expressed in Bernoulli's equation should be constant at the free surface.

$$p_a + \rho g z + \frac{1}{2}(\nabla\phi\nabla\phi) = const. \quad at \quad z = \zeta(x, y) \tag{3.12}$$

The kinematic boundary condition states that the flow velocity must be tangential to the free surface. This implies that the no particles at the free surface leaves the free surface.

$$\phi_x \zeta_x + \phi_y \zeta_y + \phi_z = 0 \quad at \quad z = \zeta(x, y) \tag{3.13}$$

The solution of the potential flow equations described above are not unique, meaning that there are several solutions existing. This is a consequence of the loss in information introduced by the reduction of the NS equations when implementing the potential flow assumptions. As a result of this, the radiation condition is included to avoid non physical solutions such as free surface waves traveling upstream of the disturbance.

Linearization of the Free Surface Boundary Condition

On the initially unknown wavy free surface, the free surface boundary conditions 3.13 and 3.12 are non linear, and must be satisfied on the free surface. The solution to this problem as suggested by Dawson (1977), is to linearize the free surface boundary conditions around a known

base flow as an estimation, and then introduce a perturbation due to the waves. This is done by dividing the velocity potential (ϕ) into a velocity potential for the perturbation(φ) and a velocity potential for the base flow (Φ).

$$\nabla\phi = \nabla\varphi + \nabla\Phi \tag{3.14}$$

$$\zeta = H + h \tag{3.15}$$

where H is the known surface elevation, and h is the estimated surface elevation. Applying the linearized free-surface boundary conditions to the dynamic and kinematic boundary condition yields the following form:

$$\Phi_x h_x + \Phi_y h_y \varphi_x H_x + \varphi_y H_y - \Phi_z - \varphi_z = 0 \tag{3.16}$$

$$\zeta = \frac{1}{2g}\left(U_\infty^2 - \Phi_x^2 - \Phi_y^2 - \Phi_z^2 - 2\Phi_x\varphi_x - 2\Phi_y\varphi_y - 2\Phi_z\varphi_z\right) \tag{3.17}$$

The boundary conditions in equation 3.16 and 3.17 have to be satisfied at the unknown free surface. The location of the wavy free surface is unknown, and as a consequence these equations are transferred to the estimated surface ($z = h$).

$$\nabla\phi_{(z=\zeta)} \approx \nabla\Phi_{(z=H)} + \nabla\varphi_{(z=H)} + h\frac{\partial\nabla\Phi}{\partial z} \tag{3.18}$$

The method of linearization suggested by Dawson (1977) neglect the transfer term, the last term in equation 3.18 as well as the higher order terms. This may lead to inconsistent linearization, but for practical applications more consistent linearization methods are known to perform equally well, and accordingly this method has proven to be sufficient. The combined linear free surface boundary condition on the known surface ($z = H$) becomes:

$$\begin{aligned}
&-\frac{1}{2g}\Phi_x\frac{\partial}{\partial x}\left(\Phi_x^2 + \Phi_y^2 + \Phi_z^2 + 2\Phi_x\varphi_x + 2\Phi_y\varphi_y + 2\Phi_z\varphi_z\right)\\
&-\frac{1}{2g}\Phi_x\frac{\partial}{\partial x}\left(\Phi_x^2 + \Phi_y^2 + \Phi_z^2 + 2\Phi_x\varphi_x + 2\Phi_y\varphi_y + 2\Phi_z\varphi_z\right)\\
&+\varphi_x H_x + \varphi_y H_y - \Phi_z - \varphi_z = 0
\end{aligned} \tag{3.19}$$

3.3.3 Method of Solution for the Free Surface Problem

There are several methods to express the velocity potentials in order to solve the Laplace equation. The method used in the SHIPFLOW code, as described by Raven (1989), is to express the velocity potentials Φ and φ by Rankine sources and dipoles distributed on the wetted surface of the body as well as the free surface. The free surface problem described in the previous subsection is solved in two steps.

Linear Free Surface Solution

The solution of the linear free surface problem starts with calculating the base solution. The base solution is found by treating the free surface as a symmetry plane. Treating the free surface as a symmetry plane implies that the submerged part of the body is mirrored above the water plane, also known as the double body solution, Φ. By the calculation of the double body, the meshing of the free surface is not included, and only body panels have to be included, which makes for an efficient solver.

When the base flow is estimated, the velocity potential for the perturbation, φ, can be solved. The free surface problem is now solved by adding the boundary conditions from equation 3.12 and 3.13 on the free surface panels. The streamlines obtained in the double body solution are used to set up the free surface grid, since these streamlines does not penetrate the hull. The solution for the perturbation is added to the base flow, and the sum of these potentials constitutes the linear free surface potential flow solution.

Non Linear Solution Method

In order to improve the accuracy of the solution, the results from the linear case are used as an estimate for the non linear solution. The hull and free surface panels are moved, and the perturbation is calculated again. This procedure iterates until a set limit of convergence is reached. The change in wave height is the governing factor for the convergence criteria. The non linear solution is known to be more accurate as it is no longer an approximation, as for the linear case. The non linear solution also takes into account the curvature of the hull at the new free surface, which often can give significant contributions.

3.3.4   Calculation of The Wave Resistance

The direct pressure integration method calculates the wave resistance by integration of the pressure on the wetted surface of the hull as seen in equation 3.20. Since the pressure on the hull consists of contributions from both the hydrodynamic pressure as well as the dynamic pressure the linear solution and the non-linear solution will have different contributions from the two pressure terms. For the linear solution, the hydrostatic pressure sums up to zero, and only the hydrodynamic pressure needs to be integrated to determine the wave resistance. For the non-linear solution the hydrostatic pressure does not cancel and both pressure terms have to be integrated to determine the wave resistance. The accuracy of the pressure integration method can be affected by the difference in pressure contributions for the linear and the non-linear solution if the number of panels at the hull surface is insufficient.

$$R_W = -\int_{S_B} Pn_1 dS \tag{3.20}$$

3.4   Calculation of Total Resistance

The wave resistance is made dimensionless and the wave resistance coefficient is defined by:

$$C_W = \frac{R_W}{\frac{1}{2} \cdot \rho \cdot U^2 \cdot S} \tag{3.21}$$

Where S is the wetted surface of the hull, the density of the water is defined as $rho = 1025[kg/m^3]$, and U is the velocity of the vessel in $[m/s]$.

The viscous resistance coefficient is calculated with the ITTC'57 formula for frictional resistance and is defined as:

$$C_F = \frac{0.075}{(log_{10}[Re] - 2)^2} \tag{3.22}$$

where Rn is the Reynolds number defined as:

$$Re = \frac{L_{WL} \cdot U}{\nu} \tag{3.23}$$

Where L_{WL} is the length of the vessel in the waterline, ν is the kinematic viscosity set to be $\nu = 1.1 \cdot 10^{-6}$ and U is the velocity if the ship in $[m/s]$.

The calculation of the total resistance coefficient C_T is obtained using equation 3.24

$$C_T = C_W + C_F(1 + k) \tag{3.24}$$

Where k is the form factor and it is computed using MARINTEKs standard formula [1]. The total resistance can then be defined as:

$$R_T = C_T \cdot \frac{1}{2} \cdot \rho \cdot V^2 \cdot S \tag{3.25}$$

[1]Steen (2011)

Chapter 4

Validation

As for all numerical schemes, there will be some simulation error defined as the difference between the truth and the simulated result. When dealing with a potential code to calculate the wave resistance of a ship hull, there will be some errors that originates from the simplifications of the potential theory as well as some numerical errors related to the refinement of the mesh. The numerical errors related to the meshing of the surface can to some point be reduced by a mesh refinement, but is constrained by the boundary conditions at the free surface not containing the effects of spray and wave breaking. In order to determine if the level of accuracy in the SHIPFLOW potential code is sufficient to carry out further investigations on the bulbous bow, some validation of the code has to be established. This chapter will firstly consider the amount of panels to be used in the grid for the hull surface as well as the free surface for future calculations. Secondly, this chapter will evaluate the validity of the SHIPFLOW potential code by comparisons with the potential code ShipX WaveRes as well as comparisons with experimental data for the KRISO container ship(KCS). On the basis of the results, the question of whether the potential code SHIPFLOW is adequate to carry out further investigations will be answered.

4.1   Grid Resolution

The number of panels distributed on both the body and the free surface will affect the accuracy of the numerical simulations. A refinement of the grid will lead to a reduction in the loss of accuracy due to the discritization error, and it is therefore desirable to represent the free surface and the hull with a sufficient amount of panels. Second order panels are used to represent the hull

33

and free surface due to their superiority compared to first order panels since the number of panels needed to represent the hull without a loss in accuracy is reduced. The objective of this thesis is to evaluate a large number of design candidates, and it is therefore of importance to keep the amount of panels to a bare minimum to reduce computational time without a substantial loss in accuracy.

4.1.1 Hull panels

To capture the effect of the large wave scales, Mierlo (2006) suggests that a minimum of 20-30 panels per wavelength in the longitudinal direction is sufficient. Since the waves generated by the ship is affected by the Froude number at which the vessel is sailing, the grid needs to be evaluated at each Froude number in the operating profile subject to investigation. The length of a wave generated by a vessel sailing at a constant Froude number is defined as follows:

$$\lambda = F_n^2 \cdot 2\pi \cdot L_{pp} \tag{4.1}$$

where F_n is the Froude number, λ is the wavelength and L_{pp} is the length of the vessel.

For the main body of the vessel to be discretized by the same resolution for the different Froude numbers in the operating profile, the number of panels are defined as a function of the Froude number as seen in equation 4.2. For the investigations in this thesis, 25 panels per wavelength are used.

$$\text{Number of panels} = 25 \cdot \frac{1}{F_n^2 \cdot 2\pi} \tag{4.2}$$

To capture the nonlinear effects which is prominent in the bow and stern region, these regions are distributed with 30 and 25 panels in the longitudinal direction respectively. In addition, the panels on the main body are stretched with a hyperbolic tangent stretching function with spacing specified to 0.025 in percentage of L_{pp} at the two ends. In the transverse direction, the number of panels are set to the default fine grid value defined in SHIPFLOW, which corresponds to 22 panels. Figure 4.1 demonstrate the grid used for the investigation of the various design candidates for the body at $F_n = 0.26$.
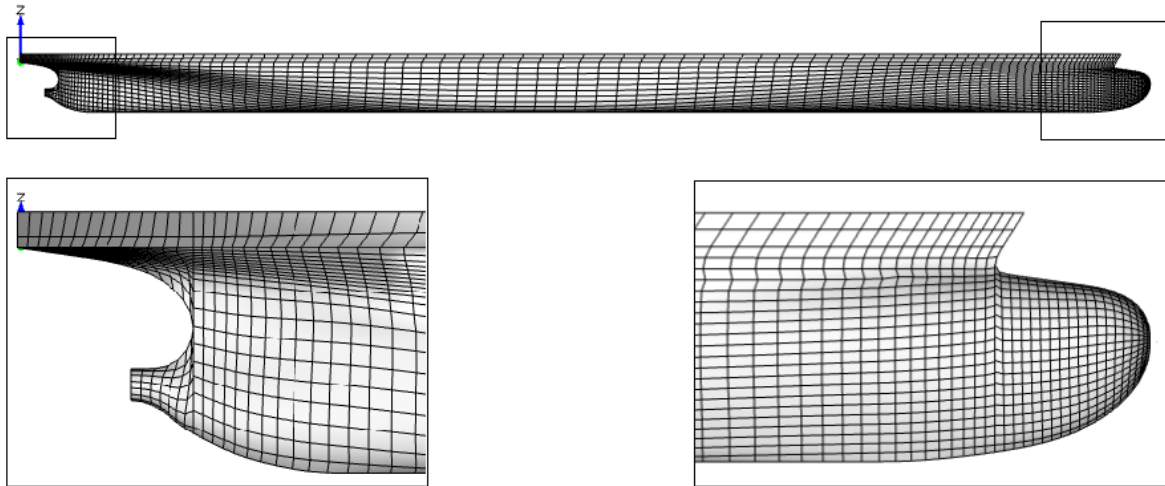
Figure 4.1: Illustration of the panel distribution on the hull surface at $F_n = 0.26$.

4.1.2 Free Surface Panels

The number of panels on the free surface is chosen on the same basis as the hull panels with 25 panels per wavelength in the longitudinal direction. The number of panels in the transverse direction is defined such that the aspect ratio stays reasonable. Figure 4.2 demonstrate the grid used for the investigation of the various design candidates for the free surface at $F_n = 0.26$.
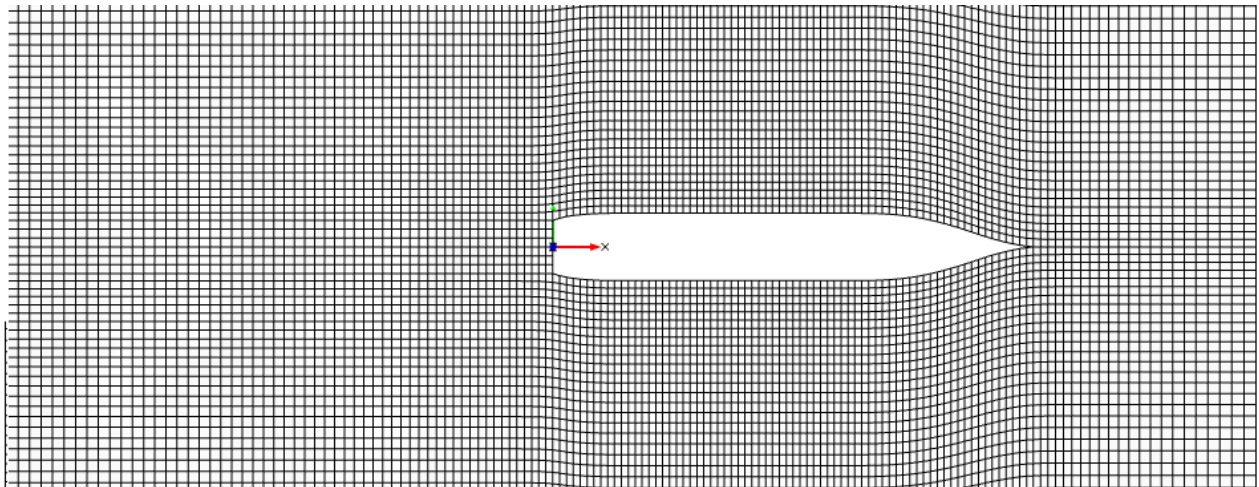
Figure 4.2: Illustration of the panel distribution on the free surface at $F_n = 0.26$.

4.2 The Potential Flow Codes Shipflow and ShipX-WaveRes

To get an idea of the accuracy of the numerical scheme used in the wave resistance calculation of SHIPFLOW, a trend analysis of the wave resistance for the KCS is executed with the potential code used in ShipX-WaveRes and the potential code used in SHIPFLOW. Validation based on the resistance results from both schemes is not possible because there is not enough information in the resistance results to determine the numerical uncertainties introduced by both schemes. However, a trend analysis of the two numerical schemes is possible. If the trend of the two schemes are comparable, the program will be useful in the design cycle. For the results to be comparable, the same number and the distribution of panels on the hull and free surface are used in both simulations. The model was free to move in heave and pitch, with no initial trim at the design draft. The simulations were carried out through a series of 6 speeds ranging from 14 to 24 knots equally spaced.

4.2.1 Hull Geometry Conversion

To compare the two different potential theory codes, it is crucial that the subject of investigation is of the exact same geometry. The files supported for resistance calculations in the two programs differ, and means to convert the file format from one program to the other had to be established. After investigation, it was clear that the two file-formats containing the information about the hull geometry that were the most alike were the NAPA-file format in ShipX, and the Offset-file format in SHIPFLOW. The SHIPFLOW software enables the user to format the surface model of the hull, usually described by an IGES or a STL file, to an offset file. The purpose of the offset file is to describe the hull geometry of the vessel by a list of coordinate values of points lying on the hull surface. These points are defined by its x, y and z-coordinates, and allocated to describe the stations of the hull at constant x-planes. The stations are grouped to describe the different parts of the geometry such as the bow, bulb, main body, aft, boss and transom stern. As for the offset file format, the NAPA file format also describes the form of the stations with a set of points defined by its x, y and z-coordinates in the constant x-plane. In addition to the stations in the x-plane, the NAPA file format contains a set of points located at the intersection between the center line of the hull and the stations, known as knuckle points. Since the two file formats are fundamentally alike, but with information allocated differently, the process of converting one file format to another, is simply a process of reallocating the information given. The conversion of the file formats were done with a MATLAB-script, where the input is the offset file

from SHIPFLOW.
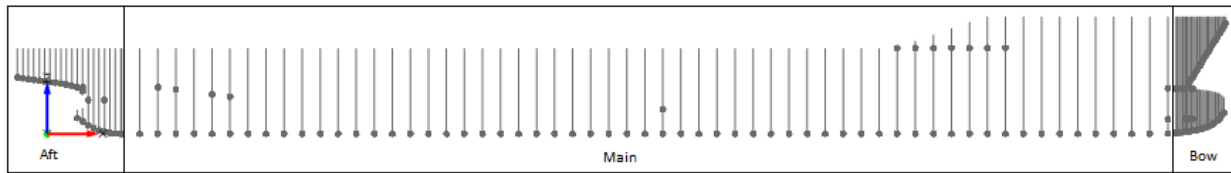
Figure 4.3: An exaple of the grouping of the offset-file format for the KCS in SHIPFLOW.

In order for the MATLAB script to run and generate the NAPA geometry file, a manual export of the offset file from SHIPFLOW is needed. The boss and bulb, as well as the overhang in the stern and the bow region introduces more than one point at the intersection of the stations and the center line for a constant x-plane. To account for this, these regions are treated differently to obtain the right connection between the center-line and the knuckle points. In the manual export of the offset geometry file, the number and the distribution of the stations describing the aft, main and the bow part of the hull is determined. The grouping of the different hull regions used in the manual part of the geometry conversion is illustrated in figure 4.3. The geometry of the KCS with the offset file format in SHIPFLOW and the NAPA file format in ShipX is shown in figure 4.4 and 4.5 respectively.
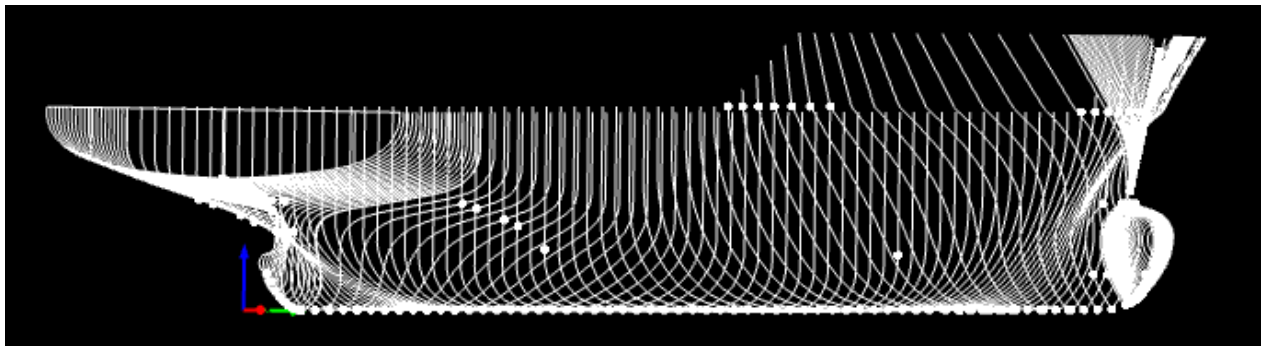
Figure 4.4: The offset file geometry shown in the SHIPFLOW environment.
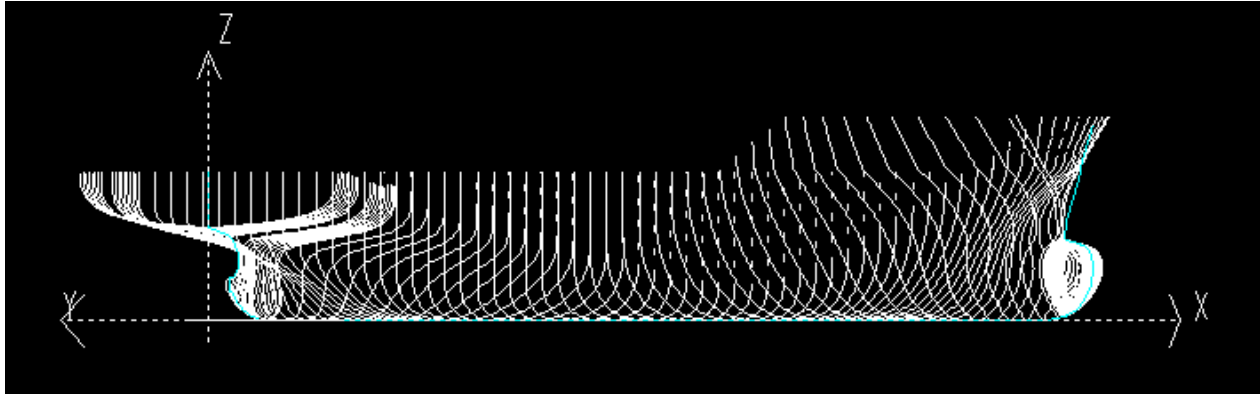
Figure 4.5: The Napa file geometry shown in the ShipX environment.

4.2.2 Validation Results: the Comparison of SHIPFLOW and ShipX

The treatment of the non linear solution in the bow region differs in the SHIPFLOW code and the ShipX-WaveRes code, and some differences in the results are expected. As seen in figure 4.6, the wave resistance show a similar trend over the changing speed regime, however the wave resistance calculated by ShipX-WaveRes is slightly lower than the wave resistance calculated by SHIPFLOW. Compared to the experimental data the potential code SHIPFLOW predict the wave resistance well in the region between 14 and 20 knots, and overestimates the resistance in the higher Froude regime.
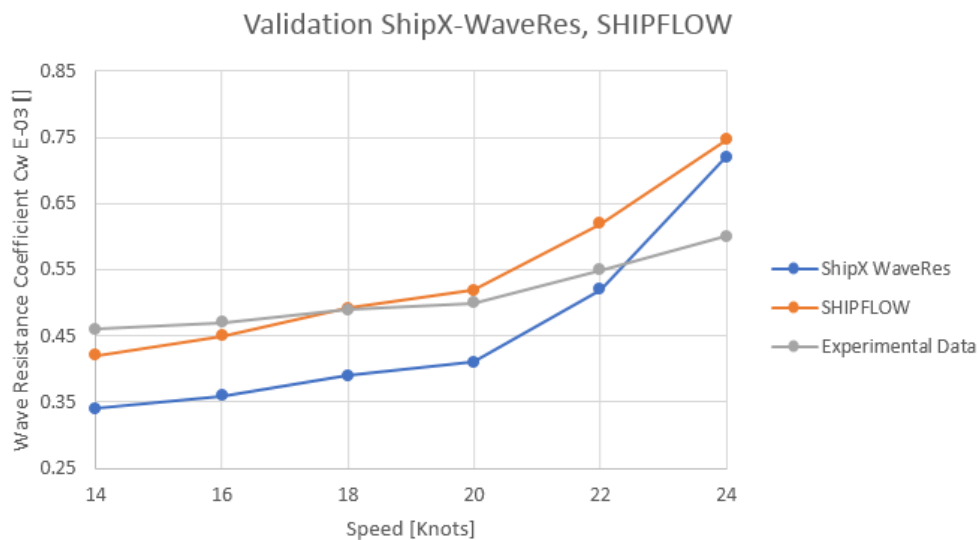
Figure 4.6: The wave resistance of the KCS obtained from ShipX WaveRes, SHIPFLOW and experimental data Choi et al. (2011).

4.3 Experimental Data

The experimental data from towing tank tests done for the KCS in the KRISO towing tank is the basis for validation of CFD simulations for the KCS ship. The ship was towed at a constant Froude number of 0.26, which corresponds to a full scale ship speed of 24 knots. The model was fixed in heave and pitch at the full scale static draft with zero trim angle. Measurements of the global wave pattern, as well as the wave elevation at several longitudinal wave cuts were obtained through photo analysis Kim et al. (2001).

4.3.1 Evaluation of the Wave Generation.

When using a potential code such as SHIPFLOW to predict the wave resistance of the hull, it is assumed that the main particulars of the flow is captured. The overall quality of the solution method can be established by comparison between the computed and measured wave field. As seen in figure 4.7 the global wave pattern from the SHIPFLOW simulation and the global
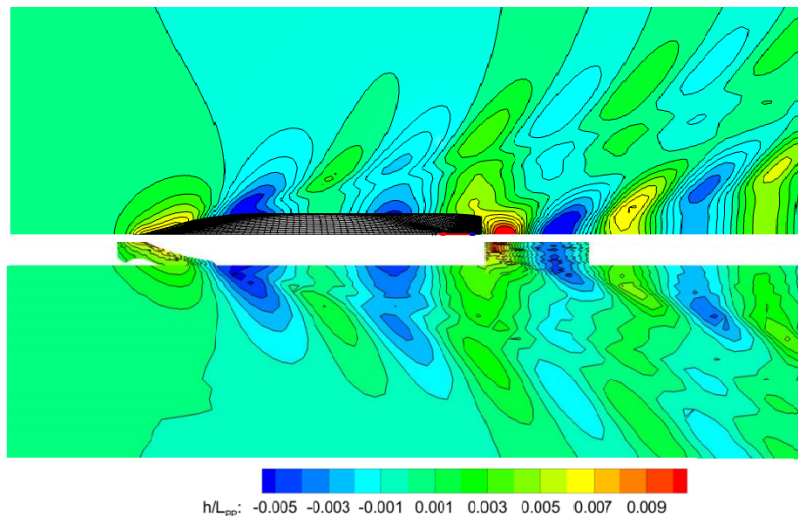
Figure 4.7: Comparison between measured and computed wave field. Top: numerical simulation in SHIPFLOW. Bottom: measurements from experimental data.

wave pattern from the experimental measurements are in excellent agreement. The position and the magnitude of both the transverse and longitudinal wave crests and troughs are well estimated.

Wave elevation

Figure 4.8 and 4.9 shows the comparison between the free surface elevation at the hull surface as well as at the longitudinal wave cut located at $y/L_{pp} = 0.1$. The results are obtained from experimental measurements and the simulations in SHIPFLOW.
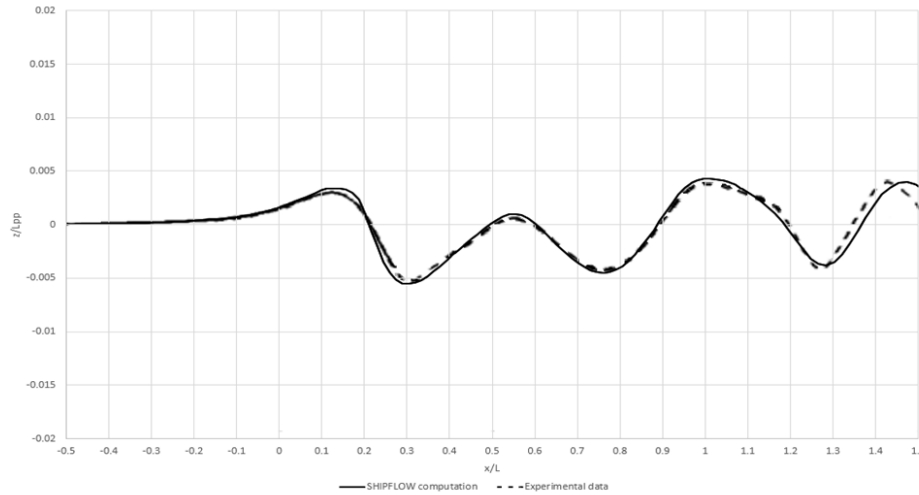
Figure 4.8: Comparison of the longitudinal wave cut for the KCS hull at $y/L_{pp} = 0.1$.
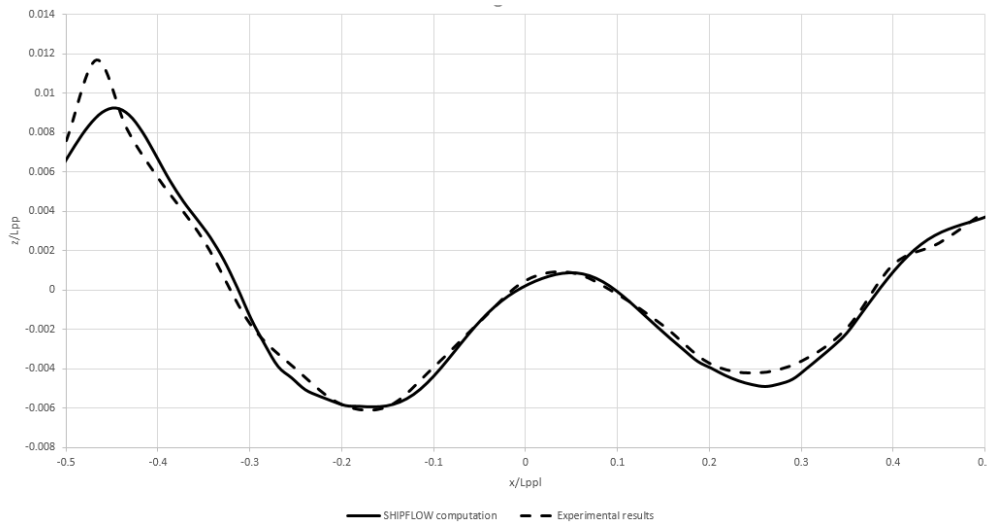
Figure 4.9: Comparison of the longitudinal wave cut for the KCS hull at the hull surface.

For the wave cut at the hull surface, the wave elevation obtained from the SHIPFLOW simulation corresponds well both in location and magnitude to the experimental data. Some differences are seen in the bow and stern region. The bow wave is underestimated and this could lead to a reduction in the calculated resistance. For the longitudinal wave cut located at $y/L_{pp} = 0.10$,

the the wave elevation from SHIPFLOW and the experimental data is in good agreement. Additionally, it should be mentioned that the experimental data were captured with the use of photo analysis instead of wave probes, which can cause uncertainties in the measurements.

4.4 Conclusion

As seen in the results from the validation evaluation, the potential code SHIPFLOW is in overall fairly good agreement with both the comparable potential code ShipX-WaveRes and experimental data. The trend analysis done with the potential code ShipX WaveRes demonstrates that SHIPFLOW is in fact a suitable potential code to rank the performance of the different bulb design candidates, and will be used for further investigations in this thesis.

Chapter 5

Parametric Design

This chapter aims to provide an understanding of parametric design for engineering problems. Firstly, a literature review of the current state of parametric modelling and how multi objective optimization algorithms now constitutes the state-of-the-art modeling procedures is carried out. Secondly, a description of how the parameterization of the bulb geometry is modelled in the CAESES framework with the use of spline curves.

5.1   The Current State of Engineering Design

Conventional ship design have in the past manly been based the ship designers ability to design a new ship hull based on past experience and database regression models, to meet a set of given dimensions and requirements proposed by the contractors. These requirements often include main operation speed, payload capacity, main dimensions and operating range. Since the requirements from the contractors are becoming more detailed and diverse, traditional ship design methods, which is manly based on the experience and intuition of the designer, has reached a limit and more accurate and demanding methods are needed. In addition, the traditional design approach does not take into account variations in the operating profile, which can lead to ineffective ship design for large periods of time.

The first efforts of optimization with structural design methods have been present in the field of aeronautical and aerospace industry since the 1960s, and the automatic CFD-based design methods arise later in the 1970s, manly based on the work of Hicks and Henne (1978). Since then, the development of design methods both in the field of aeronautical and aerospace as

well as the field of naval architecture have seen a tremendous change with the introduction of reliable and validated flow solvers. In the 1990s a number of papers concerned around the optimization of ship design with the use of singe objective optimization methods with flow solvers ranging from potential flow to RANSE methods resulted in efficient ship design methods as seen in Janson and Larsson (1996) and Tahara et al. (2001). However, ship design, as with the vast majority of engineering problems, is a multi objective problem with conflicted objectives, concerning a set of different disciplines such as hydrodynamic performance, maneuvering, stability and structural strength. The degree of importance of these objectives is again influenced by the operating profile of the vessel. During the last decades, following the development of parametric modelling in computer aided design(CAD), the relationship between parametric modelling and CFD have been the topic of interest when modelling the hull geometry with respect to hydrodynamic performance. The use of control points and B-spline surfaces as a means to develop the parametric design of the ship hull surface has been introduced with favorable results as seen in Mancuso (2006) and Pérez et al. (2007). The use of control point movement as design variables in the parametric design in solid modelling to create bulb geometries in accordance to change in the length and breadth parameters was investigated by Blanchard et al. (2013) and gave promising results. Over the years, especially with the development of high performance computers, optimization has become an integral part of engineering. State-of-the-art modelling procedures coupled with advanced optimization algorithms now constitutes an essential part in the design of large complex multi-variable systems such as ship design. As described by Wagner and Bronsart (2011), a detailed service profile considering the economical and ecological constraints as well as the vessels operating profile, can be used as basis of the development of the optimal ship design. Wagner et al. (2014) performed a scenario based optimization of a container vessel with respect to its projected operating conditions to analyze improved performance in the bulb geometry. The latter paper forms the basis of the methodology for the various optimization procedures described in chapter 6.

5.2   Parametric Modelling

When optimizing the bulb geometry of the hull it is of advantage to create a large number of bulb geometries that can be evaluated by the potential code SHIPFLOW to calculate the resistance. Because of the complex geometry of the bulb, designing and optimizing the hull surface can become a difficult task when using conventional computer aided drag and drop design methods. It is therefore beneficial to design the bulb geometry with a set of given bulb geometry param-

eters that controls the deformation of the bulb geometry, also known as parametric modelling. If done right, parametric modelling is an effective and reasonable method for generation of hull form deformations. While it is possible to describe the parametric model with a large number of parameters to create a large design space, it is of great importance that the number of variables that describes the deformation of the geometry is kept at a minimum in the design process. An increase in variables will lead to an increase in the complexity of the optimization process, which again will lead to vast computational cost multiples.

In order to keep the computational cost of the optimization process low, the bulbous bow geometry is modified locally without interacting with the rest of the hull geometry. Sariöz (2006) and Pérez et al. (2007) proposes that automatic modelling of hull form geometries with the use of a set of mathematical representations of the 3-D geometries using eg. Bézier or B-spline curves and surfaces results in high-quality fairing surfaces. These mathematical representations have the ability to describe the bulb geometry in a sufficient manner. Furthermore the B-spline curves and surfaces can describe the deformation of the geometry with movement of the control points defining the surface, which makes it ideal for the parametric modelling.

5.2.1 NURBS Curves

The following subsection will give a brief introduction to the definition of the NURBS curves and surfaces, for a more in detail description of NURBS and its applications see Piegl and Tiller (2012). Non-uniform rational B-splines (NURBS) are mathematical representations of a 3-D geometry that can be accurately describe any shape from a simple 2-D line, circle, arc or curve. With the use of the NURBS method, good-quality curves and surfaces can be obtained by describing the bulb with less design variables than conventional ship design, as the initial relationship between the hull form and the hull parameters is retained, and the deformations is described by movement of some control points, which makes for an efficient and feasible design process.

In addition to employ the ability of efficient and effective bulb geometry variant generation, it is also compatible with most industry-standard CAD and engineering analysis programs, which is of big advantage. For the reasons mentioned above, the parametric modeling done in this thesis is by the use of B-spline curves and surfaces, a particular case of the NURBS method.

5.2.2 The Modelling in CAESES

The parameterization of the bulb geometry is done with the use of the CAD software CAESES. CAESES is chosen as the CAD software because it enables innovative CAD capabilities, such as the B-Spline surface modelling, to create variable geometry models that are geared towards simulation. The CAESES software is coupled with the potential code SHIPFLOW, which makes it perfectly suited for a fully-automated workflow between the modelling and the resistance calculations.

In the CAESES-enviroment the process of curve generation is defined by a number of control points on the surface that describes the parametric curve of that given surface. These control points can be manipulated in order to deform the initial geometry. A visualization of the morphing of the bulb geometry in the x, y and z-direction is shown in figure 5.2 5.1 and 5.3 respectively.

(a)	(b)	(c)
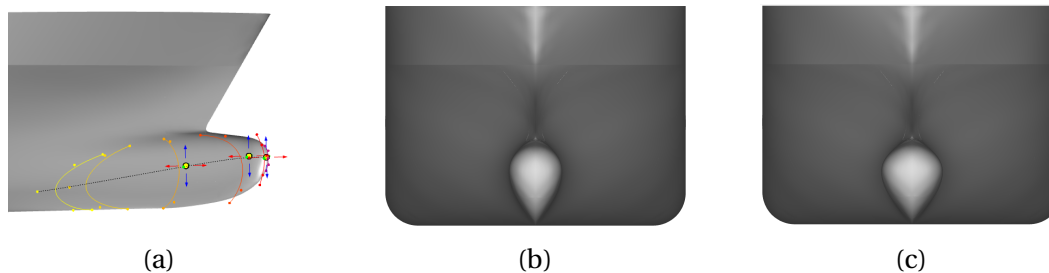
Figure 5.1: Illustrative figure of how modeling of the change in the bulb geometry in the y-direction with the use of a B-spline surface works.

The B-spline surface that controls the deformation of the bulb in the y-direction consists of a B-spline surface of third degree, modeled with 25 control points on the bulb surface. These 25 control points forms 6 B-spline curves which again constitutes the B-spline surface. Three control points placed on the maximum breadth line of the bulb is subject to change in order to morph the bulb geometry. The three control points are carefully placed on the surface to retain the ∇-shape of the bulb, as well as to improve the fairing of the hull in the bulb-hull transition. The control points defining the deformation of the surface are controlled by one parameter describing the movement of all three control points in the y-direction. However, the movement of the three control points is defined such that the most forward control point only is subject to half of the movement compared to the two other points. This is done to retain the oval shape of the bulb such that the stagnation point on the tip of the bulb does not increase substantially although the breadth, and thus the volume, increases. The modeling of the B-spline surface and

the position of the control points is shown in figure 5.1a.

<div align="center">(a)   (b)   (c)</div>
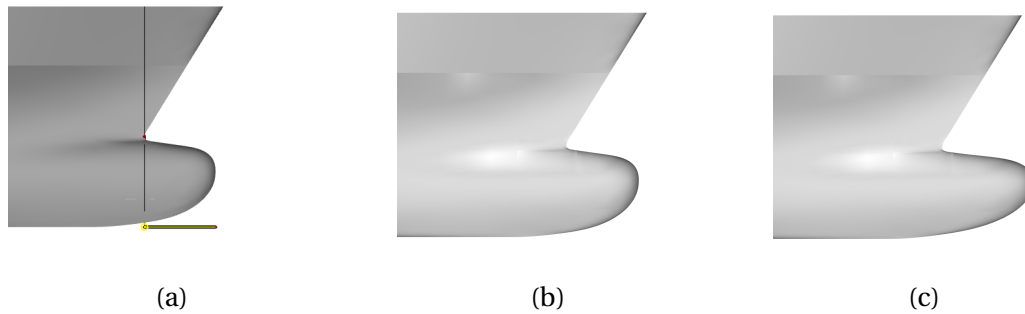
Figure 5.2: Illustrative figure of how modeling of the change in the bulb geometry in the x-direction with the use of a B-spline curve works.

<div align="center">(a)   (b)   (c)</div>
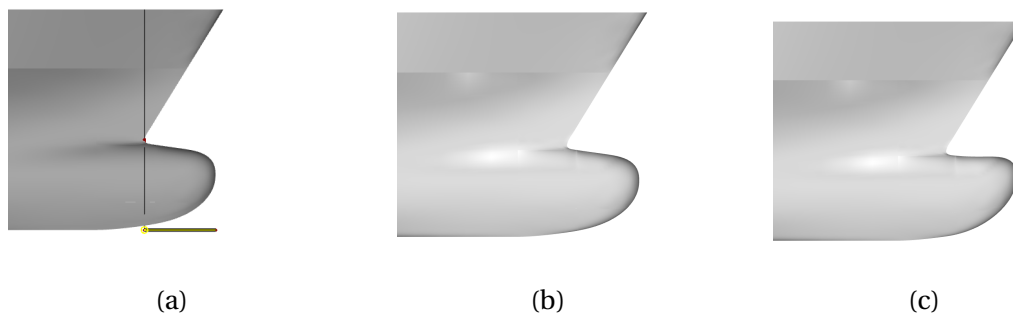
Figure 5.3: Illustrative figure of how modeling of the change in the bulb geometry in the x-direction with the use of a B-spline curve works.

The deformation of the bulb in the x and z-direction is controlled by an F-spline curve. The F-spline curve is a fairness optimized curve created within the CAESES framework. The input for the deformation consist of two control points, where the most forward point controls the deformation in both the x and z-direction. The movement of the control points defining the deformation of the bulb in the x and y-direction is described by one parameter respectively. In order not to deform the parts of the bow that is positioned above the bulbous bow with the F-spline curve, a curve generator which prohibits the top part of the bow from deformation was implemented. The modeling and deformation is illustrated in figure 5.2 and 5.3

Deformation of the bulb with respect to the change in the length, breadth and height of the bulb is described by three individual parameters as described previously in this chapter. The change in these parameters is completed within the CAESES framework, and can be implemented to change automatically in an optimization procedure to create a large number of design candidates in a short period of time.

Chapter 6

Design of The Flexible Bulb Geometry

This chapter is implemented to present a design method for the flexible bulb geometry. The procedure of the flexible bulb design is divided into separate parts relevant to assess the design parameters of the bulbs influence on the resistance of the vessel, and to obtain and evaluate the flexible bulb configurations. To appraise the value of the flexible bulb configuration and the design procedure presented, a case study with a suitable vessel and operating profile will be performed.

6.1 Initial Geometry and Operating Profile for the Case Study

Figure 6.1: The KRISO container ship.

The KRISO container ship(KCS), with main dimensions listed in table 6.1, is used as the initial hull for the investigation of the flexible bulb in the case study. The KCS was developed at The Korea Research Institute for Ships and Ocean Engineering in 1997 to provide validation for CFD calculations and flow physics. Although the ship has never been build, the hull is meant to represent a modern container ship with a bulbous bow and stern with an estimated capacity of 3600 TEU. Because the hull geometry is available to the public for research, the hull has been a subject of study at many well renown CFD-workshops [Larsson et al. (2010), Kim (2015)]. The

magnitude of the available data of the flow around the KCS, both from experimental fluid dynamics(EFD) and CFD makes this ship ideal as initial geometry since the CFD software used in the optimization process can be validated for accuracy.

Table 6.1: Main dimensions of the KCS.

Ship Data	Value
Length between perpendiculars	230.00[m]
Beam	32.20 [m]
Draft	10.8 [m]
Displacement	52030 [m^3]
Block coefficient-C_B	0.6507[]
Wetted surface area-S_W	9424 [m^2
Design Speed	24.00 [Knots]

To evaluate the potential value of having a flexible bulb, which is driven by the variation in operating conditions, historical operating conditions have to be analyzed. This requires sophisticated data breakdown coupled with stochastic modeling and time series analysis. The operating profile used for the KCS in this case study is based on the work of fellow stud. techn. Jon Hovem Leonhardsen. The results from this work will be used as input in the case study without further explanation.

Because of its similarities in the main dimensions to the KCS, the container ship ANL BAREGA is used as a reference ship for the operating profile. The analysis of the historical data for the sailing speed is shown in figure 6.2a. To asses the value of flexibility in the bulb design, a fictive operating profile, as illustrated in figure 6.2b, is implemented. This fictional operating profile is implemented with the aim to establish the value of flexibility, should the operating profiles for container ships in this size segment be reversed to the operating profiles typical before slow steaming was introduced. This fictional operating profile has an increased mean speed, and a general higher weighting, in accordance to a non slow steaming operating profile.
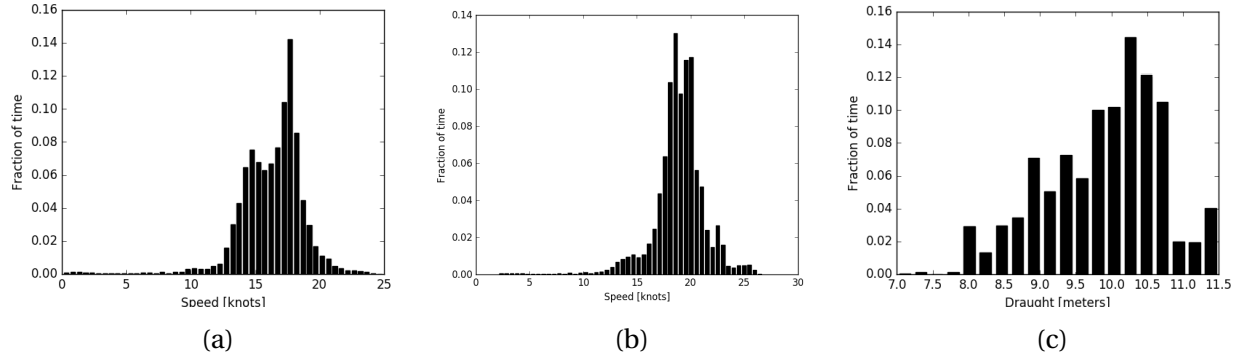
Figure 6.2: Figure (a): Operating profile of ANL BRAGA based on time series analysis of historical AIS data. Figure (b): Fictional operating profile resembling a typical non slow steaming profile.Figure (c): Draft profile of ANL BAREGA.

The analysis of the historical data yields a detailed breakdown of the different speeds and drafts used as input in the case study. To use this information in the optimization process, the number of speed and draft conditions have to be reduced in order to keep the computational cost reasonable. Table 6.2 shows an averaged operating profile of five different speed conditions and their respected percent of time spent at each condition during operation. Table 6.3 is defined in a similar manner as the operating profile for ANL BAREGA. These averaged operating profiles are used to illustrate the value of flexibility in the case study.

Table 6.2: Operating profile 1: The operating profile for ANL BAREGA represented in percent of time spent at each condition defined by the ship speed and draft.

Draft/ Speed	12 kn	15kn	18kn	21 kn	24 kn
10.50m	11.00 %	27.00 %	40.00 %	19.00 %	3.00 %

Table 6.3: Operational Profile 2: a higher weighted fictional operating profile resented in percent of time spent at each condition defined by the ship speed and draft.

Draft/ Speed	12 kn	15kn	18kn	21 kn	24 kn
10.5m	0.50 %	12.00 %	31.00 %	39.00 %	17.50%

6.2   Design Procedure of The Flexible Bulb

In order to obtain the most suitable flexible bulb configuration for the ship in question, a design procedure of the flexible bulb is implemented. The procedure is divided in two stages. The first stage is to analyze sailing data for an equivalent vessel to the KCS, in terms of the vessels main

dimensions, to establish an applicable operating profile for the case study. The operating profile used the case study is presented in the previous section. Stage two of the the design procedure consists of an optimization process of the flexible bulb geometry with respect to a minimization of the weighted effective power over the operating profile.

Because of the change in sailing speed during operation, the optimization process becomes a multi-objective optimization problem. A multi-objective optimization problem is a multiple criteria decision making problem where more than one objective function is optimized simultaneously, and there are often trade-offs between the objective functions. For the optimization of the bulb shape over the operating profile, the objective functions for the different speed conditions differs substantially. In mathematical terms, the multi-objective optimization problem can be described as:

$$min(f_1(x), f_2(x), .. f_k(x)) \qquad k \geq 2 \tag{6.1}$$

where k is the number of objectives corresponding to the number of sailing speeds in the operating profile, and x is a set of decision variables corresponding to the design parameters of the bulb.

Like all optimization processes, the objectives, constraints and design variables must be specified in detail. The following subsections will discuss in detail the reasoning behind the chosen objectives, constraints, design variables.

Objectives

As discussed in section 2, the total resistance (R_T) of a ship hull propagating in calm water can be divided into two subdivisions. Wave resistance (R_w), related to the Froude number, and frictional resistance (R_F) related to the Reynolds number.

$$R_T = R_W + R_F \tag{6.2}$$

The objective of the bulb is to reduce the wave resistance, which will result in a reduction of the total resistance. Subsequently, the objective when optimizing the bulb geometry is to reduce the wave resistance of the hull. Since the reduction in wave making resistance is the object of study, emphasis have been put into the evaluation of this resistance component rather than the frictional resistance. The objective function is defined as the minimization of the effective power

of the vessel for the various speeds in the operating profile. In this thesis the wave resistance is calculated by the potential code SHIPFLOW, while the frictional resistance is calculated by the use of the ITTC57 friction formula, both described in chapter 3.

Design Variables
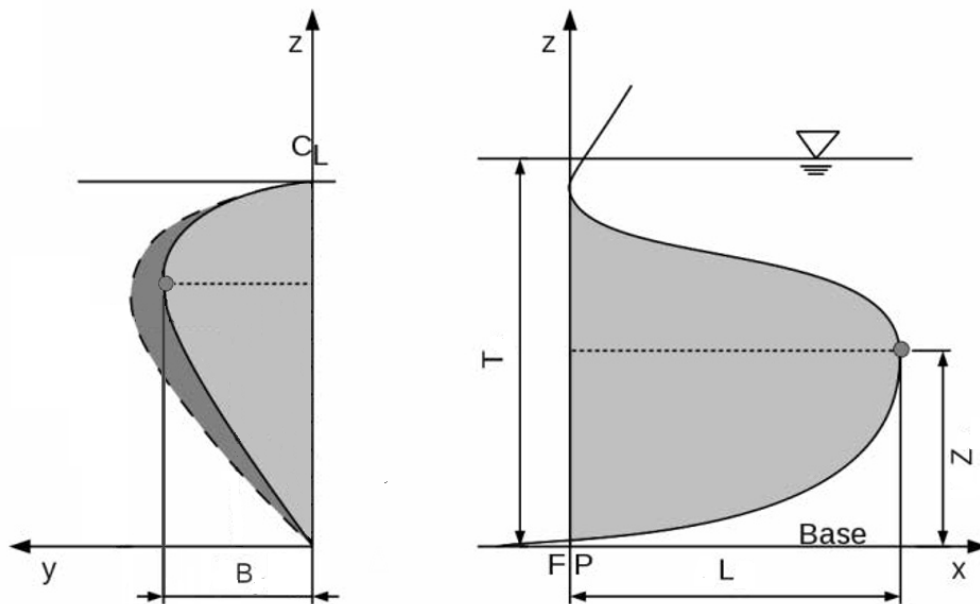
Figure 6.3: Design parameters of the bolbous bow Wagner et al. (2014).

To generate new hull variants efficiently the variation of parameter is only subjected to the bulbous bow section of the hull. As described in section 2.1.2 the goal of the change in geometry of the bulb is to change the total volume and the length of the bulb to reduce the total wave generation by the hull through cancellation of the intersecting waves. On the basis of this, three design variables are considered in the case study. The length of the bulb, defined as the position of the most forward point of the bulb in the longitudinal axis. This variable will have an impact on the total volume of the bulb as well as the phase of the wave generated by the bulb. The height of the tip position of the bulb, defined as the tip position of the bulb in the z-direction. This variable will impact the bulb's ability to be submerged for different draft conditions. The last design variable is the maximum breadth of the bulb. This variable will have a great impact on the volume of the bulb. Together these variables will have the ability to change the volume distribution of the bulb as well as the phase of the wave generated by the bulb, and thus they are suited to be good design variables for the optimization of the bulb geometry. The design vari-

ables described above are illustrated in detail by figure 6.3. The change in the design variables during the optimization procedure is completed by the parametric modelling of the bulb within the CAESES framework as described in chapter 5

Constraints

For the optimization process not to introduce nonphysical bulb geometries and retain the typical ∇-bulb shape, some constrains have to be introduced. The constraints for the design space of the design variables ΔL, ΔB and ΔZ were decided through visual inspection of the bulb shapes generated when the parameters were changed individually. In order not to change the hydrostatic properties of the vessel, a change in displacement of $\pm 1.0\%$ is set as the inequality constraint for the optimization algorithms. The design space for the design variables are listed in table 6.4

Table 6.4: Constraints for the design space of the three design variables.

Design variable	Min value	Original value	Max value
ΔL	-2.0m	0.0	3.0m
ΔB	-1.5m	0.0	2.0m
ΔZ	-1.3m	0.0	1.0m

6.3 The Optimization Procedure of the Flexible Bulb Configuration
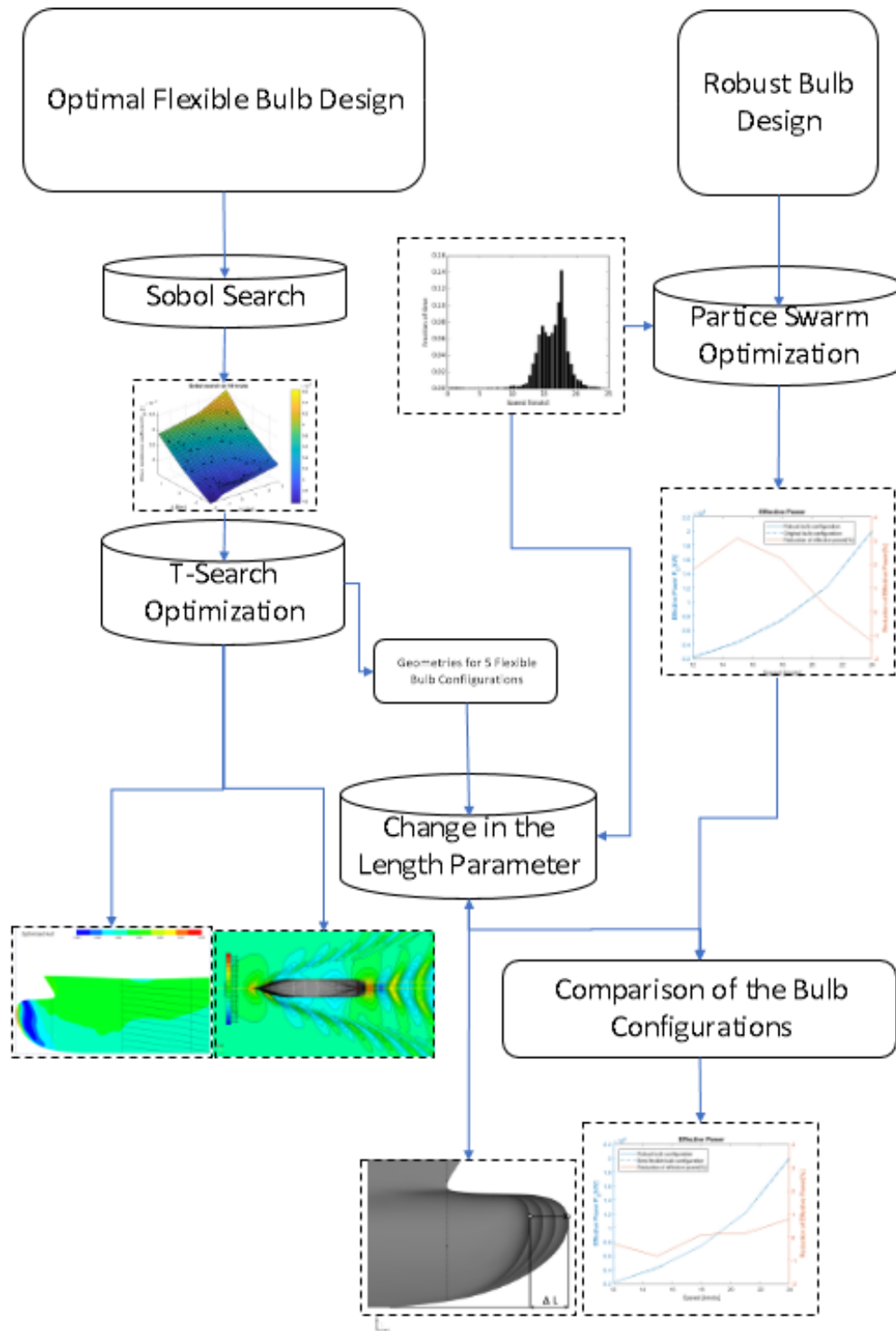
Figure 6.4: Flowchart of the optimization procedure of the flexible bulb configuration.

The general flow of the optimization procedure of the flexible bulb is illustrated in figure 6.4. The optimization of the flexible bulb configuration is a process which is divided into three separate parts. The first part constitutes a search of the design space to identify the influence of the design parameters on the wave resistance for the various speeds in the operating profile. Furthermore, this part will aggregate the optimization of the flexible bulb geometries to be studied later in the optimization procedure. The second part of the optimization procedure is to establish an optimized robust bulb configuration, which will be used as a reference, as this bulb configuration is industry standard. The last part of the optimization procedure consists of evaluating the flexible bulb geometries with a change in the length parameter. The performance of the flexible bulb configurations and the robust bulb configuration is compared, with respect to the weighted effective power over the operating profile, to establish the best flexible bulb configuration and to demonstrate the potential of flexibility in the bulb design.

6.3.1   Establishment of the Higher and Lower Bonds of Potential Savings

Since the flexible bulbous bow is a concept which is very much still in the conceptual stage, it is of desire to investigate the potential savings of flexibility compared to a robust bulbous bow design. As described in section 1.1.2, the robust bulb design is best practice when designing ships, and this design will therefore indicate the lower bond of potential savings in resistance compared to the original shape of the bulb. In addition, the identification of the true optimum, a scenario where the bulb have the ability to change all the design variables during operation, will constitute the higher bond of potential savings in resistance. The flexible bulb design will lie somewhere in the middle of these bonds, depending on the number of physical and mechanical constraints introduced by the structure mechanics of the flexible bulb. In order to evaluate the value of flexibility, the lower and higher bonds have to be stated. The optimization procedure for the three different configurations, robust, flexible true optimum and flexible length, differs both in their objective functions as well as the best suited optimization algorithms. The following subsections will elaborate in detail how and why the objective functions change for the various bulb configurations as well as carefully describe how these methods affect the optimization process.

6.3.2 True Optimum Flexible Bulb Design

The procedure of the true optimum flexible bulb design at each operating condition in the operating profile for the vessel, is far less complex than the robust design. While the robust design accounts for the the weighted fraction of time spent at each condition, the true optimum design is a single objective optimization process subject to finding the best bulb geometry at each speed in the operating profile separately. Accordingly this optimization procedure will result in one geometry for each operating condition, resulting in five bulb geometries. These bulb geometries will differ drastically in their shape and form, and the chances for a mechanism that can change these design parameters during operation is unlikely. However, these design candidates demonstrate the higher bond of the potential of the flexible bulb. The objective function of the true optimum design is to minimize the effective power for each speed variation separately as described in equation 6.3.

$$P_{E_i} = R_{T_i} V_i \tag{6.3}$$

The first step in the optimization procedure is to perform the optimization for the true optimum design. The results from this optimization process will give valuable information on the response of the design variables within the design space. As described in section 6.2 the height variable, ΔZ, indicates the bulb's ability to be submerged for various draft conditions, and does not affect the change in volume of the bulb in a significant manner. Since the subject of investigation in this case study is to evaluate the impact of speed variation on the bulb geometry, while the draft is kept constant, the ideal height parameter is established beforehand, and then kept constant for the remaining optimization procedure. To establish the ideal height parameter of the bulb, a brute force optimization where ten different height parameters governing the design space of said parameter is the subject of investigation. The breadth parameter, ΔB, and the length parameter, ΔL, were kept at the original value. The ideal height for each speed in the operating profile is used during the rest of the optimization procedure of the true optimum flexible bulb design.

When the height parameter is kept constant, it is possible to establish the impact of the remaining design variables(ΔB and ΔL) in an illustrative manner, as shown in figure 6.4. To get a general idea of the the behaviour of the different bulb geometries as well as identifying some starting design variants for the optimization process, a Sobol algorithm is used. The Sobol algorithm is a deterministic algorithm that imitates the behaviour of random sequencing, also known as a

quasi-random sequence. 40 quasi-random design variants covering the design space is used for each speed in the operating profile. The best candidates from the Sobol search are used as initial design in the optimization algorithm to find the best point optimized bulb geometries for each speed in the operating profile.

Because of the reduced complexity of the optimization problem, as well as no change in the operating condition during the optimization process, a tangent search algorithm within the CAE-SES framework is utilized as the optimization algorithm. The tangent search method promises to be a reliable solver for small scaled, single-objective optimization problems with inequality constraints. The method employs a descent search in the solution space, to ensure fast improvement in the most favorable search direction, as well as keeping the search in the feasible domain.

To evaluate the hydrodynamic effects imposed by the change of the bulb geometry, the 5 true optimum point optimized bulb geometries obtained from the T-search optimization are evaluated at their respective optimized speeds as illustrated in 6.4
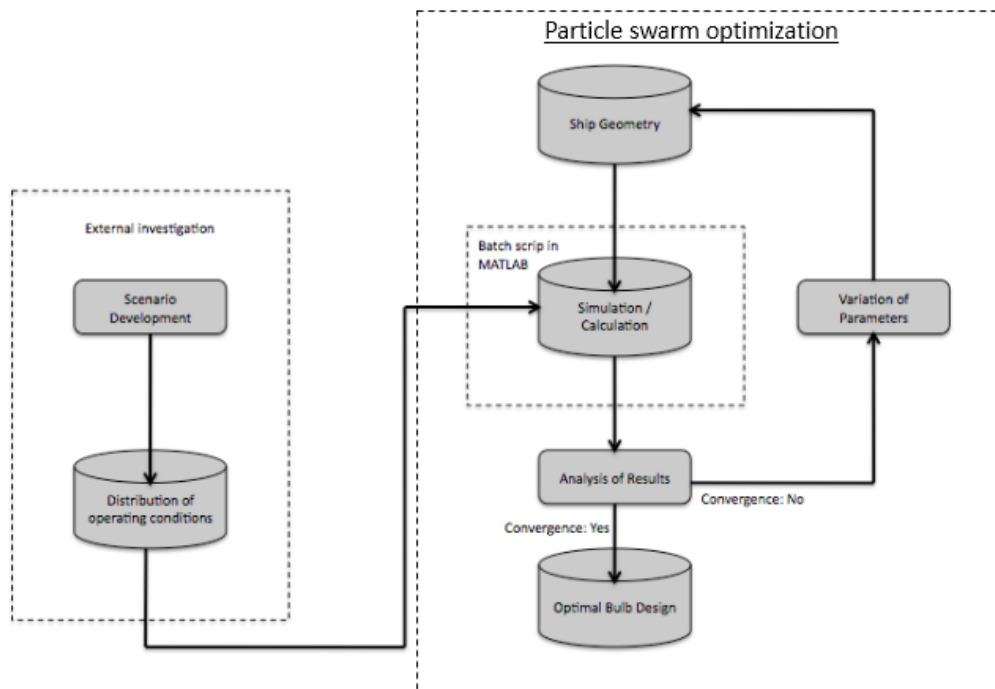
6.3.3   Robust Bulb Design

Figure 6.5: Flowchart of the optimization procedure of the robust bulb configuration with the use of a particle swarm optimization algorithm.

The robust bulb design is a multi objective optimization problem where the different speed conditions constitutes a drastic change of the optimal bulb geometry within the design space. While the optimal bulb geometry in the higher and lower Froude regimes may differ drastically, the goal of the robust bulb design is to optimize the bulb geometry with respect to the weighted fraction of time spent at each condition. The robust design yields a bulb geometry with slightly reduced hydrodynamic performance properties for most operating conditions compared to a point optimized design, often designed for one operating condition. However, with large variations in the operating conditions, the total reduction of resistance with respect to the operating profile is reduced, and accordingly this design method is common practice when the uncertainties in the operating profile is expected. The objective function for the robust design optimization is to minimize the weighted effective power over the operating profile as described in equation 6.4.

$$P_{E_w} = \sum_{i=1}^{m} w_i R_{T_i} V_i \qquad (6.4)$$

where w_i is the weighting, R_{T_i} is the total resistance and V_i is the speed of the vessel at their respective operation conditions.

Since the optimal bulb geometry for the different operating conditions may vary broadly within the design space, a suitable optimization algorithm with the ability to rank different design candidates over a large design space is implemented. A particle swarm optimization(PSO) algorithm is used to find the optimal solution. The PSO algorithm have the desired ability to search a large design space, and in an iterative manner converge towards an optimal solution. See Eberhart and Kennedy (1995) for a detailed description of the algorithm. The PSO algorithm written in MATLAB is a modified version of Ehlers (2012). The input parameters for the PSO algorithm are listed in table 6.5

Table 6.5: PSO parameters.

Input parameter	Value
Particle swarm size	20
Number of generations	15
Scaling parameter ϕ_p	2
Scaling parameter ϕ_g	2
Inertia(ω) at the begining	1.4
Inertia reduction factor	0.8
Number of rounds to improve the results before the inertia is reduced	4

The optimization process is executed by a PSO code written in MATLAB, and both the geometry change in the CAESES software, and the resistance calculation from SHIPFLOW is carried out by running the programs in batch-mode.

Batch-script in MATLAB
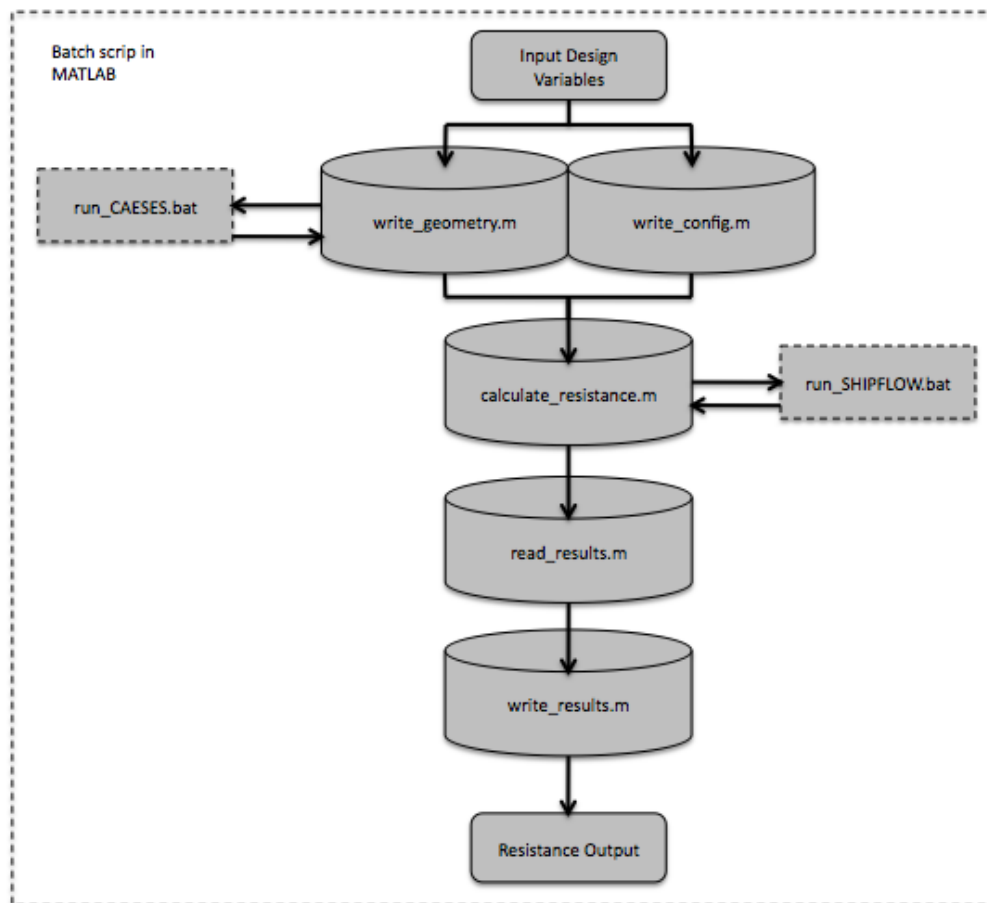
Figure 6.6: Flowchart of the batch script in MATLAB used in the particle swarm optimization algorithm.

In order to run the PSO through MATLAB, the modeling in CAESES as well as the flow simulations from SHIPFLOW run in batch. The process includes calling upon CAESES to write the geometry file with the updated design variables, writing a configuration file for the SHIPFLOW calculation, as well as reading the result files from the SHIPFLOW calculation. The configuration of the optimization process and the flow of the batch-script for the resistance calculation is illustrated in the flow charts in figure 6.5 and 6.6 respectively.

6.3.4 Flexible Bulb Design
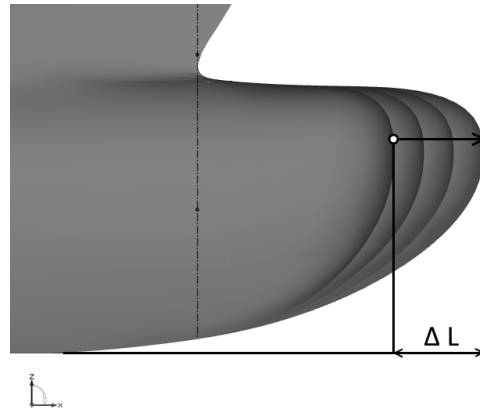
Figure 6.7: Change in the longitudinal parameter ΔL while the parameters ΔB and ΔZ are kept constant.

As a consequence of the significant change in operating conditions within the operating profile, flexibility in a given set of the design parameters of the bulbous bow during operation introduces potential savings in terms of reduced resistance. The introduction of the flexibility to the bulb design, is an active method of creating value, contrasting the standard passive robust design approach. The aim of the modelling procedure in this thesis is to establish *what bulb shape is best suited for a change in the length parameter during operation.*

The initial thought of the concept of flexibility in the bulb geometry is that the bulb would be subjected to change in the longitudinal direction of the bulb. This change, corresponds to the design parameter ΔL in the parametric modelling. With the addition of another design variable in the optimization procedure, the number of evaluations needed to establish the best flexible bulb candidate, with the use of an optimization algorithm, will be to time consuming within the time constrains of this thesis. As an alternative, a brute force optimization where the 5 bulb candidates from the true optimum bulb design process will be evaluated with a change in the bulb geometry in the longitudinal direction. In this process, the height of the tip position and the breadth of the bulb, described with the ΔZ and ΔB parameters respectively, will be held constant while the length of the bulb will be able to move longitudinally. Figure 6.7 illustrates how the change in bulb geometry in the longitudinal direction is modeled within the CAESES framework to represent the flexible bulb design. The objective function for the flexible bulb optimization is to minimize the weighted effective power over the operating profile as described in equation 6.5.

$$P_E = \sum_{i=1}^{m} w_i R_{T_i} V_i \tag{6.5}$$

To asses the value of flexibility, the flexible bulb configurations will be evaluated for the operating profile for ANL BAREGA, as well as the fictional higher weighted operating profile listed in table 6.2 and 6.3 respectively. The weighted effective power of the flexible bulb configurations is compared to the weighted effective power of the robust bulb design to evaluate the performance of the flexible bulb design.

The case study will use the optimization procedure for the flexible bulb configuration described in the previous sections, and the results will be presented in chapter 7 while a discussion of the results and findings will be discussed in chapter 8

Chapter 7

Results

The results from the case study obtained from the numerical simulations with SHIPFLOW will be presented in this chapter. The results from the various design procedures as described in chapter 6 will be presented without an in depth discussion as this takes place in chapter 8.

7.1 Robust Bulb Design

The results from the particle swarm optimization algorithm yielded a robust bulb geometry with dimensions listed in table 7.1.

Table 7.1: The dimensions and the performance characteristics for the robust bulb design.

	$\Delta L[m]$	$\Delta B[m]$	$\Delta Z[m]$	P_{E_w} OP1[kW]	P_{E_w} OP2[kW]	γ OP1[%]	γ OP1[%]
Robust Bulb	-1.00	-0.85	0.70	5587.21	11085.45	2.07%	0.23%
Original Bulb	0.00	0.00	0.00	5705.52	11110.95	0.00	0.00

The γ OP1 and γ OP1 values represent the reduction in weighted effective power over operating profile 1 and 2 respectively, compared to the original bulb configuration. The performance of the robust bulb candidate with respect to the effective power is compared to the original bulb configuration in the figure below.
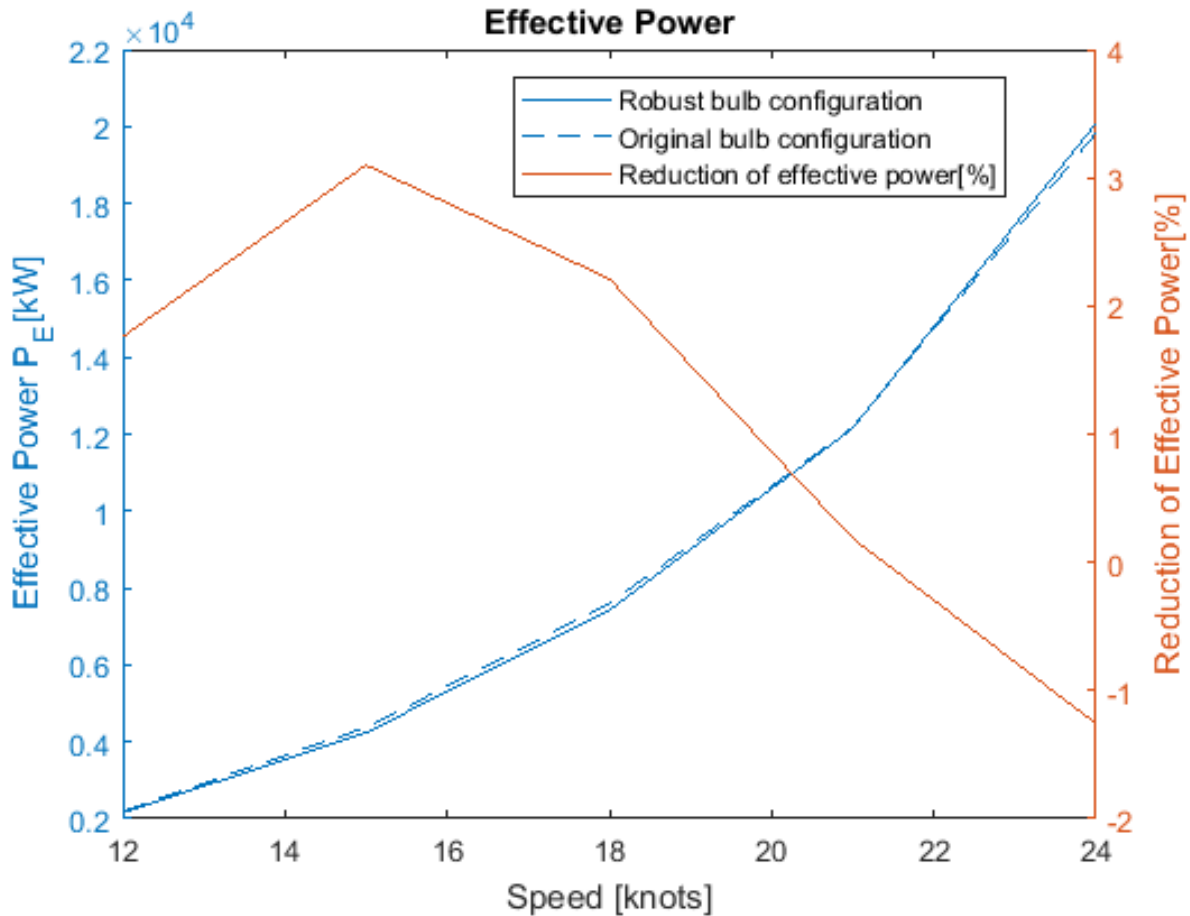
Figure 7.1: Comparison of the effective power for the robust bulb configuration and the original bulb configuration.

7.2   True Optimum Design

The individual search for the ideal height parameter ΔZ for each speed in the operating profile is presented in table 7.2. These height parameters will be used for further investigations. As discussed in section 6.3, the search for the optimal bulb design at each operating condition will give valuable insight on how the different design variables affect the bulb performance within the design space. As a consequence of this, the findings from this design process will be presented in detail as it constitutes the candidates to be evaluated for the flexible design process. The results from the Sobol search are presented in a 3-D and 2-D surface plot. The colored plane in the plot represent a linear interpolation of the the wave resistance from the various ΔL and ΔB design parameter combinations. The wave elevation within the vessels wake, as well as the

pressure distribution at the hull surface are presented for each true optimum bulb configuration at their respective speeds to give an insight of the hydrodynamic effects imposed by the change in the bulb geometry.

7.2.1   Brute Force Optimization: the Height Parameter

Table 7.2: The ideal height parameters for the true optimum bulb configurations at each speed regime in the operating profile.

Speed [Kn]	12	15	18	21	24
Ideal Height ΔZ [m]	0.60	0.60	0.70	0.80	1.00

7.2.2   True Optimum: 12 knots

(a)   (b)

Figure 7.2: Figure (a) show the results from the Sobol search for the optimal bulb shape at 12 knots. In this figure an interpolated surface plane is added in order to illustrate the trend of the change in design variables. Figure (b) also show the results Sobol search for 12 knots in a 2D plot.

Figure 7.3: The figure illustrates the global wave pattern of the optimal bulb configuration in the upper part, and the global wave pattern of the original bulb configuration in the lower part at 12 knots.

Figure 7.4: The figure shows the pressure coefficient on the hull as well as the wave elevation curvature at the top of the hull at 12 knots sailing speed. To the left: the optimal bulb configuration. To the right: original bulb configuration.

7.2.3   True Optimum: 15 knots

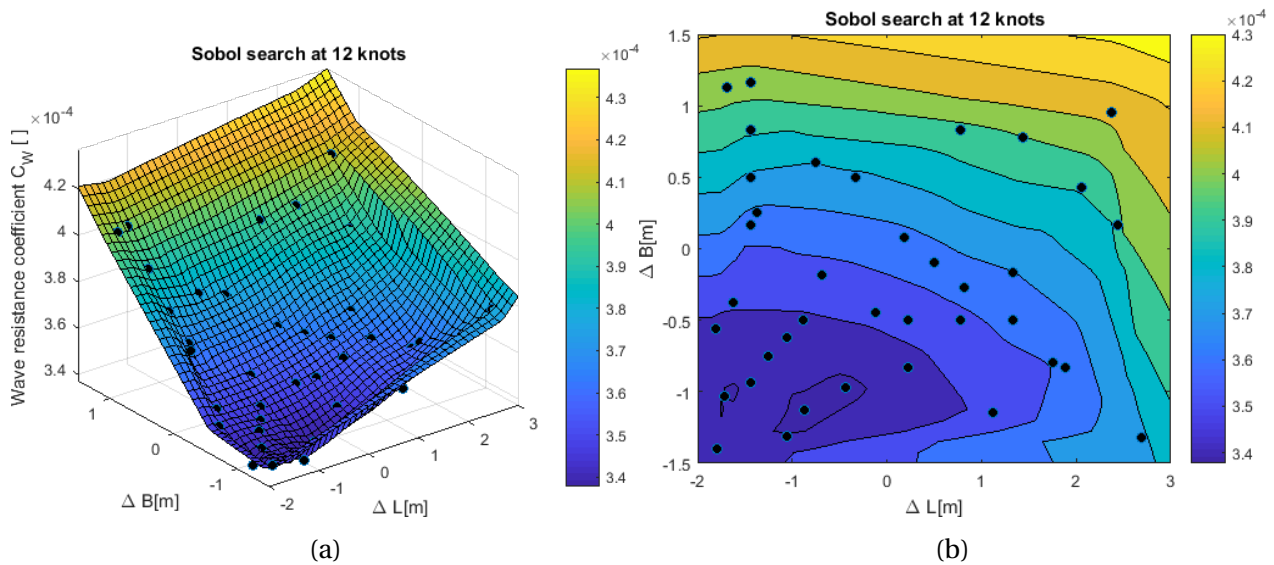(a)   (b)

Figure 7.5: Figure (a) show the results from the Sobol search for the optimal bulb shape at 15 knots. In this figure an interpolated surface plane is added in order to illustrate the trend of the change in design variables. Figure (b) also show the results Sobol search for 15 knots in a 2D plot.

Figure 7.6: The figure illustrates the global wave pattern of the optimal bulb configuration in the upper part, and the global wave pattern of the original bulb configuration in the lower part at 15 knots.

Figure 7.7: The figure shows the pressure coefficient on the hull as well as the wave elevation curvature at the top of the hull at 15 knots sailing speed. To the left: the optimal bulb configuration. To the right: original bulb configuration.

7.2.4 True Optimum: 18 knots

(a)   (b)

Figure 7.8: Figure (a) show the results from the Sobol search for the optimal bulb shape at 18 knots. In this figure an interpolated surface plane is added in order to illustrate the trend of the change in design variables. Figure (b) also show the results Sobol search for 18 knots in a 2D plot.
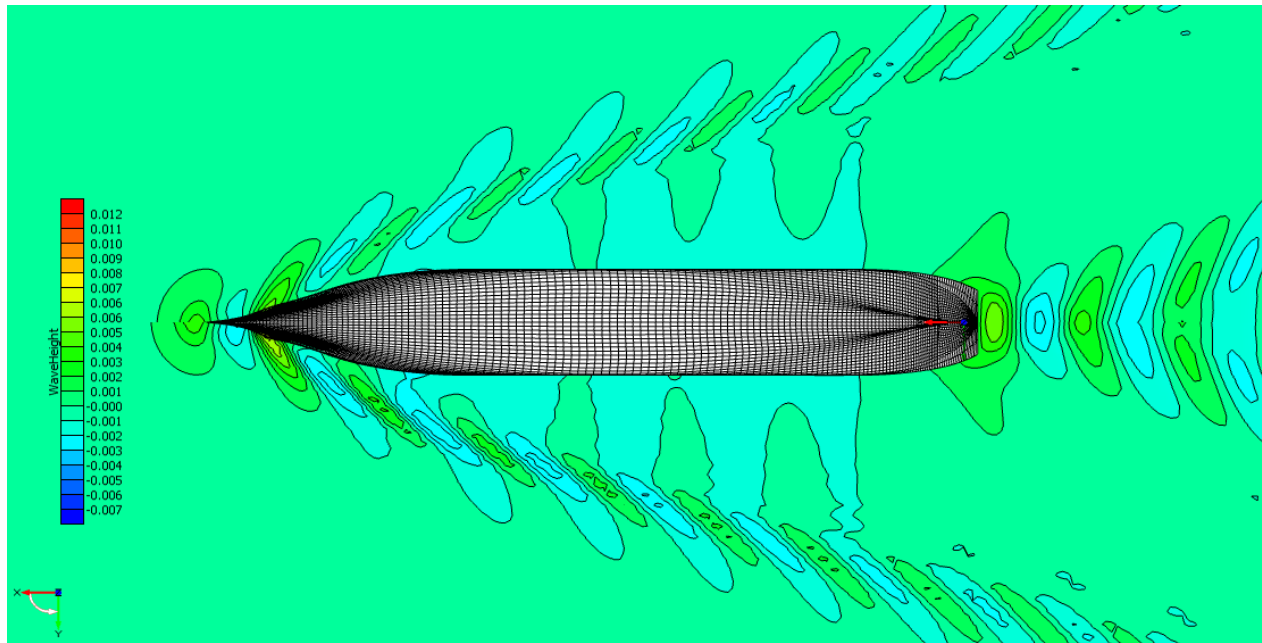
Figure 7.9: The figure illustrates the global wave pattern of the optimal bulb configuration in the upper part, and the global wave pattern of the original bulb configuration in the lower part at 18 knots.
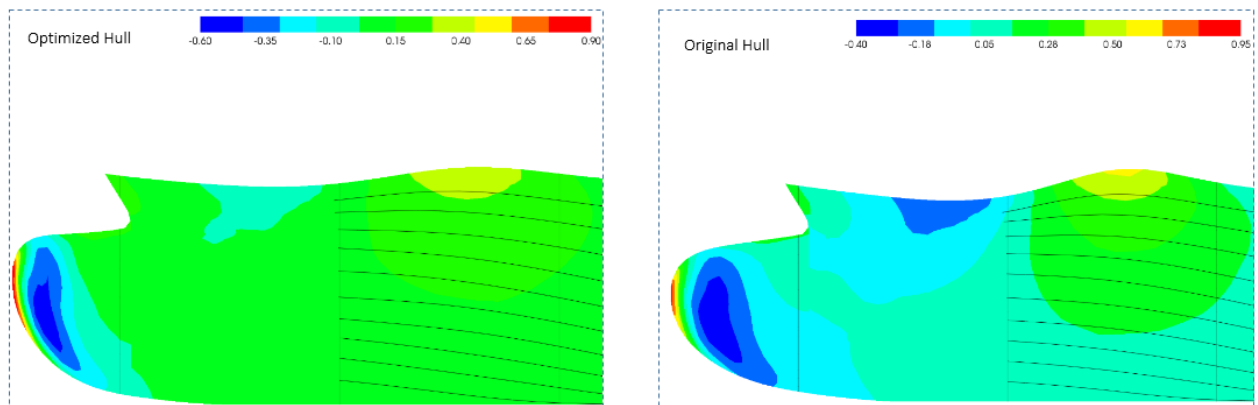

Figure 7.10: The figure shows the pressure coefficient on the hull as well as the wave elevation curvature at the top of the hull at 18 knots sailing speed. To the left: the optimal bulb configuration. To the right: original bulb configuration.

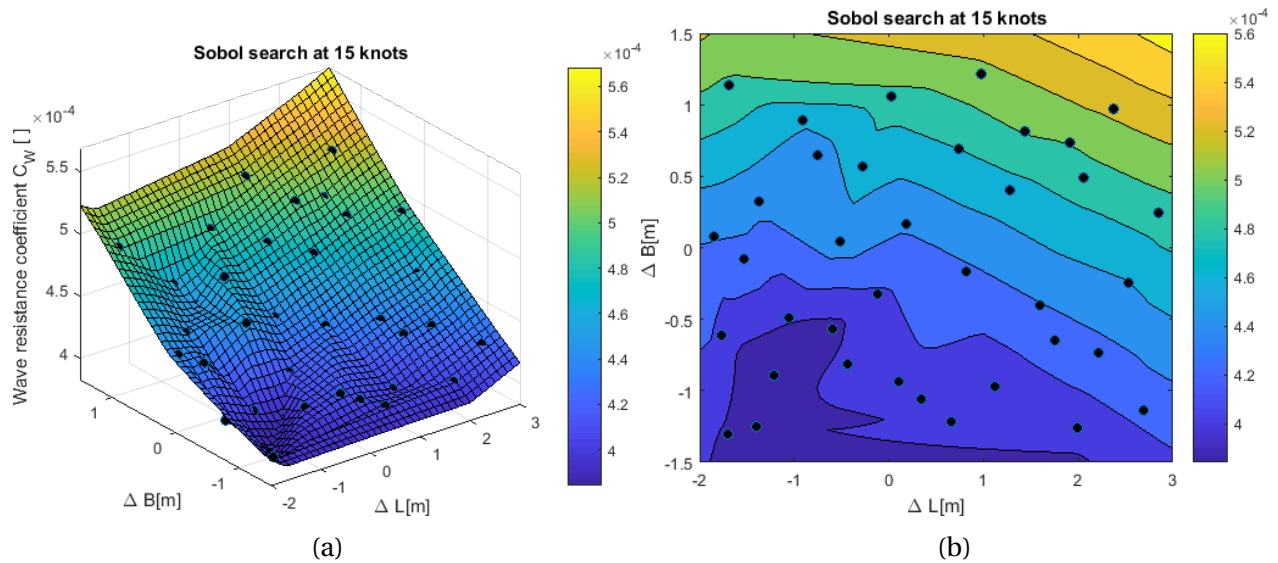### 7.2.5 True Optimum: 21 knots

(a)

(b)
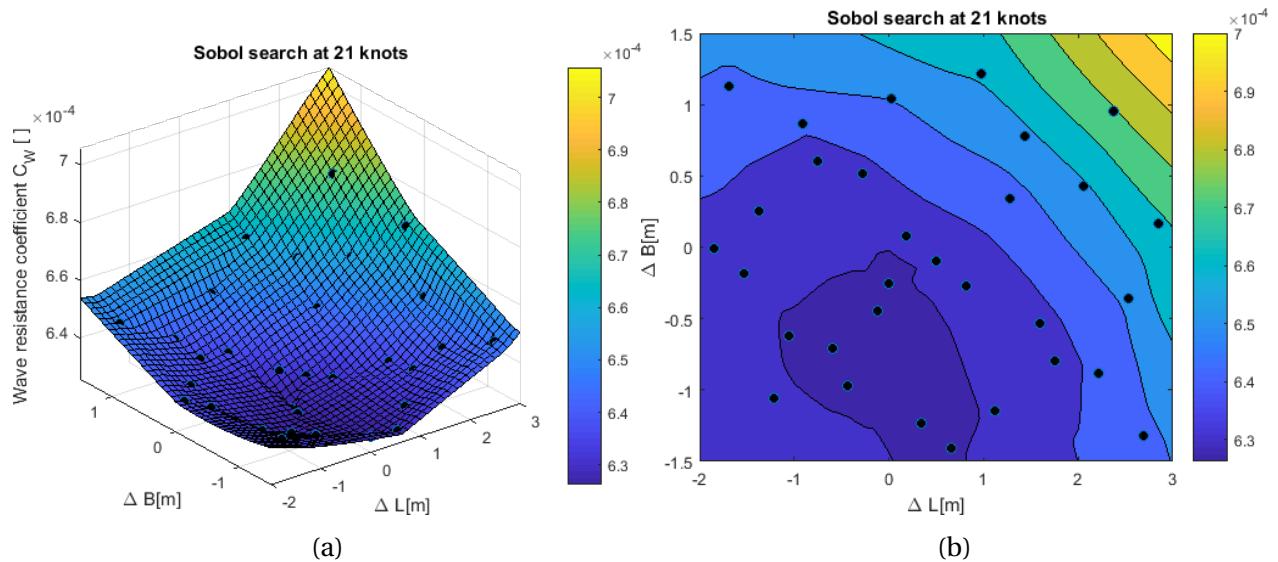
Figure 7.11: Figure (a) show the results from the Sobol search for the optimal bulb shape at 21 knots. In this figure an interpolated surface plane is added in order to illustrate the trend of the change in design variables. Figure (b) also show the results Sobol search for 21 knots in a 2D plot.
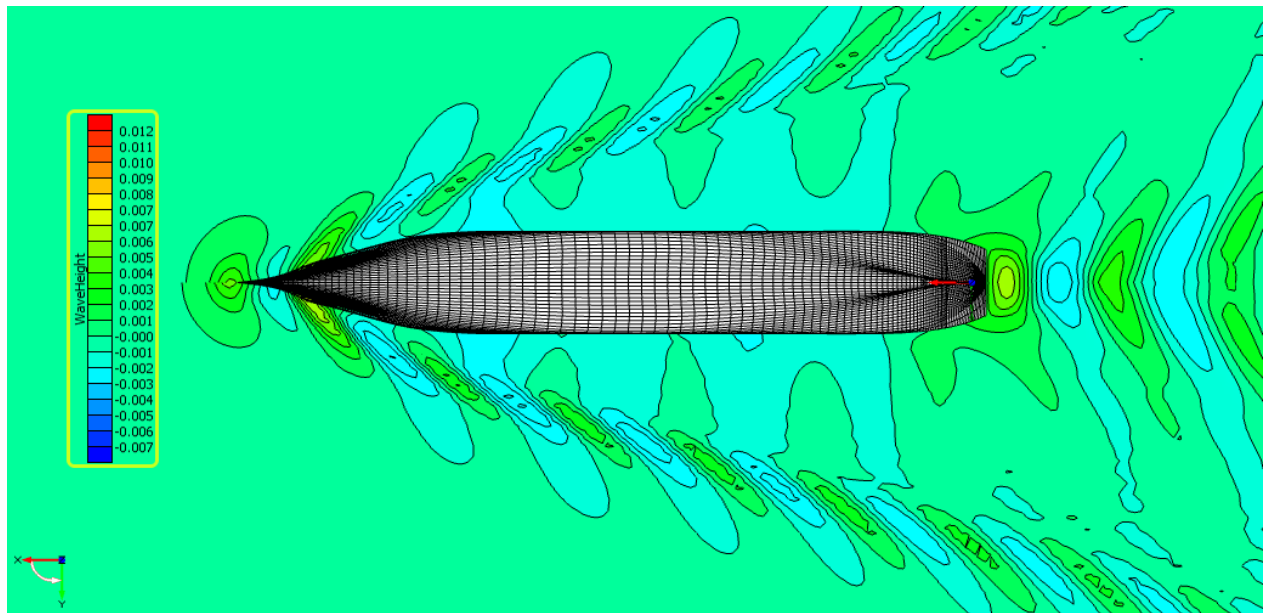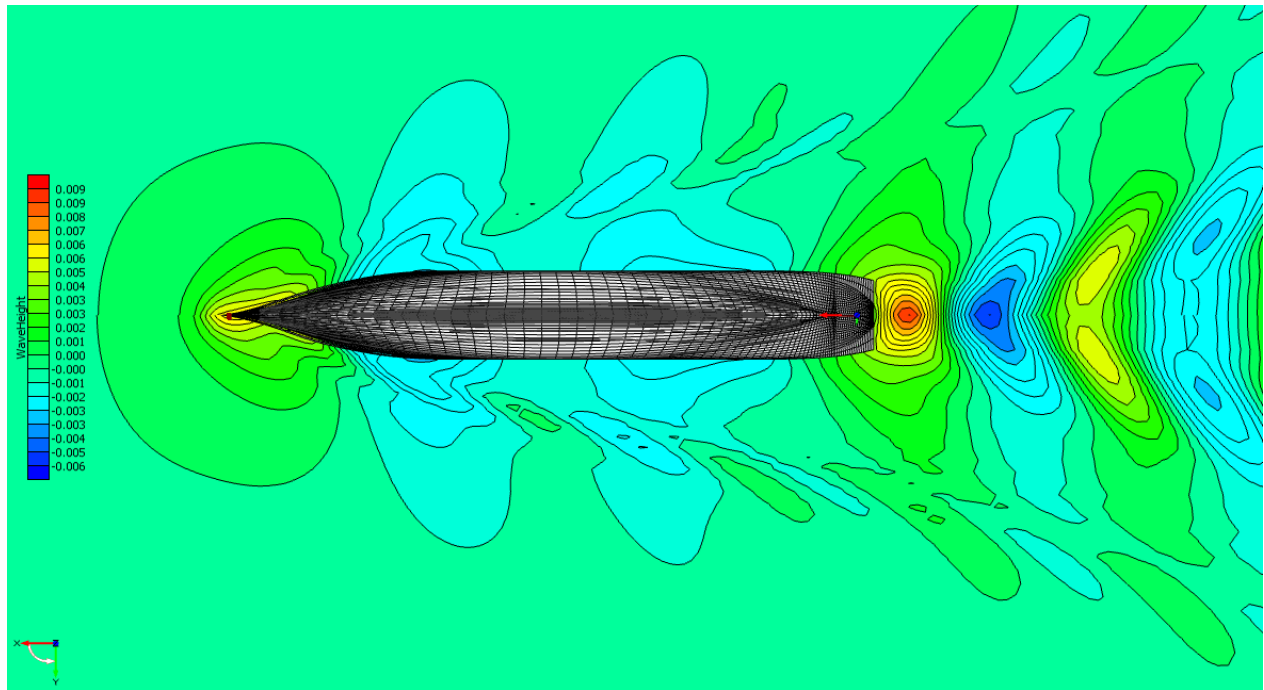

Figure 7.12: The figure illustrates the global wave pattern of the optimal bulb configuration in the upper part, and the global wave pattern of the original bulb configuration in the lower part at 21 knots.
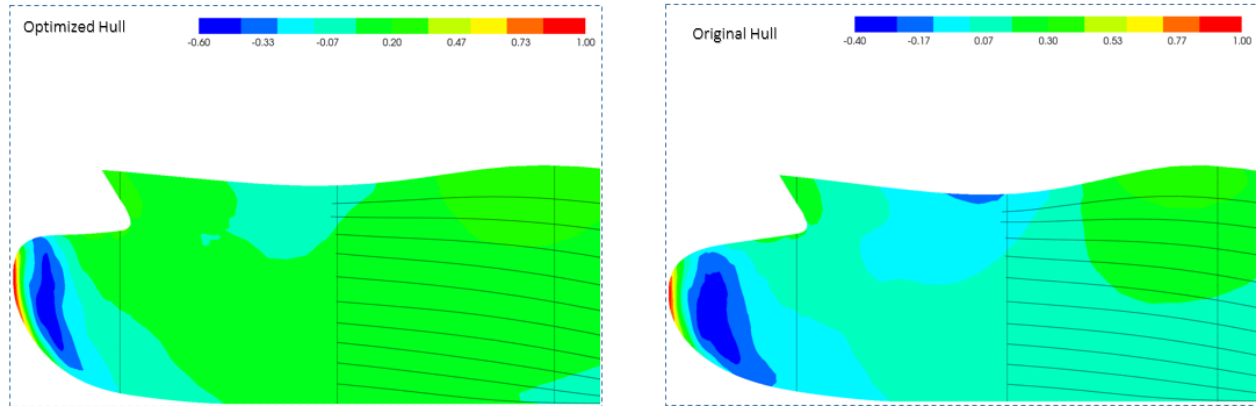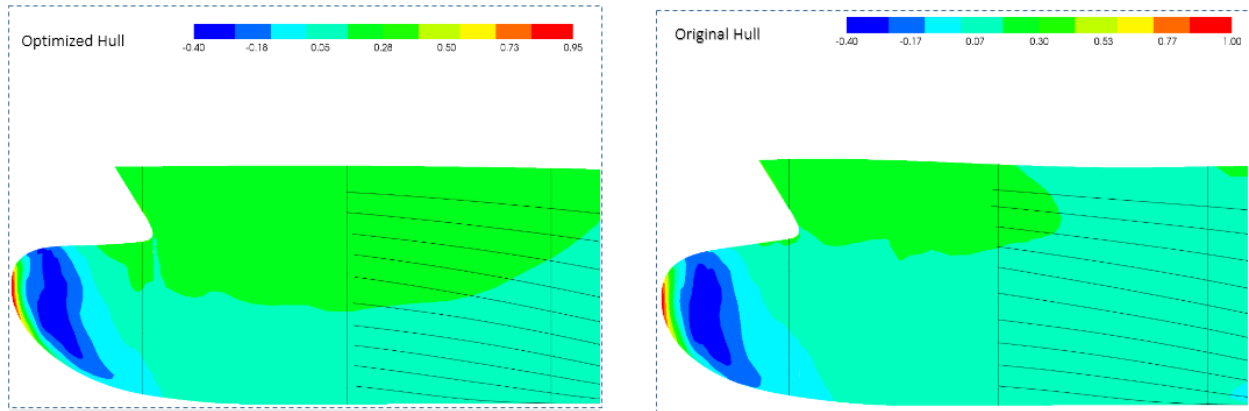
Figure 7.13: The figure shows the pressure coefficient on the hull as well as the wave elevation curvature at the top of the hull at 21 knots sailing speed. To the left: the optimal bulb configuration. To the right: original bulb configuration.

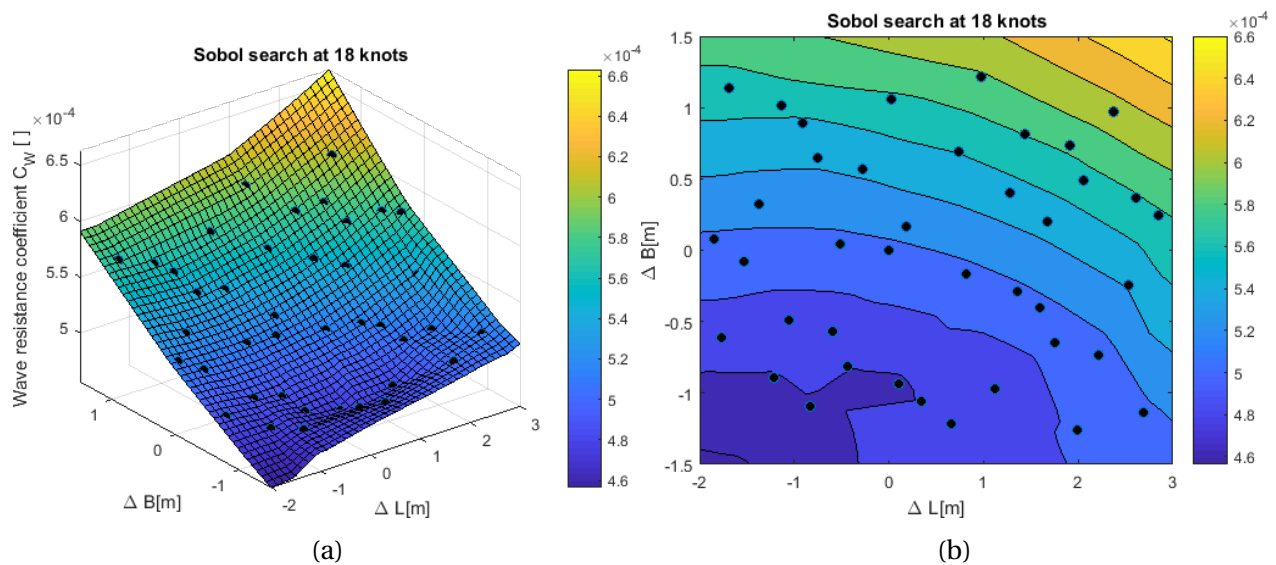### 7.2.6 True Optimum: 24 knots

(a)

(b)
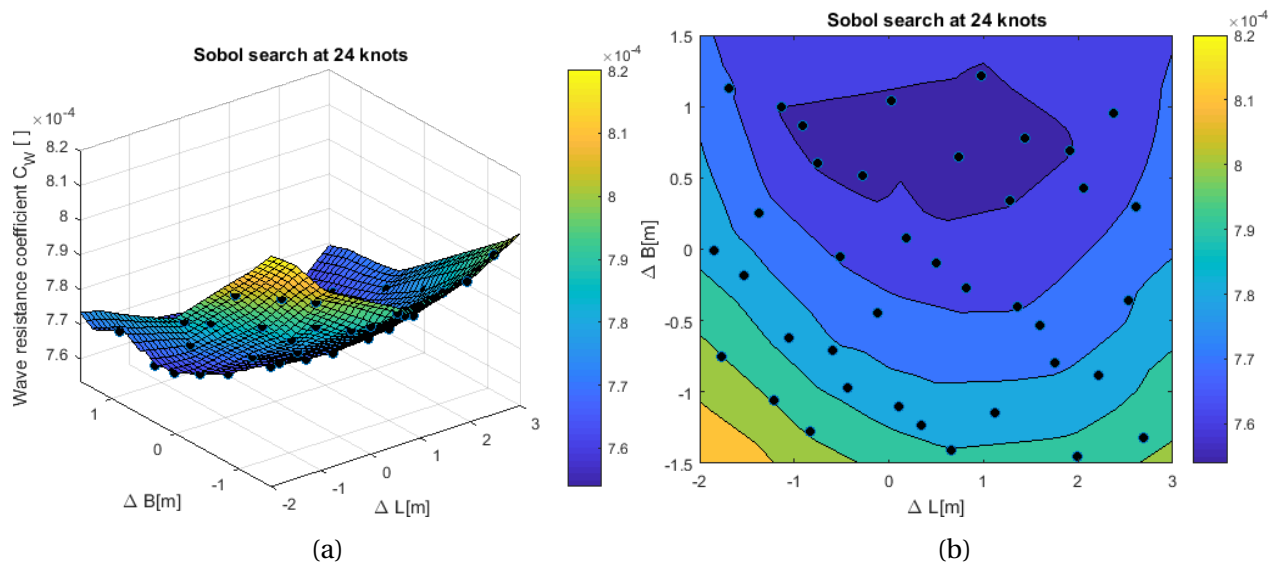
Figure 7.14: Figure (a) show the results from the Sobol search for the optimal bulb shape at 24 knots. In this figure an interpolated surface plane is added in order to illustrate the trend of the change in design variables. Figure (b) also show the results Sobol search for 24 knots in a 2D plot
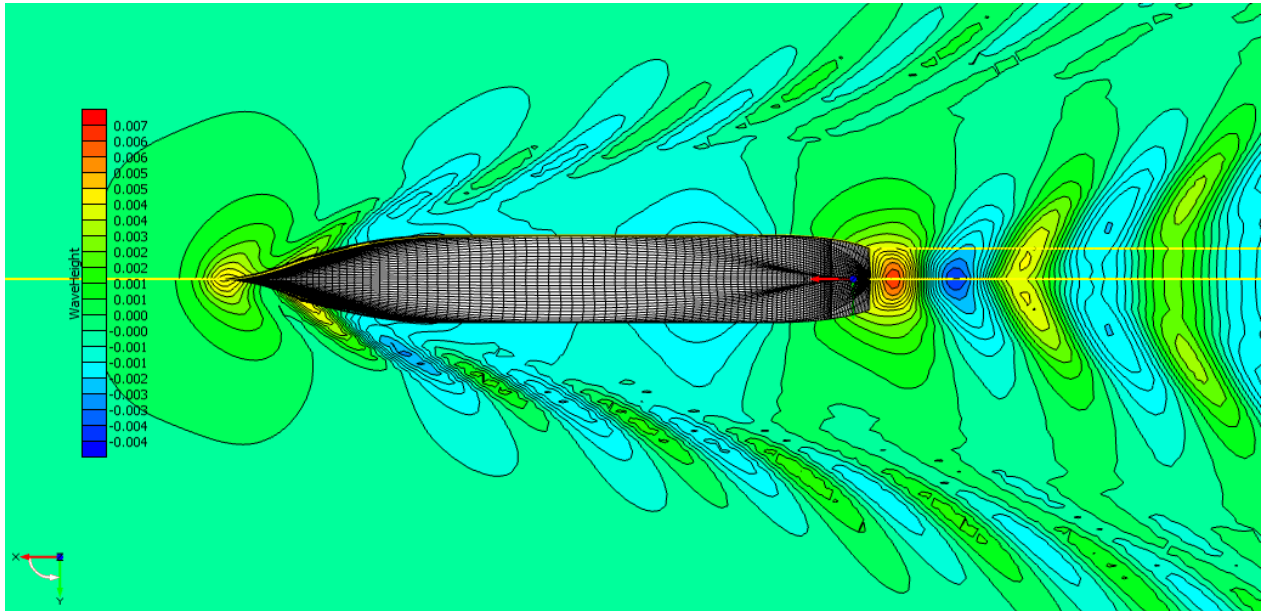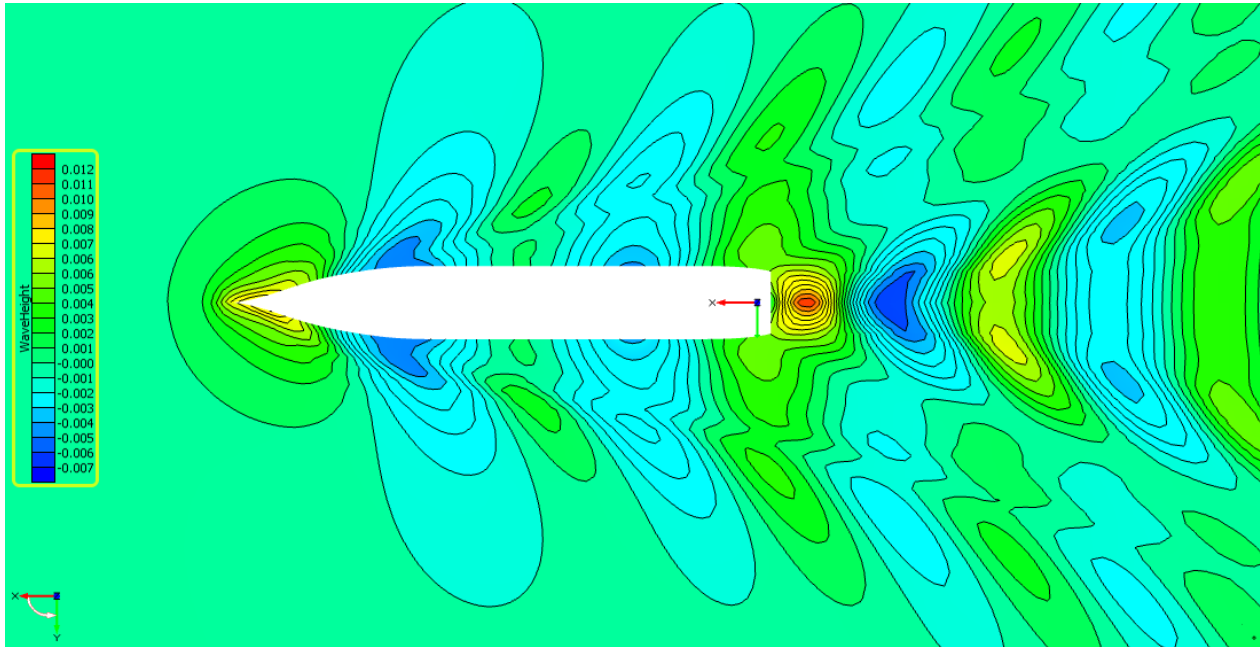
Figure 7.15: The figure illustrates the global wave pattern of the optimal bulb configuration in the upper part, and the global wave pattern of the original bulb configuration in the lower part at 24 knots.
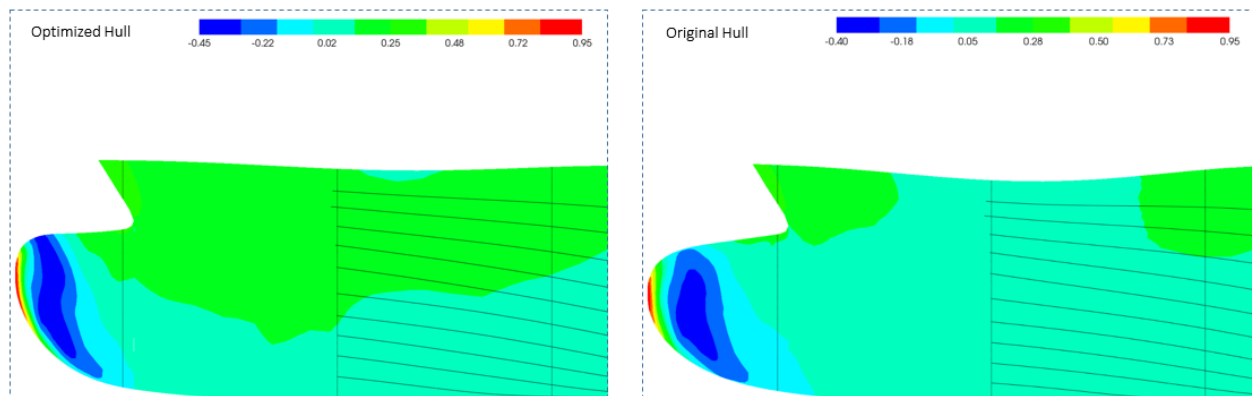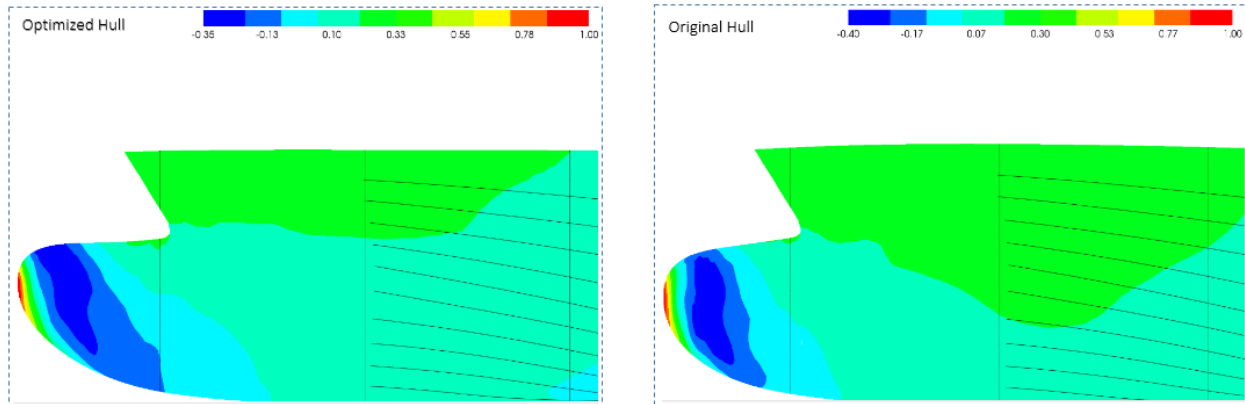

Figure 7.16: The figure shows the pressure coefficient on the hull as well as the wave elevation curvature at the top of the hull at 24 knots sailing speed. To the left: the optimal bulb configuration. To the right: original bulb configuration.

7.2.7 True Optimum Design: Best Candidates

The performance of the 5 true optimum bulb configurations, obtained from the T-search optimization, with respect to the effective power for the various speeds in the operational profile are presented in the figures below. Figure 7.17 show the performance of all the bulb candidates

for all speeds in the operating profile, while figure 7.18 show the performance of the optimum flexible design compared to the original bulb design. Figure 7.19 show the performance of the optimum flexible design compared to the robust bulb design. The optimum bulb design is allowed to change all design variables at each speed variation in order to always have superior performance criteria. Table 7.3 show the dimensions and the performance characteristics of the point optimized true optimum bulb configurations. Table 7.4 show the weighted effective power of the true optimum flexible bulb geometry for the two operating profiles. The γ OP1 and γ OP1 values represent the reduction in weighted effective power over operating profile 1 and 2 respectively compared to the robust design, and indicates the higher bond of potential savings by introducing flexibility in the bulb design.
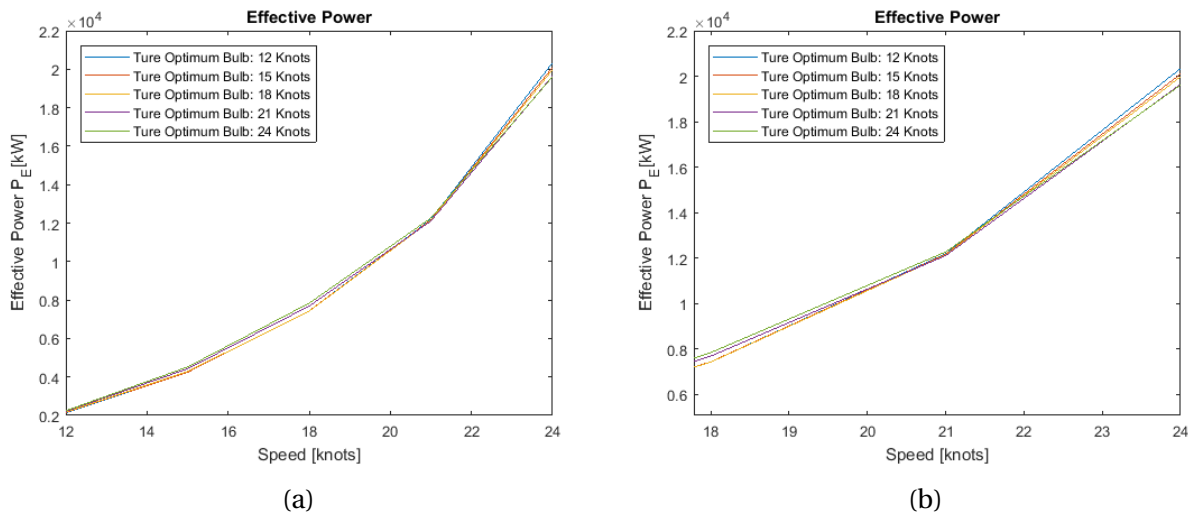
Figure 7.17: Figure (a) show the performance of the true optimum bulb configurations with respect to the effective power over the speeds in the operating profile in the lower speed regime. Figure (b) show the performance of the true optimum bulb configurations with respect to the effective power over the speeds in the operating profile in the higher speed regime.
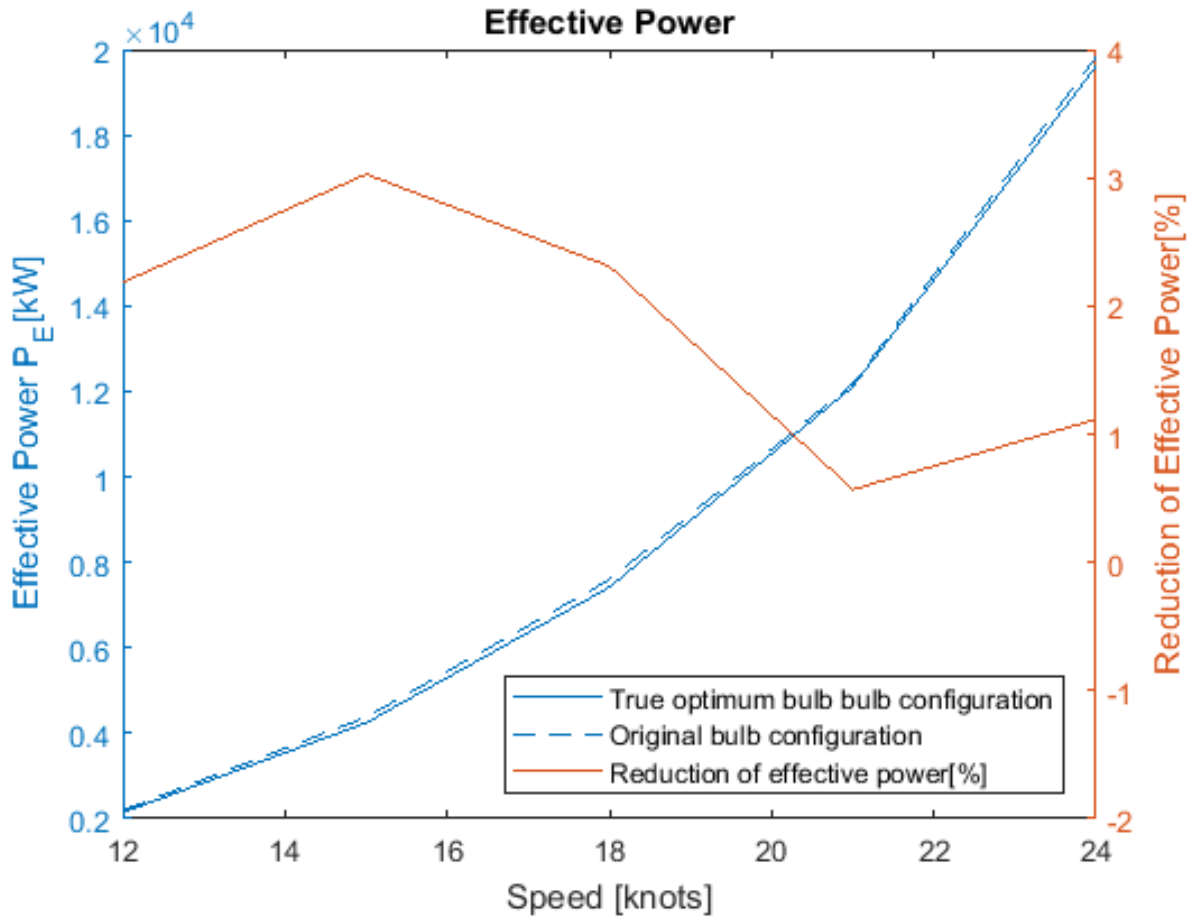
Figure 7.18: The performance of the true optimum flexible bulb configuration and the original bulb configuration with respect to the effective power over the speeds in the operating profile.

Table 7.3: The dimensions and the performance characteristics for the true optimum bulb design candidates.

Bulb optimized for [Kn]	$\Delta L[m]$	$\Delta B[m]$	$\Delta Z[m]$	$P_E[kW]$	P_{E_w} OP1 [kW]	P_{E_w} OP2 [kW]
12.00	-1.45	-1.32	0.60	2145.31	386.16	10.73
15.00	-1.23	-0.85	0.60	4243.95	1612.70	509.27
18.00	-1.00	-1.04	0.70	7420.11	2893.84	2300.23
21.00	-0.51	-0.55	0.80	12108.54	484.34	4722.33
24.00	0.74	0.49	1.00	19612.31	196.12	3432.15
Sum					5573.16	10974.72

Table 7.4: The performance characteristics for the true optimum flexible bulb design.

	P_{E_w} OP1[kW]	P_{E_w} OP2[kW]	γ OP1[%]	γ OP1[%]
Ture Optimum Bulb	5573.16	10974.72	0.25	1.00

Figure 7.19: Comparison of the effective power for the true optimum flexible bulb configuration and the robust bulb configuration.

7.3 Flexible Bulb Design

The height parameter ΔZ and the breadth parameter ΔB for the five bulbs to be evaluated with a change in the length parameter ΔL during operation are listed in table 7.3. The performance of the five flexible bulb candidates will be presented below. The candidates are now numbered from 1 to 5, corresponding to the true optimum bulb candidates designed for 12 to 24 knots

respectively. For each configuration, the wave resistance coefficient for all the length parameters the bulb can be subjected to is presented to illustrate how the flexibility can take advantage of the change in speed by changing the length. The performance of each bulb candidate with respect to the effective power is compared to the best robust bulb configuration and the original bulb configuration to show the potential of the flexible bulb design.

The tabulated values for the effective power for each flexible bulb configuration is found in the tables below. These tables are included to show how the best length parameter of the bulb are different for the different speeds in the operating profile. The green values represent the best length configuration for the flexible bulb configurations at each speed in the operating profile. The values in the table represent the effective power for their respective bulb configuration at each speed in the operating profile and for each length configuration.

7.3.1 Flexible Bulb Configuration 1

Figure 7.20: Wave resistance coefficient for all length variations of flexible bulb configuration 1.

	12 [Knots]	15 [Knots]	18 [Knots]	21 [Knots]	24 [Knots]
Delta L = -1.50 [m]	2145.31 [kW]	4249.72 [kW]	7428.04 [kW]	12191.18 [kW]	20336.72 [kW]
Delta L = -1.00 [m]	2153.10 [kW]	4242.77 [kW]	7410.66 [kW]	12179.03 [kW]	20165.59 [kW]
Delta L = -0.50 [m]	2158.79 [kW]	4248.53 [kW]	7417.64 [kW]	12147.13 [kW]	20085.15 [kW]
Delta L = -0.00 [m]	2167.22 [kW]	4258.74 [kW]	7432.71 [kW]	12167.19 [kW]	20042.99 [kW]
Delta L = -0.50 [m]	2179.10 [kW]	4271.91 [kW]	7456.06 [kW]	12197.64 [kW]	20022.12 [kW]

Figure 7.21: The tabulated values for the effective power in kW for flexible bulb configuration 1.The green cells represent the best length configuration at the given speed.

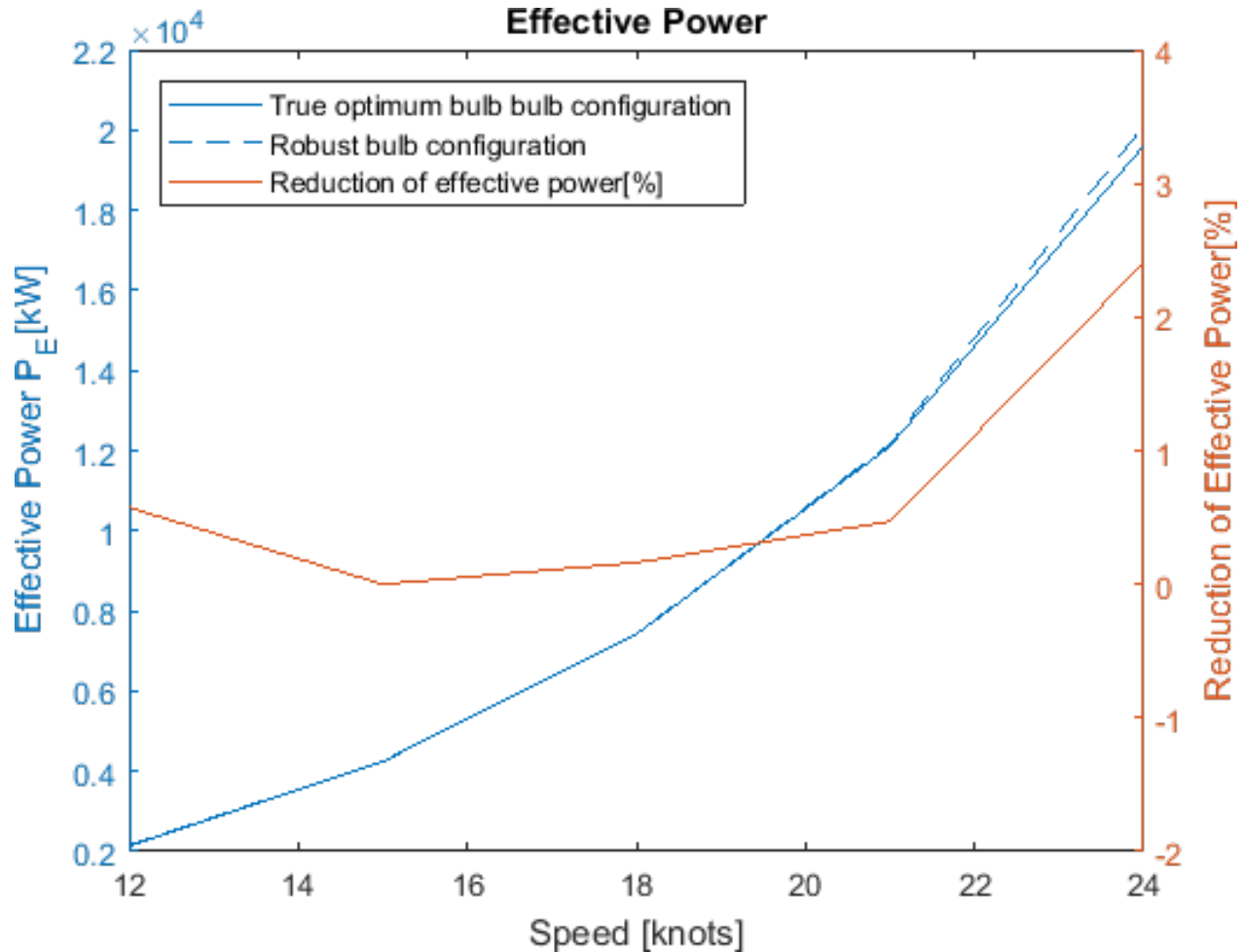Figure 7.22: Figure (a): Comparison of the effective power for the flexible bulb configuration 1 and the robust bulb configuration. Figure (b): Comparison of the effective power for the flexible bulb configuration 1 and the original bulb configuration.

7.3.2 Flexible Bulb Configuration 2

Figure 7.23: Wave resistance coefficient for all length variations of flexible bulb configuration 2.

	12 [Knots]	15 [Knots]	18 [Knots]	21 [Knots]	24 [Knots]
Delta L = -1.50 [m]	2157.47[kW]	4267.95 [kW]	7447.67 [kW]	12175.51 [kW]	20263.25 [kW]
Delta L = -1.00 [m]	2157.72[kW]	4243.95 [kW]	7432.14 [kW]	12165.86 [kW]	20095.66 [kW]
Delta L = -0.50 [m]	2163.14[kW]	4267.39 [kW]	7437.26 [kW]	12139.28 [kW]	20016.89 [kW]
Delta L = -0.00 [m]	2171.56 [kW]	4277.45 [kW]	7456.07 [kW]	12159.83 [kW]	19979.61 [kW]
Delta L = -0.50 [m]	2182.99 [kW]	4290.78 [kW]	7480.38 [kW]	12194.78 [kW]	19965.72 [kW]

Figure 7.24: The tabulated values for the effective power in kW for flexible bulb configuration 2. The green cells represent the best length configuration at the given speed.

(a)

(b)

Figure 7.25: Figure (a): Comparison of the effective power for the flexible bulb configuration 2 and the robust bulb configuration. Figure (b): Comparison of the effective power for the flexible bulb configuration 2 and the original bulb configuration.
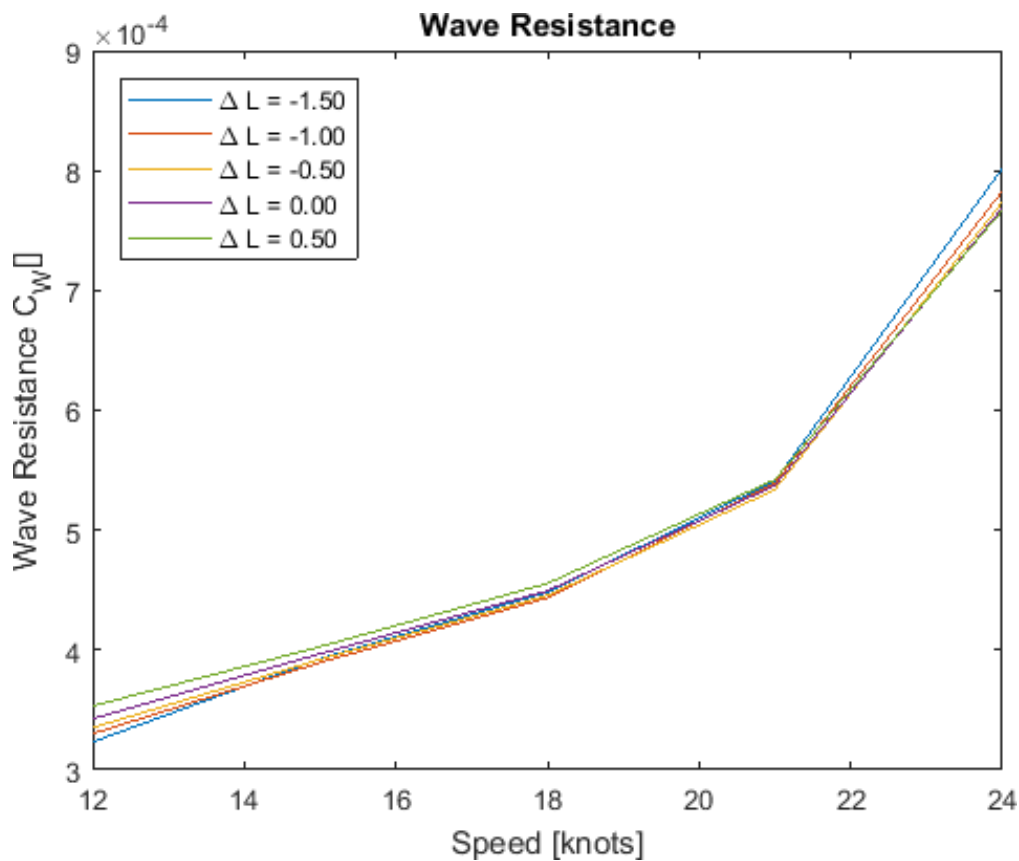
7.3.3 Flexible Bulb Configuration 3

Figure 7.26: Wave resistance coefficient for all length variations of flexible bulb configuration 3.

	12 [Knots]	15 [Knots]	18 [Knots]	21 [Knots]	24 [Knots]
Delta L = -1.50 [m]	2157.47[kW]	4267.95 [kW]	7447.67 [kW]	12175.51 [kW]	20263.25 [kW]
Delta L = -1.00 [m]	2157.72[kW]	4243.95 [kW]	7432.14 [kW]	12165.86 [kW]	20095.66 [kW]
Delta L = -0.50 [m]	2163.14[kW]	4267.39 [kW]	7437.26 [kW]	12139.28 [kW]	20016.89 [kW]
Delta L = -0.00 [m]	2171.56 [kW]	4277.45 [kW]	7456.07 [kW]	12159.83 [kW]	19979.61 [kW]
Delta L = -0.50 [m]	2182.99 [kW]	4290.78 [kW]	7480.38 [kW]	12194.78 [kW]	19965.72 [kW]

Figure 7.27: The tabulated values for the effective power in kW for flexible bulb configuration 3. The green cells represent the best length configuration at the given speed.
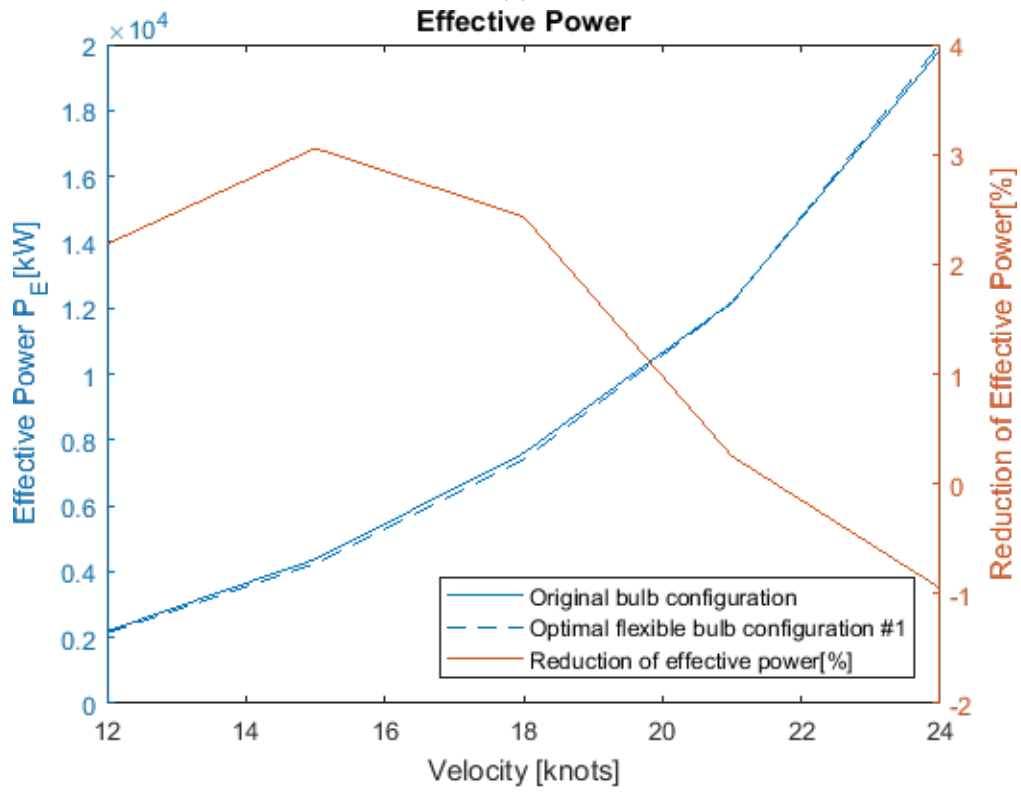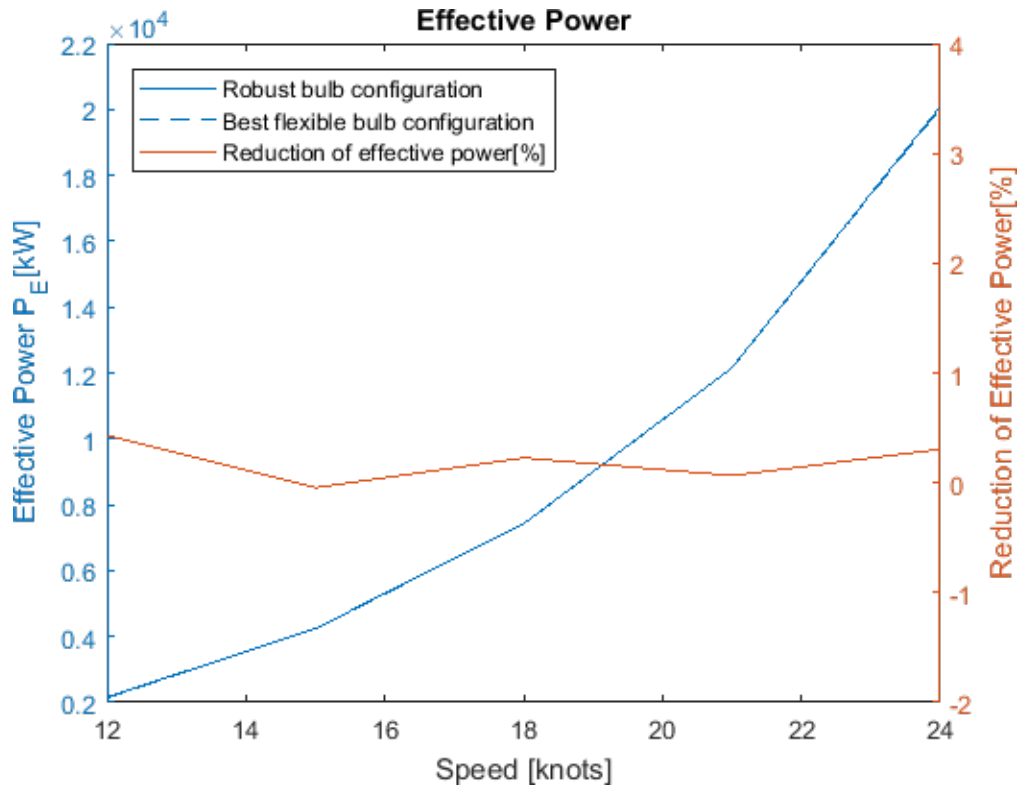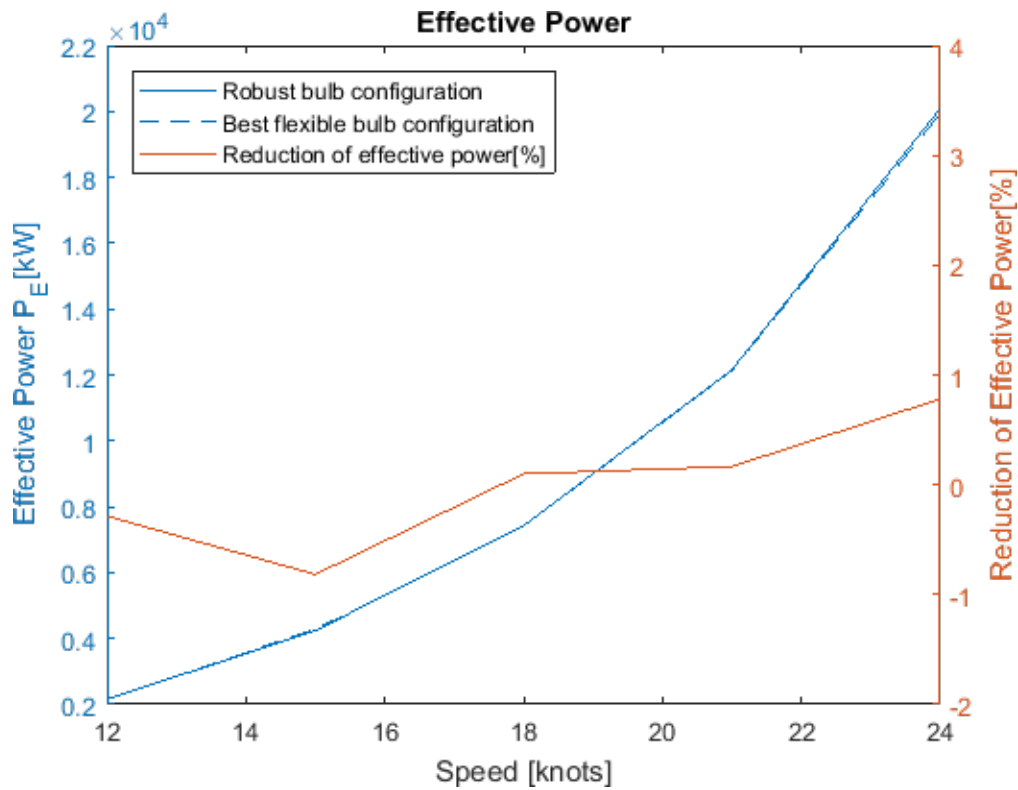
(a)
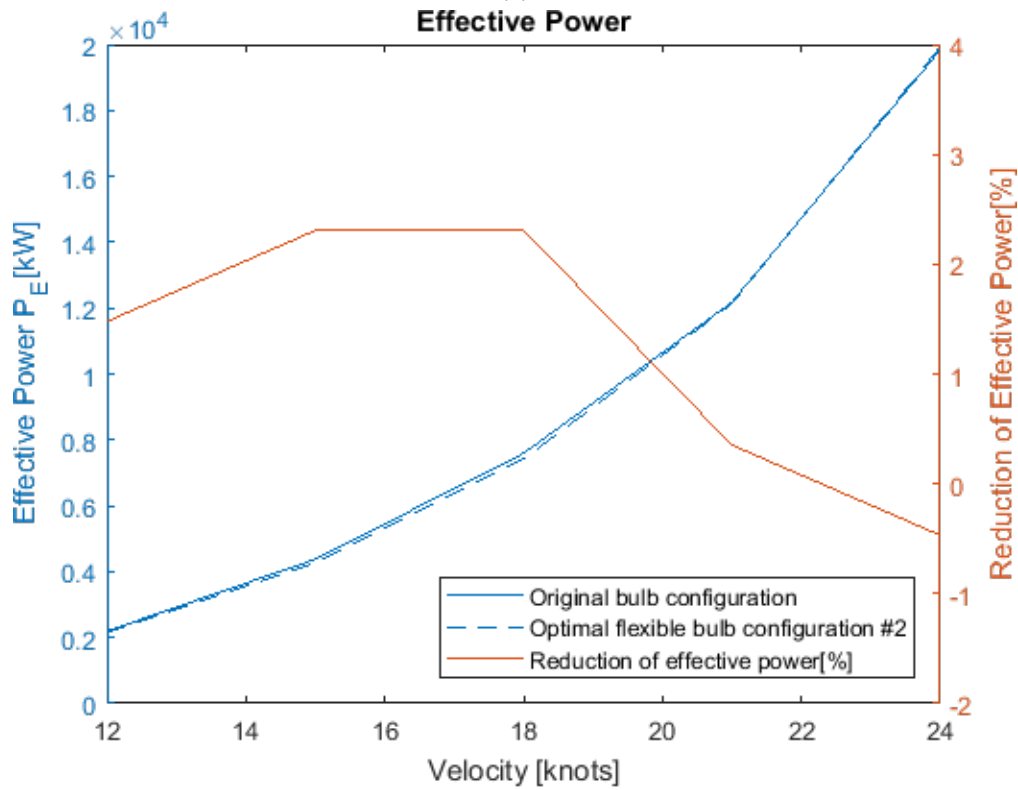
(b)

Figure 7.28: Figure (a): Comparison of the effective power for the flexible bulb configuration 3 and the robust bulb configuration. Figure (b): Comparison of the effective power for the flexible bulb configuration 3 and the original bulb configuration.

7.3.4 Flexible Bulb Configuration 4
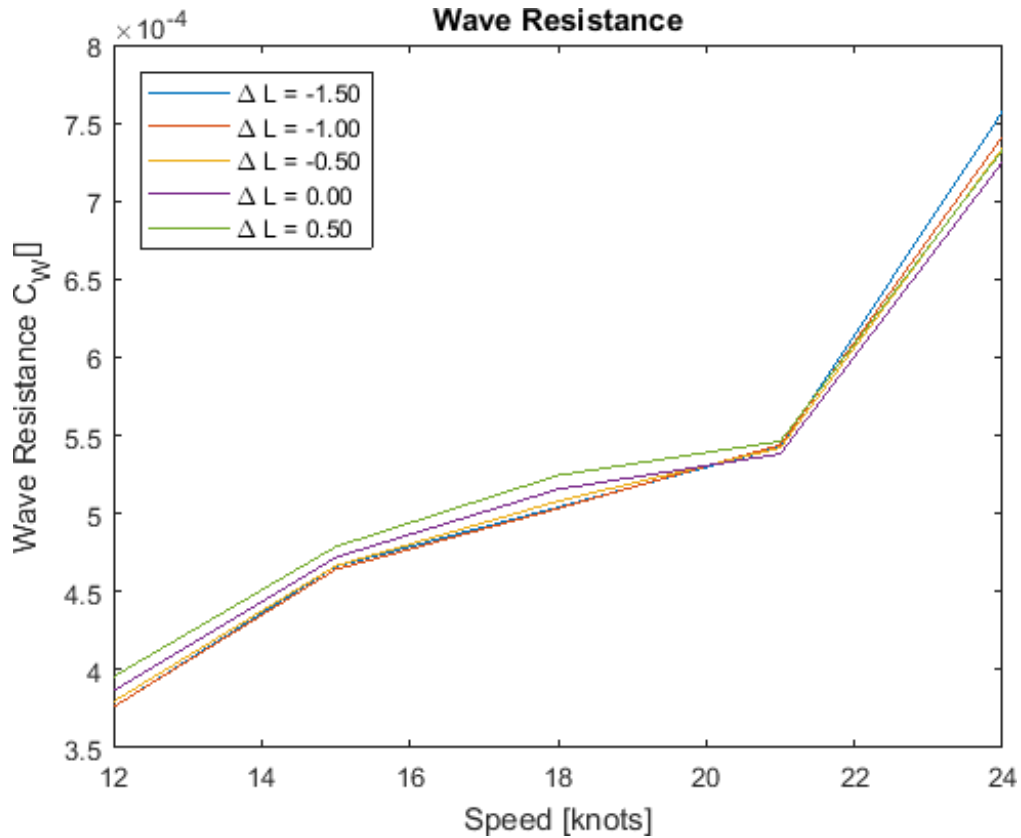
Figure 7.29: Wave resistance coefficient for all length variations of flexible bulb configuration 4.

	12 [Knots]	15 [Knots]	18 [Knots]	21 [Knots]	24 [Knots]
Delta L = -1.50 [m]	2204.77 [kW]	4411.36 [kW]	7640.02[kW]	12134.23 [kW]	19938.00 [kW]
Delta L = -1.00 [m]	2204.90 [kW]	4407.08 [kW]	7636.85 [kW]	12142.97 [kW]	19794.18 [kW]
Delta L = -0.50 [m]	2208.79 [kW]	4412.19 [kW]	7654.94 [kW]	12131.65 [kW]	19728.21 [kW]
Delta L = -0.00 [m]	2216.44 [kW]	4424.22 [kW]	7683.91 [kW]	12108.54 [kW]	19647.33 [kW]
Delta L = -0.50 [m]	2226.69 [kW]	4439.07 [kW]	7717.78 [kW]	12156.47 [kW]	19715.87 [kW]

Figure 7.30: The tabulated values for the effective power in kW for flexible bulb configuration 4. The green cells represent the best length configuration at the given speed.
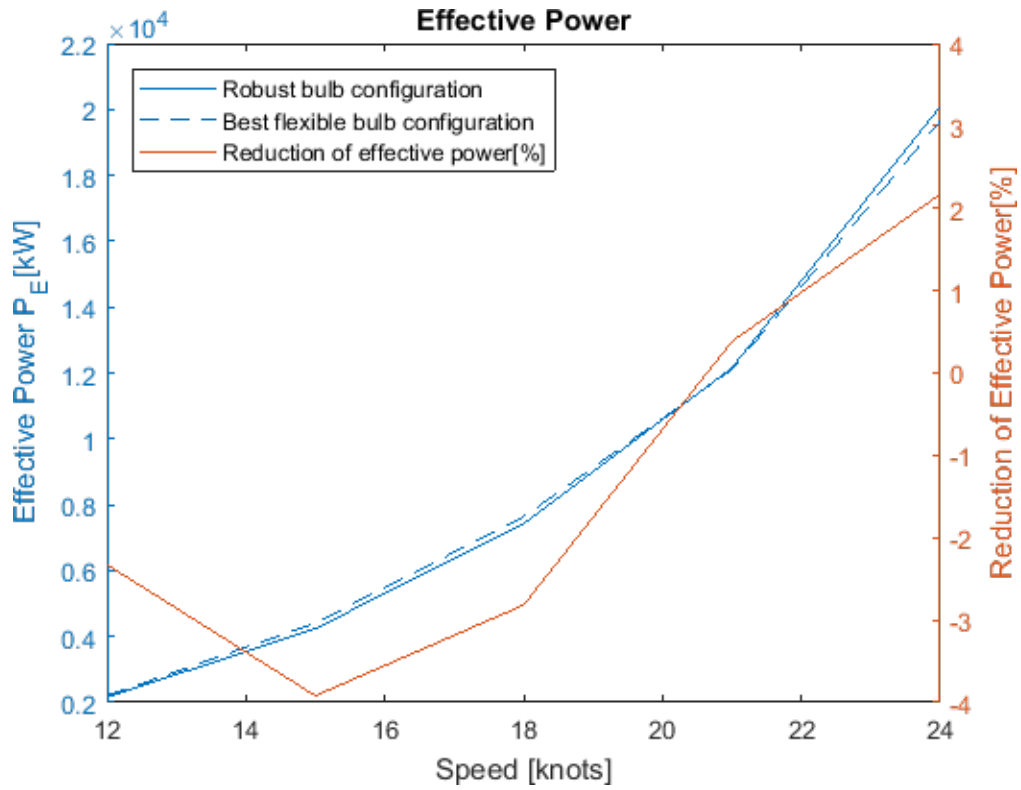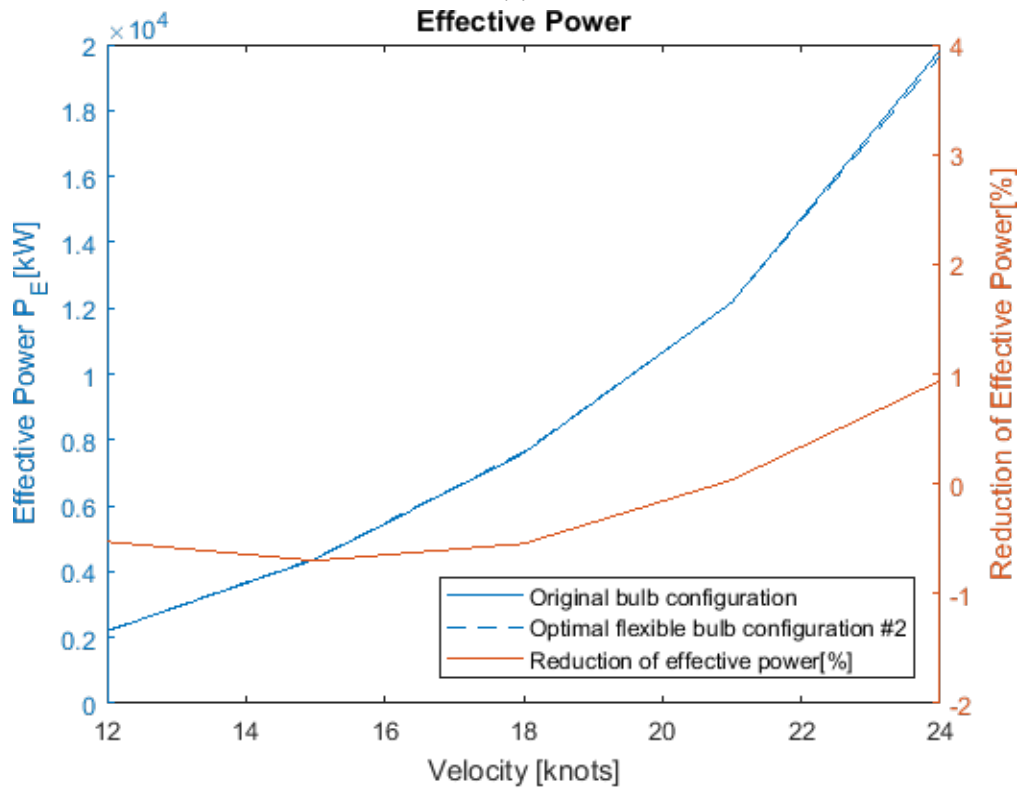
Figure 7.31: Figure (a): Comparison of the effective power for the flexible bulb configuration 4 and the robust bulb configuration. Figure (b): Comparison of the effective power for the flexible bulb configuration 4 and the original bulb configuration.
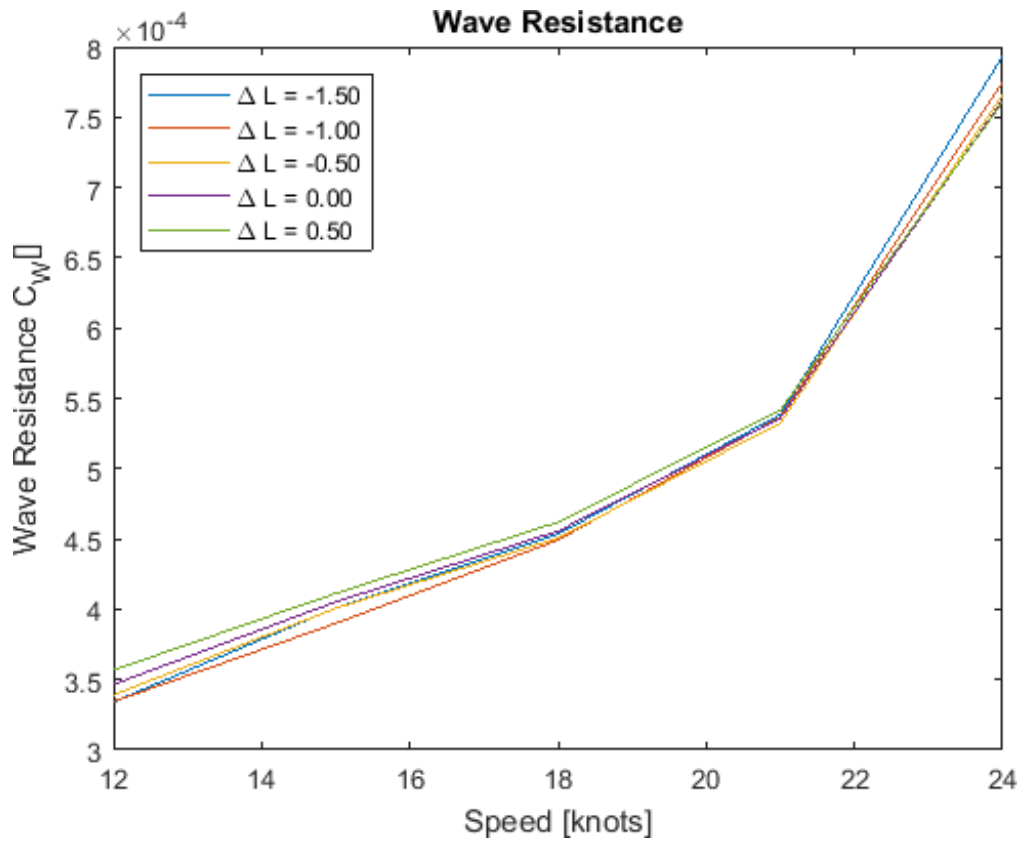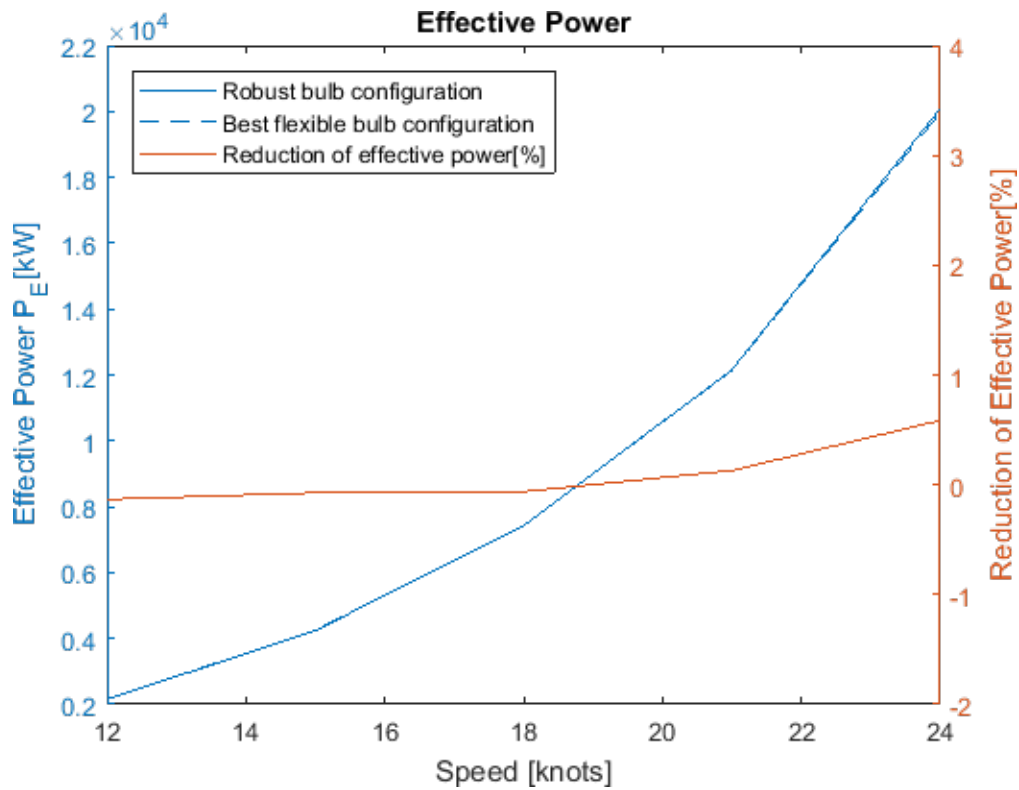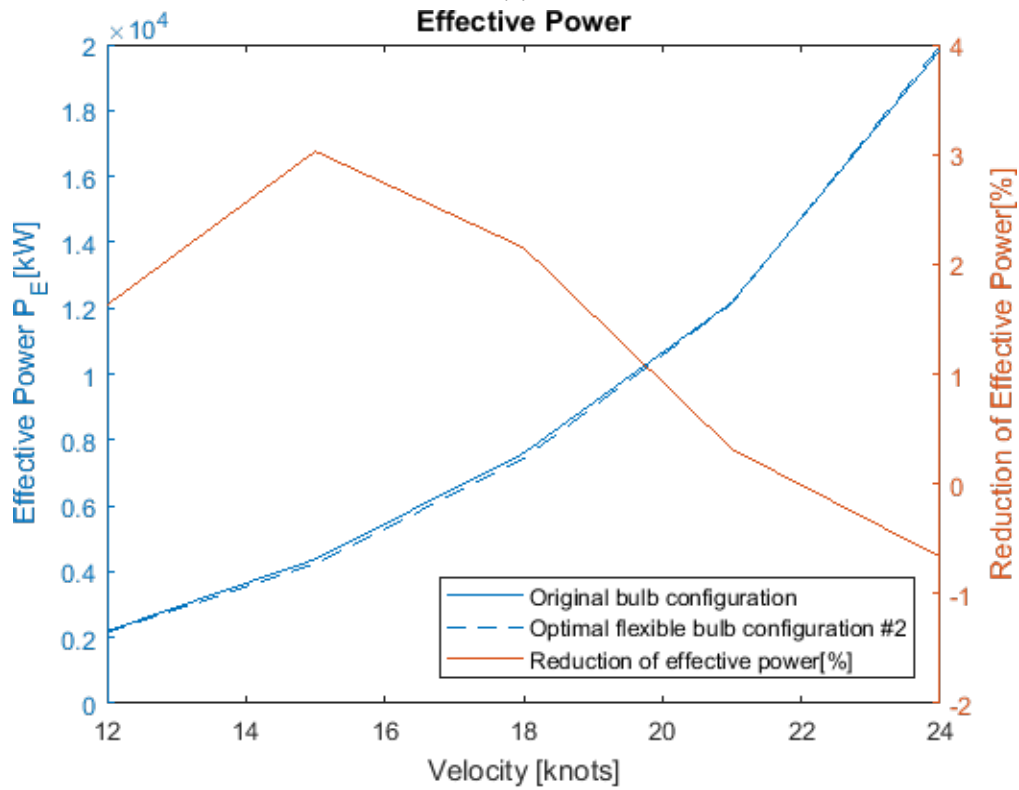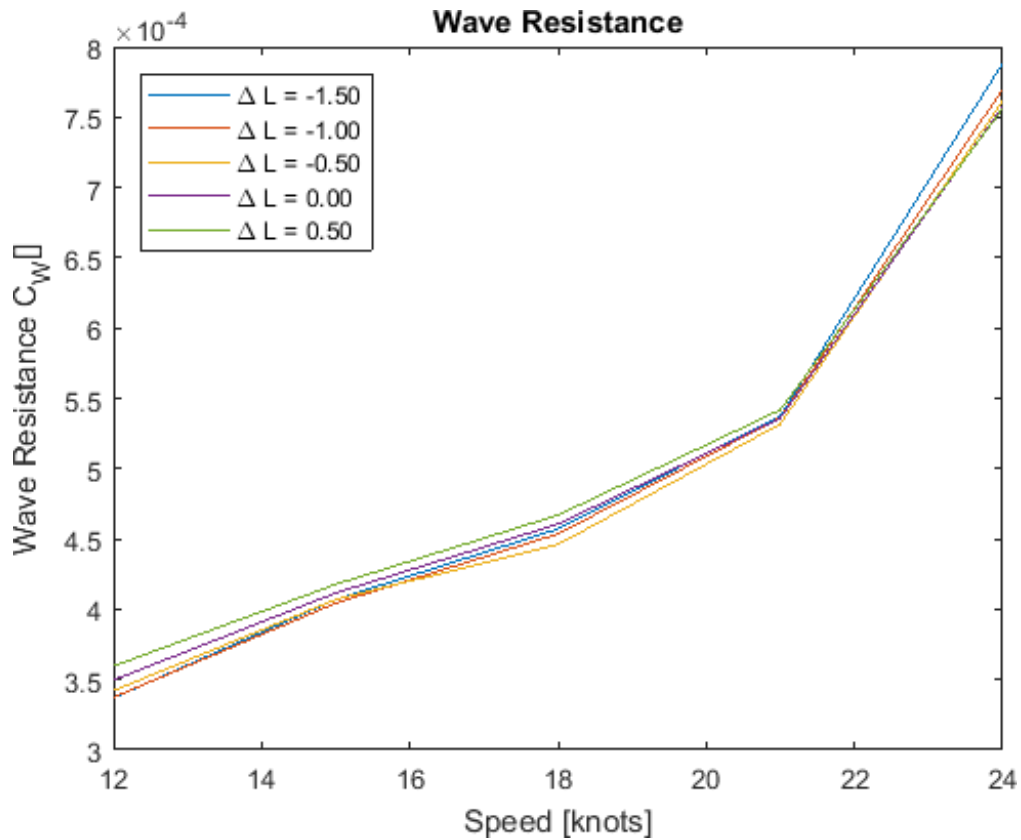
7.3.5 Flexible Bulb Configuration 5
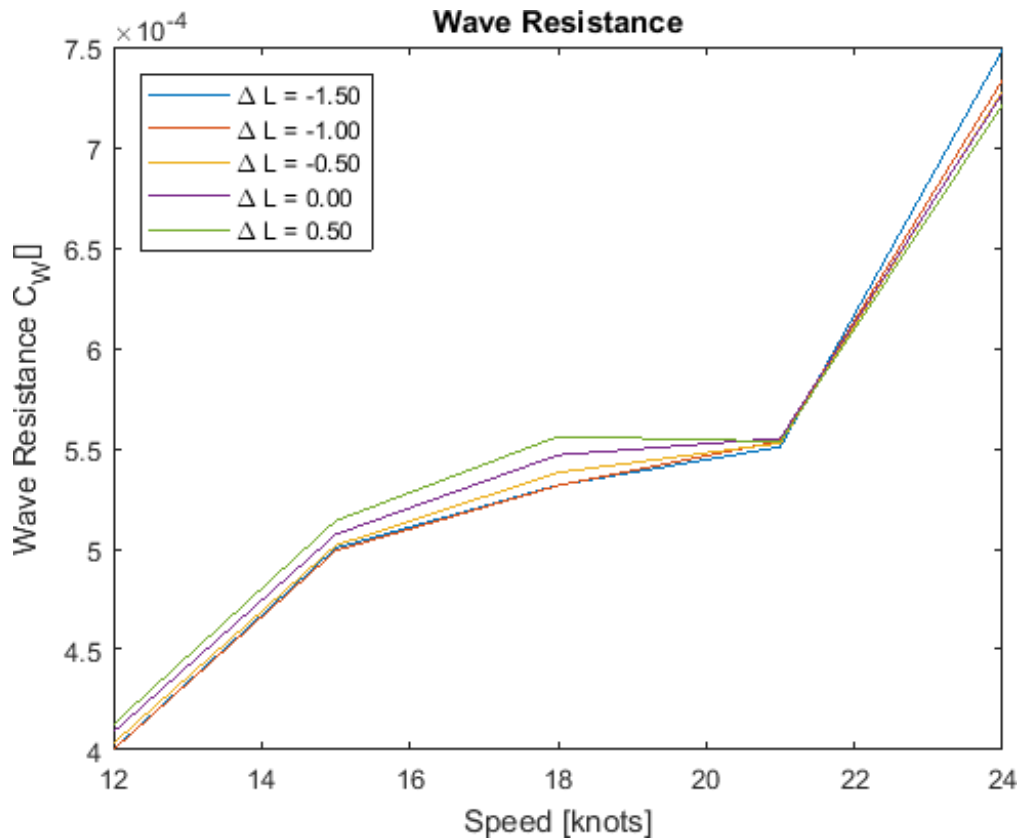
Figure 7.32: Wave resistance coefficient for all length variations of flexible bulb configuration 5.

	12 [Knots]	15 [Knots]	18 [Knots]	21 [Knots]	24 [Knots]
Delta L = -1.50 [m]	2231.98[kW]	4486.76[kW]	7745.54[kW]	12249.64[kW]	19858.79[kW]
Delta L = -1.00 [m]	2231.75[kW]	4483.85[kW]	7744.89[kW]	12267.63[kW]	19722.41[kW]
Delta L = -0.50 [m]	2235.43[kW]	4489.60[kW]	7769.51[kW]	12261.30[kW]	19671.84[kW]
Delta L = -0.00 [m]	2241.69[kW]	4501.66[kW]	7802.55[kW]	12275.98[kW]	19662.66[kW]
Delta L = -0.50 [m]	2246.12[kW]	4516.70[kW]	7837.80[kW]	12266.59[kW]	19612.31[kW]

Figure 7.33: The tabulated values for the effective power in kW for flexible bulb configuration 5. The green cells represent the best length configuration at the given speed.
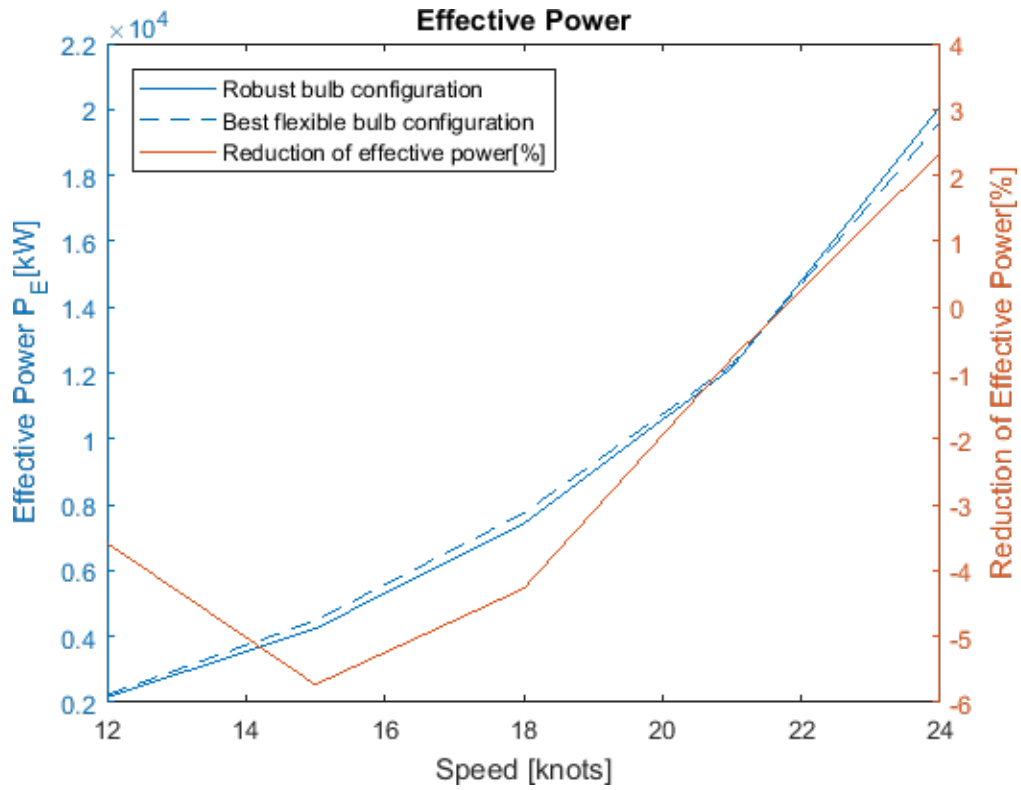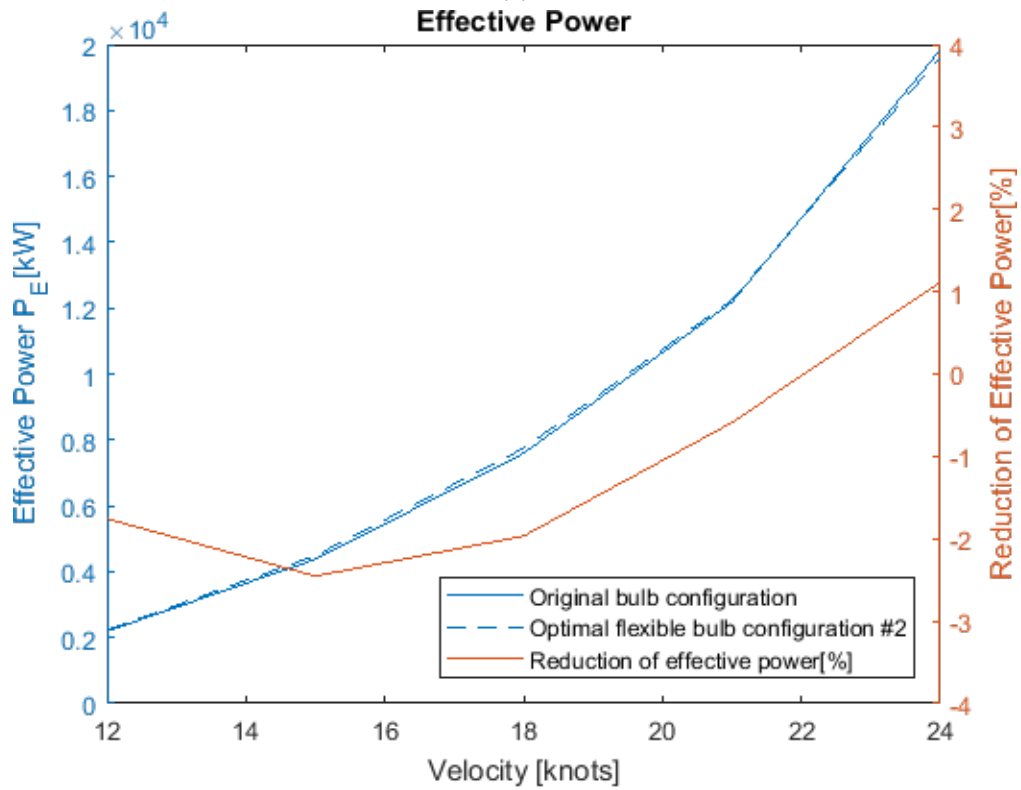
Figure 7.34: Figure (a): Comparison of the effective power for the flexible bulb configuration 5 and the robust bulb configuration. Figure (b): Comparison of the effective power for the flexible bulb configuration 5 and the original bulb configuration.

7.3.6   Overall Performance of the Flexible Bulb Configurations

The overall performance for the flexible bulb configurations are listed in table 7.5.The values γ OP1 and γ OP2 represent the reduction in the weighted effective power for the flexible bulb configuration compared to the robust bulb configuration, thus indicating the potential of the flexible bulb design.

Table 7.5: The performance characteristics of the 5 flexible bulb configurations.

Bulb Configuration #	P_{E_w} OP1[kW]	P_{E_w} OP2 [kW]	γ OP1[%]	γ OP1[%]
1	5574.67	11058.41	0.22	0.24
2	5584.81	11052.34	0.04	0.30
3	5592.12	11043.80	-0.09	0.38
4	5730.73	11067.91	-2.57	0.16
5	5812.66	11164.20	-4.04	-0.71

Chapter 8

Discussion

As section 2.3 showed, bulb design depends heavily on the operating conditions as well as the requirements the ship in question is exposed to. Optimal bulb geometry varies across different operating conditions and ship types, hence, the design of bulb is closely attached to analyses of the uncertainties in the operating profile. From the taxonomy of the various bulb designs and their typical operating profile, it is clear that the large variance in sailing speed and displacement in the operating profile for the container vessel segment propose an untapped potential for resistance reduction of the ship with the introduction of flexibility in the bulb design.

To investigate the potential of the flexible bulb design, the modern container ship, KCS coupled with a typical slow steaming profile was studied with fully non linear potential theory simulations with free surface for a set of five speed configurations ranging from 12-24 knots, weighted corresponding to a typical slow steaming profile. The simulations were performed with the commercial panel code SHIPFLOW within the CAESES framework.

8.1   Robust Bulb Configuration

The particle swarm optimization procedure performed to obtain the ideal robust bulb configuration resulted in a bulb with main dimensions corresponding to a length parameter of $\Delta L = -1.05$, a breadth parameter of $\Delta B = -0.85$ and a height parameter of $\Delta Z = -0.90$. As presented in section 7.1 the robust optimized bulb configuration show an improved performance of 2.07% and 0.23% in the weighted effective power compared to the original bulb configuration, over operating profile 1 and 2 respectively. The robust bulb configuration outperforms the orig-

89

inal bulb configuration in the lower and mid speed regime, and as a result of the low weighting of operating profile 1 the robust bulb configuration shows worse performance in the the higher speed regime compared to the original bulb configuration. Based on the fact that the original hull form has been designed to operate in the higher speed regime, the robust bulb configuration is expected to show poorer performance in this speed regime. The outcome of the obtained robust bulb design is in compliance to the outcome of similar studies related to the topic of hull form optimization for the KCS with respect to a slow steaming operating profile. As an example Wagner et al. (2014) states that multi objective hull form optimization typically yields a reduced, less distinctive bulb geometry. As previously noted, this hull will be used as reference hull for the flexible bulb configurations, as robust bulb designs constitutes the benchmark for bulbous bow design.

8.2 True Optimum Design

As discussed in section 6.3, the search for the optimal bulb design at each operating condition will give valuable insight on how the different design variables affect the bulb performance within the design space. The Sobol pseudo-random search especially gave great insight into:

1. What design variable introduces the greatest potential of resistance reduction with the introduction of flexibility for the given operating condition.

2. The wave elevation within the vessels wake, as well as the pressure distribution at the hull surface for each true optimum bulb configuration at their respective speeds give great insight on the hydrodynamic effects imposed by the change in the bulb geometry.

3. The overall potential of the flexible bulb design for that operating condition.

The Lower Speed Regime

The surface plane as illustrated in figure 7.2 and 7.5, which illustrates the Sobol search for the speeds 12 knots and 15 knots respectively, indicates that the best bulb geometry is located in the corner of the design space of the design variables ΔL and ΔB for both velocities. This is in accordance to theory which states that slender, shorter bulbs are subjected to ships sailing in the lower speed regime. The slope of the surface planes also indicates that a change in the breadth parameter of the bulb has the most significant impact on the wave resistance, compared to the

length parameter of the bulb. Both the change in length, as well as the change in breadth of the bulb introduces a significant change in the volume of the bulb section of the bow, and should, according to linear wave theory, lead to a significant change in the wave making of the bulb. As seen in figure 7.6, the change in the bow wave elevation is reduced for the optimized bulb shape. The reduction of bow wave elevation is a result of the new slender bulb, leading to a reduction of the stagnation pressure, as well as the forward shifted area of overpressure. Furthermore, because of the smaller wave heights in the lower speed regime, the reduction in wave resistance by the improved fairing of the bow section, as a result of the slender bulb geometry, can take presence over interference effect of the bulb.

Considering the fact that the change in the length parameter of the bulb for the speeds 12 knots and 15 knots does not introduce a significant change in the wave resistance, the potential for a significant reduction in wave resistance by introducing flexibility in the length parameter for this speed regime is low.

The Mid Speed Regime

The investigation of the influence of the design parameters within the design space for 18 knots, which is illustrated in figure 7.8 leads to the same findings as for the optimal bulb at 12 knots and 15 knots; a shorter and more slender bulb. While the change in the breadth parameter still compose the most significant contribution to the change in wave resistance, the influence of the length parameter of the bulb is more prominent for this speed than for the lower speed regime. As seen in figure 7.10 the effect of the shorter and more slender bulb leads to a lifting of the underpressure at the top of the bow, in affiliation with a shift in the overpressure this results in a reduction of the bow wave elevation. These findings is confirmed by the comparison of the wave elevations for the original hull and the optimized hull in figure 7.9, where it is clear that the reduction of the vessels wake is caused by an more favourable wave interference.

The Sobol investigation for 18 knots suggests that a flexibility in the length parameter of the bulb will introduce a potential of resistance reduction as the wave resistance increases if the length of the bulb is altered forward.

The Higher Speed Regime

The Sobol investigation illustrated by the surface plane in the figures 7.11 and 7.14 show a shift in trend compared to the mid and lower speed regime. While in the lower speed regimes the

change in breadth parameter was the dominating factor with respect to reduction of wave resistance, the trend in the higher speed regime indicates that the change in the length parameter has the most significant impact on the wave resistance. Figure 7.11 illustrates that the optimal bulb shape for 21 knots sailing speed lies in the region of $\Delta L = 0.00$, while figure 7.14 indicates that the optimal bulb shape for 24 knots sailing speed lies in the region of $\Delta L = 0.50$. In addition to the change in influence of the length parameter of the bulb, the optimal breadth parameter of the bulb see a shift towards fuller bulb shapes compared to the lower speed regimes. This indicates that the potential of flexibility in the bulb design is much more prominent in this speed regime, since the length of the bulb can be altered to the ideal length when sailing in this speed regime.

As illustrated in figure 7.13 the change in the height parameter of the bulb introduces an uplifting of the underpressure at the top of the bulb, as well as a minor forward shift of the overpressure, leading to a reduced bow wave. Figure 7.12 indicates that the improved bulb geometry results in an effective wave interference, as the wave elevation within the vessels wake for the optimized hull is reduced compared to the original hull. The ideal bulb geometry optimized for a sailing speed of 24 knots resulted in main dimensions of the bulb which is similar to the original bulb geometry. Based on the fact that the original hull form has been designed to operate in the higher speed regime, the true optimum bulb configuration for 24 knots is expected to show similar performance. As a result, the optimized hull and the original hull show similar characteristics with respect to the bow wave elevation, as well as the wave elevation within the vessels wake.

The influence of the length parameter on the hydrodynamic performance of the bulb clearly shows that flexibility in the length parameter introduce a severe potential of reduction in the wave resistance.

True Optimum Design: Overall Performance

To establish how well the optimum bulb configuration perform, the effective power of the hull with the optimum bulb configuration were compared to the effective power of the hull with the original bulb shape. The plot in figure 7.17 show the performance of each of the optimum bulb configurations for all the velocities in the operating profile. It is evident that there is a distinct difference in performance for the bulb shapes optimized in their respective optimized region.

In general, this opens for the introduction of flexibility in the bulb design, but as seen in table 7.4 the savings in percentage in terms of the weighted effective power over operating profile 1 has a reduction 0.25% and a reduction of 1.00% over operating profile 2. The reasoning for the difference in the reduced weighted effective power over the two different operating profiles lies in the weighting of the time fraction spent in each speed in the respective operating profiles. Since operating profile 1 is based on time series analysis of the vessel ANL BAREGA in a time period where the vessel was slow steaming, the higher velocities is weighted low, giving little contribution to the total reduction in the weighted effective power in the higher speed regimes. For operating profile 2, the weighting is centred around the mid to high speed regime, and the advantage of the increased length is captured, thus opening a potential for reduced resistance.

The findings from the optimum design, described above, clearly show that the potential of flexibility is largely governed by the breadth parameter in the lower to mid speed regime, while in the higher speed regime the length parameter is the governing factor. In the lower speed regime, the ideal bulb shapes consists of slender and shorter bulbs, while in the higher speed regime, the ideal bulb shapes comprise of fuller and longer bulbs. However, the variation in the breadth parameter of the bulb introduce the most significant change on the wave resistance for the different speeds weighted high in operating profile 1, and both the breadth parameter and the length parameter have a significant impact on the wave resistance for the different speeds weighted high in operating profile 2. Moreover, the objective of this thesis is to investigate the potential savings in reduction of the wave resistance by introducing flexibility in the length parameter. Bearing this in mind, further investigations on the value of flexibility in the bulb design will involve the influence of flexibility in the length parameter of the bulb.

The optimal bulb geometry for the three lowest velocities in the operating profile 12, 15 and 18 knots are very similar in terms of the main dimensions $\Delta L, \Delta B$ and ΔZ as seen in table 7.3. Naturally, their hydrodynamic performance in the various velocities in the operating profile are similar. A mechanical mechanism that is able to dynamically change between these configurations will not not be cost effective nor possible with the technology available in the marked today Bang et al. (2017). As described in section 6.3.2, the optimal bulb design for each speed configuration constitutes the higher bond of potential resistance reduction in terms of flexibility, if the mechanical configuration is disregarded.

8.3 Flexible Bulb Configuration

As stated in section 6.3.4, the investigation of the best bulb geometry to be subjected to a change in the length parameter during operation is a process of evaluating the best candidates from the optimum design process. The breadth and height parameter of the five different design candidates are listed in table 7.3. To evaluate the performance of the different design candidates the breadth and height parameters were kept constant while the length were allowed to change. From the search of the design space in the optimum bulb design, it is evident that a bulb ideally would be able to change the length between $\Delta L = -1.5$ and $\Delta = 0.5$ to capture the ideal length for the bulb at all the velocities in the operating profile. All the bulb candidates were evaluated with a length parameter of $\Delta L = -1.50$, $\Delta L = -1.00$, $\Delta L = -0.50$, $\Delta L = 0.00$ and $\Delta L = 0.50$.

8.3.1 The Difference in Wave Resistance

Figure 7.20, 7.23, 7.26, 7.29 and 7.32 shows the wave resistance coefficient for all length variations for all the flexible bulb candidates over the speed regime. The idea of the flexible bulb configuration is that the the length parameter of the flexible bulb that yields the lowest wave resistance for the vessel at the current sailing speed will be used during operation at that sailing speed. The figures illustrates how the length variations in the bulb geometry affect the wave resistance of the vessel, and thus constitutes the ideal length for the bulb at each speed. As seen in figure 7.20, 7.23 and 7.26, the performance of flexible bulb configuration number 1, 2 and 3 show similar trends with lower wave resistance than flexible bulb configuration number 4 and 5 in the lower speed regime. The reasoning for this is along the lines that was described in section 8.2.

8.3.2 The Overall Performance of the Flexible Bulb Configurations

Figure 7.22a, 7.25a, 7.28a, 7.31a and 7.34a shows the performance, in terms of effective power, for the 5 flexible bulb candidates, as well as how their performance compares to the robust bulb configuration. From the figures it is evident that flexible bulb configuration 1, 2 and 3 show the greatest potential in reduction of the resistance compared to flexible bulb configuration 4 and 5, with flexible bulb configuration number 1 showing the greatest potential. However, with a reduction in the weighted effective power of 0.22%, 0.04% and −0.09% over operating profile 1

respectively, the introduction of flexibility in the bulb design have little to no impact on the total resistance of the vessel.

Flexible bulb configuration number 1 have main dimensions corresponding to a fixed breadth parameter of $\Delta B = -1.44$ and a fixed height parameter of $\Delta Z = -0.80$, and a length parameter of $\Delta L = -1.50$ when sailing at 12 knots, $\Delta L = -1.00$ when sailing at 15 and 18 knots, $\Delta L = -0.50$ when sailing at 21 knots and $\Delta L = 0.50$ when sailing at 24 knots to take advantage of the flexibility. However small, the reconfigurable length ability of the flexible bulb indicates how the flexible bulb design can take advantage of the interfering effect on the wave system.

The hypothesis of the flexible bulb configuration builds upon the the fact that the variations in the operating profile for vessels have large variance due to the short term effects governing the given trade. While slow steaming is a result of a combination of bunker prices, as well as the demand in the global trading marked, the introduction of flexibility in the bulb design opens a possibility for the vessel to sail at higher velocities without a loss in reduction, compared to the robust design. Should the demand in the global trading marked see a change where the demand is higher, the flexible bulb design would be more suitable than the robust designed bulb. The intention of operating profile 2 is to imitate such an event, and as seen in table 7.5, flexible bulb configuration 1, 2 and 3 will perform better than the robust bulb configuration. flexible bulb candidate number 3 shows the best performance over operating profile 2 with a reduction of 0.38% in the weighted effective power.

As substantiated by the reduction in weighted effective power compared to the robust bulb configuration it is evident that the potential savings in resistance for the flexible bulb configuration is small. The small difference in weighted effective power for the two bulb configurations, flexible and robust, indicates that the extra building costs associated with such a flexible design is not supported.

Chapter 9

Conclusion

9.1   Concluding Remarks

Based on a study of the speed variations in the operating profile for container ships, the design method for the ideal flexible bulb configuration coinciding the to the optimal performance of the bulb at each sailing speed in the operating profile has been built. The design of the flexible bulb is divided into three main parts; one part subjected to parametrically model the bulbous bow geometry in CAESES to search for the optimal bulb geometry in a systematic manner, one part devoted to evaluate the variations in resistance over the operating profile due to the changes in geometry in SHIPFLOW, and one part devoted to present a systematic design procedure which describes the steps completed to obtain the ideal flexible bulb geometry, and how to evaluate the performance of the ideal flexible bulb compared to the robust bulb design. To evaluate the potential in terms of reduced resistance for the flexible bulb, a case study was performed for the KRISO container ship, where the operating profile for the comparable container ship ANL BAREGA was applied.

The work of parameterizing the geometry of the bulbous bow within the CAESES framework can conclude on the following:

- The chosen design variables, as well as the chosen method to model each design variable has shown desirable effects to achieve reductions in the resistance of the hull at the different speed variations.

- The use of spline curves to represent the change in geometry of the bulb were found to be a suitable way to parameterize the bulb, as the design variants created resembled typical

∇-bulb shapes with quality fairing curves. Furthermore, the parameterization of the bulb geometry with the use of spline curves has shown to be an efficient way to model the bulb, which enabled a good workflow in the design procedure of the flexible bulb.

- The seamless integration between the two programs, CAESES and SHIPFLOW, enabled a a clean and robust parametric geometry that was ideal for resistance calculations.

The results from the numerical resistance calculations obtained with the panel code SHIPFLOW can conclude on the following:

- The panel code SHIPFLOW has shown to be an efficient solver, with computing time between 20 to 65 minutes dependent on the sailing speed studied, and consequently the number of panels in the grid of the hull surface and the free surface.

- For the optimized hull forms, the change of the area of underpressure, in conjunction with the change in the area of underpressure which resulted in a reduction of the bow wave have shown to be in line with theory. Moreover, the reduction of the wave elevation within the vessels wake clearly show the effect of the more advantageous wave interference of the optimized hull forms.

- The wave elevation in the bow region of the hull surface has shown to be slightly underestimated compared to experimental results, which can lead to reduced resistance compared to the actual resistance. However, the wave elevation at a longitudinal wave cut located at $y/L_{pp} = 0.10$ was in good accordance with the experimental results. Furthermore, the trend of the wave resistance calculation from ShipX WaveRes and SHIPFLOW were in good accordance leading to the conclusion that the potential code SHIPFLOW is well suited to study the change in resistance due to the change in the geometry of the bulb.

Section 8.2 addressed how the length parameter and the breadth parameter of the bulb influenced the wave resistance of the hull within the design space. The findings indicated a clear trend which states that the potential of flexibility in the bulb design is largely governed by the breadth parameter in the lower to mid speed regime, while in the higher speed regime the length parameter is the governing factor, leaving little room for the potential savings in terms of resistance by introduction of flexibility in the length parameter of the bulb over operating profile 1.

The robust optimized bulb configuration, with main dimensions corresponding to a length parameter of $\Delta L = -1.05$, a breadth parameter of $\Delta B = -0.85$ and a height parameter of $\Delta Z = 0.90$, leads to an overall improvement of the weighted effective power of 2.07% compared to the orig-

inal hull form. The robust bulb configuration outperformed the original bulb configuration in the lower and mid speed regime, and as a result of the low weighting of operating profile 1 the robust bulb configuration showed worse performance in the the higher speed regime compared to the original bulb configuration. Based on the fact that the original hull form has been designed to operate in the higher speed regime, the robust bulb configuration were expected to show poorer performance in this speed regime. The overall improved hydrodynamic performance indicates that the presented method for the multi objective scenario based optimization for the robust bulb configuration was well suited, as the results are comparable to reported findings from bulb retrofit studies for the KRISO container ship.

Flexible bulb configuration number 1 showed the overall best performance over operating profile 1, with a reduced weighted effective power of 0.22% compared to the robust bulb configuration. Flexible bulb configuration number 1 have main dimensions corresponding to a fixed breadth parameter of $\Delta B = -1.32$ and a fixed height parameter of $\Delta Z = 0.60$. The variation in the length parameter over the operating profile, to take advantage of the flexibility, corresponding to $\Delta L = -1.50$ when sailing at 12 knots, $\Delta L = -1.00$ when sailing at 15 and 18 knots, $\Delta L = -0.50$ when sailing at 21 knots and $\Delta L = 0.50$ when sailing at 24 knots. Based on the improvement of the resistance characteristics for the flexible bulb configuration compared to the robust bulb configuration , it is concluded that the potential of flexibility in the bulb design is small, leaving limited incentives for such a configuration to be implemented in ship design.

The value of flexibility with long-term trends were analyzed in operating profile 2. Flexible bulb configuration number 1, 2,3 and 4 outperformed the robust bulb configuration with an overall reduced weighted effective power of 0.24%, 0.30%, 0.38% and 0.16% respectively over the operating profile. These findings indicates that the potential of the flexible bulb design is better suited to account for long term effects. However, as for the performance of the flexible bulb configurations over operating profile 1, the reduction is too small to account for the affiliated extra cost of such a device.

Although the results presented in this thesis indicates that the value of flexibility are limited compared to the robust bulb configuration, the thesis has presented a novel approach subjected to finding and evaluating the optimal flexible bulb geometry over a given operating profile. The methodology presented, met the objective of finding and evaluating the effect on the resistance due to a change in the bulb geometry in an efficient manner.

9.2   Recommendations for Further Work

The work related to the design approach of the flexible bulb has expanded the authhor's knowledge on the field of study. Important experience regarding the effects of the bulbous bow has been achieved, however additional experience on the influence of an increased set of design parameters describing the bulb geometry, as well as the influence of an increased set of input parameters in the operational profile, is needed to improve the design approach. The recommendations for further work is largely related to an increased computational power and can be summarized by the following:

- Increase the set of design variables in the parameterization of the bulbous bow. The introduction of an increased amount of design variables will lead to an increase in the complexity of the optimization process, which again will lead to vast computational cost multiples, suggesting that the optimization procedure is executed on a computer with increased computational power.

- Increase the input variables in the operating profile. Information such as the draft condition and trim angle of the vessel should be included as these factors impose a significant contribution to the hydrodynamic performance of the vessel. However, AIS data containing information of the coupling of the sailing speed and the draft condition is difficult to obtain. As for the increased amount of design variables, the introduction of an increased number of input variables will lead to an increased complexity of the optimization process.

- It is possible to improve the accuracy of the numerical resistance calculations by using a RANSE code instead of the potential flow code SHIPFLOW. The computational time per design variant will thereby increase, accordingly it is recommended to increase the computational power.

Bibliography

Arribas, F. P. (2007). Some methods to obtain the added resistance of a ship advancing in waves. *Ocean Engineering*, 34(7):946–955.

Bang, J., Bjørseth, J., and Hiorth, F. (2017). Design of mechanism for flexible bulb.

Blanchard, L., Berrini, E., Duvigneau, R., Roux, Y., Mourrain, B., and Jean, E. (2013). Bulbous bow shape optimization. In *5th International Conference on Computational Methods in Marine Engineering*.

Blume, P. and Kracht, A. M. (1985). Prediction of the behavior and propulsive performance of ships with bulbous bow in waves. *Transactions-Society of Naval Architects and Marine Engineers*, 93:79–94.

Choi, H.-J., Chun, H.-H., Park, I.-R., and Kim, J. (2011). Panel cutting method: new approach to generate panels on a hull in rankine source potential approximation. *International Journal of Naval Architecture and Ocean Engineering*, 3(4):225–232.

Dawson, C. (1977). A practical computer method for solving ship-wave problems. In *Proceedings of Second International Conference on Numerical Ship Hydrodynamics*, pages 30–38. DTIC Document.

DNVGL (2016). Retrofitting containerships - where the savings are. `https://www.dnvgl.com/article/retrofitting-containerships-where-the-savings-are-79963`. Accessed: 2016-11-26.

Eberhart, R. and Kennedy, J. (1995). A new optimizer using particle swarm theory. In *Micro Machine and Human Science, 1995. MHS'95., Proceedings of the Sixth International Symposium on*, pages 39–43. IEEE.

Ehlers, S. (2012). A particle swarm algorithm-based optimization for high-strength steel structures. *Journal of Ship production and Design*, 28(1):1–9.

Grech La Rosa, A., Thomas, G., and Muk-Pavic, E. (2015). Bulbous bows for energy efficient ships: Towards a novel design approach. In *Energy Efficient Ships, 4th November 2015, Rotterdam, The Netherlands.* Not publicly available.

Grey, A. (2014). Shipowners slow steam their way to profitability. `http://blog.ihs.com/q13-shipowners-slow-steam-their-way-to-profitability`. Accessed: 2016-09-1.

Hicks, R. M. and Henne, P. A. (1978). Wing design by numerical optimization. *Journal of Aircraft*, 15(7):407–412.

IMO (2016). Low carbon shipping and air pollution control. `http://www.imo.org/en/MediaCentre/hottopics/ghg/Pages/default.aspx`. Accessed: 2016-09-1.

Janson, C. (1996). A linear method for the prediction of free-surface waves, lift, and induced drag. Technical report, Technical report, Department of Naval Architecture and Ocean Engineering, Chalmers University of Technology, Sweden.

Janson, C. and Larsson, L. (1996). A method for the optimization of ship hulls from a resistance point of view, 21 st symp. on naval hydrodynamics. *Office of Naval Research, Trondheim.*

Kim, J. (2015). Tokyo 2015 workshop on cfd in ship hydrodynamics. In *KRISO, Korea*. National Maritime Research Institute.

Kim, J.-H., Choi, J.-E., Choi, B.-J., Chung, S.-H., and Seo, H.-W. (2015). Development of energy-saving devices for a full slow-speed ship through improving propulsion performance. *International Journal of Naval Architecture and Ocean Engineering*, 7(2):390–398.

Kim, W., Van, S., and Kim, D. (2001). Measurement of flows around modern commercial ship models. *Experiments in Fluids*, 31(5):567–578.

Kracht, A. M. (1978). Design of bulbous bows. *SNAME Transactions*, 86:197–217.

Larsson, L. and Broberg, L. (1990). A method for resistance and flow prediction in ship design.

Larsson, L., Stern, F., and Visonneau, M. (2010). Numerical ship hydrodynamics. In *Gothenburg 2010 a Workshop on Numerical Ship Hydrodynamics*, pages 1–32. Springer.

Maersk (2013). "nose job" for better efficiency. `http://www.maersktechnology.com/en/all-stories/nose-job-for-better-efficiency`. Accessed: 2016-09-11.

Mancuso, A. (2006). Parametric design of sailing hull shapes. *Ocean Engineering*, 33(2):234–246.

Mierlo, K. (2006). Trend validation of shipflow based on the bare hull upright resistance of the delft series. *Master Theses, Delft Univeristy of Technology.*

NASA (2017). Navier-stokes equations. `https://www.grc.nasa.gov/WWW/k-12/airplane/nseqs.html`. Accessed: 2017-03-12.

Olav, R. (2016). State of the art bulb design and operational profiles. Conference meeting.

Pérez, F., Suárez, J. A., Clemente, J. A., and Souto, A. (2007). Geometric modelling of bulbous bows with the use of non-uniform rational b-spline surfaces. *Journal of marine science and technology*, 12(2):83–94.

Piegl, L. and Tiller, W. (2012). *The NURBS book.* Springer Science & Business Media.

Raven, H. (1989). Variations on a. theme by dawson. In *Proc. 17th Symp. Naval Hydrod*, pages 151–172.

Rehn, C. F. (2015). Design theory and aspects of uncertainty in design.

Røe, M. (2010). Quantum-a container ship concept for the future. *DNV Container Ship Update*, (1):2010.

Sariöz, E. (2006). An optimization approach for fairing of ship hull forms. *Ocean Engineering*, 33(16):2105–2118.

Shipflow (2017). Shipflow website program description. `https://www.flowtech.se/products/shipflow-basic`. Accessed: 2017-14-05.

Steen, S. (2011). Motstand og propulsjon. *Propell og foilteori'(Marin Teknikk 3-Hydrodynamikk).*

Tahara, Y., Paterson, E., Stern, F., and Himeno, Y. (2001). Flow-and wave-field optimization of surface combatants using cfd-based optimization methods. In *Twenty-Third Symposium on Naval Hydrodynamics.*

Wagner, J., Binkowski, E., and Bronsart, R. (2014). Scenario based optimization of a container vessel with respect to its projected operating conditions. *International Journal of Naval Architecture and Ocean Engineering*, 6(2):496–506.

Wagner, J. and Bronsart, R. (2011). A contribution to scenario based ship design. *ICCAS 2011.*

Nomenclature

Abbreviations

CAD   Computer aided design

CFD   Computational fluid dynamics

EEDI   Energy Efficient Design Index

ESD   Energy saving devices(

FP   Forward perpendicular

IMO)   International Maritime Organizations

KCS   KRISO container ship

NS   Navier Stoke

OP   Operating profile

RANSE Reynolds-Averaged Navier-Stokes Equations

RoRo   Roll-on roll-off

TEU   Twenty-foot equivalent unit